

## Review

# Electrochemical Sensors, Biosensors, and Optical Sensors for the Detection of Opioids and Their Analogs: Pharmaceutical, Clinical, and Forensic Applications

Sayo O. Fakayode <sup>1,\*</sup>, Pamela Nicole Brady <sup>2</sup>, Cidya Grant <sup>3</sup>, Vivian Fernand Narcisse <sup>3</sup>, Peter Rosado Flores <sup>1</sup>, Catrena Higginbotham Lisse <sup>1</sup>  and David K. Bwambok <sup>4</sup>

<sup>1</sup> Department of Chemistry, Physics and Astronomy, Georgia College and State University, Milledgeville, GA 31061, USA

<sup>2</sup> Department of Chemistry, Talladega College, Talladega, AL 35160, USA

<sup>3</sup> Department of Chemistry, Forensic Science and Oceanography, Palm Beach Atlantic University, West Palm Beach, FL 33401, USA; vivian\_fernandnarcisse@pba.edu (V.F.N.)

<sup>4</sup> Department of Chemistry, Ball State University, Muncie, IN 47306, USA

\* Correspondence: sayo.fakayode@gcsu.edu

**Abstract:** Pharmaceutical opioids are intravenously or orally administered analgesics. While they are effective in relieving chronic and acute pain, their narrow window of therapeutic use contributes to the high occurrence of abuse. The associated abuse of this family of drugs can be correlated to the increase in dependency, overdose, and death of users. The negative effects of opioids extend beyond the physical and psychological effects experienced by the user to their unregulated synthesis and sale, which contribute to socioeconomic challenges and are a byproduct of this global public health epidemic. From clinical to point-of-care applications, the detection and real-time monitoring of this family of drug is critical in the fight to decrease abuse and improve use in clinical settings. Chromatographic separations and chromatography–mass spectrometry are traditional methods of opioid analyses, but the high cost, long analysis time, and absence of portability highlight the need for the development of fast, in situ, point-of-care analysis, or of community drug monitoring services. This review highlights recent electrochemical and optical (FTIR, Raman, colorimetric, and fluorescent) advances and biosensors for pharmaceutical and illicit opioid analysis. Specifically, an emphasis is placed on the detection of opioids and their metabolites in biological samples and in vitro cellular assays for clinical diagnosis and forensic applications. The challenges and prospects of the role of electrochemical sensors, biosensors, and optical sensors for opioid analysis in promoting clinical diagnosis, forensic study, point-of-care, and community drug monitoring services to reduce harm are also provided.

**Keywords:** opioids analysis; electrochemical; biosensor and optical sensors; clinical application; forensic study; community drug-checking; review



**Citation:** Fakayode, S.O.; Brady, P.N.; Grant, C.; Fernand Narcisse, V.; Rosado Flores, P.; Lisse, C.H.; Bwambok, D.K. Electrochemical Sensors, Biosensors, and Optical Sensors for the Detection of Opioids and Their Analogs: Pharmaceutical, Clinical, and Forensic Applications. *Chemosensors* **2024**, *12*, 58. <https://doi.org/10.3390/chemosensors12040058>

Received: 23 February 2024

Revised: 23 March 2024

Accepted: 2 April 2024

Published: 8 April 2024



**Copyright:** © 2024 by the authors. Licensee MDPI, Basel, Switzerland. This article is an open access article distributed under the terms and conditions of the Creative Commons Attribution (CC BY) license (<https://creativecommons.org/licenses/by/4.0/>).

## 1. Introduction

Millions of people are suffering from chronic and sharp physical pain globally. Chronic and acute pain management are significant health challenges as they are detrimental to personal health, wellness, and quality of life, leading to a host of other health challenges [1–3]. Pain management costs nearly EUR 200 billion per year in Europe and USD 150 billion per year in the United States of America [4]. Pharmaceutical opioids and their analogs are prescriptive analgesic medications widely used in hospitals and can be administered intravenously or orally for the treatment of chronic pain, surgical anesthesia, and palliative care [5–7]. However, the therapeutic efficacy of pharmaceutical drugs is highly dependent on their purity, dose, and intended use. Nonetheless, opioid drug abuse, production, and sale of illicit opioids, particularly fentanyl, have facilitated easy access to unsafe street drugs and addiction. The abuse,

dependency, tolerance, and addiction to opioid medications and their associated psychological, mental health, behavioral, and socioeconomic challenges are a global public health epidemic. For instance, long-term use of opioids and nonsteroidal anti-inflammatory drugs (NSAIDs) often leads to addiction, dependency, gastrointestinal bleeding, and cardiovascular issues [8,9].

Opioid overdose has exploded at an alarming rate in the past few decades, with exponential increases in overdose leading to nearly 91,799 fatalities in 2020 and 106,699 in 2021 [10–16]. The Centers for Disease Control and Prevention data of drug overdose deaths [17] involving opioids in the United States between 1999 and 2020 are shown in Figure 1. Other challenges of opioid overdose challenges include withdrawal management, costing billions of dollars of taxpayers' money to rehabilitate or care for drug abusers [18–21]. Opioid dependency also has negative impacts on the global workforce and human resources, [22] and is detrimental to the fabric of family structures [23]. Additionally, areas where abuse is prevalent also have increased crime rates, which promote societal disorderliness that threatens public safety [24]. Opioid abuse and related challenges are also responsible for tens of thousands of deaths globally each year [25–34].

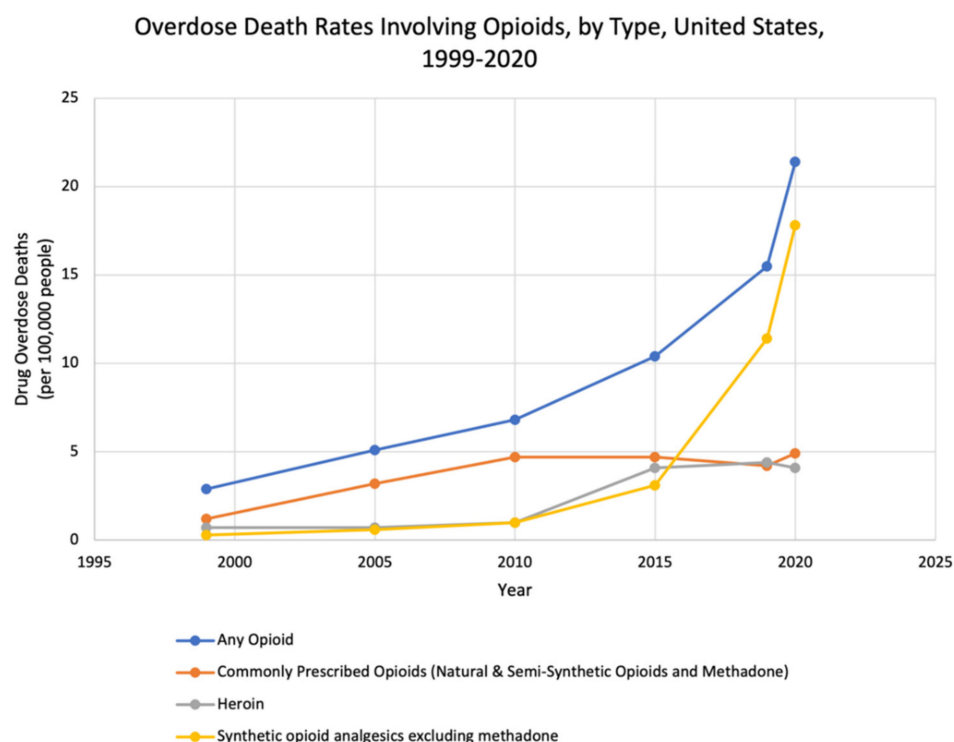


**Figure 1.** Overdose death by opioids [17].

Therefore, strict control of opioid drugs overprescription, the war against illicit drug production, and community drug-checking services are paramount to harm reduction control [25–43].

Figure 2 shows the most widely used detection methods for opioids and nitrosamine drug impurities. In general, chromatographic separation and mass spectrometry are the conventional techniques for pharmaceutical opioids and illegal drug analyses [44–46].

Enzyme-linked immunosorbent assays have also been used for opioid detection [47,48]. Liquid chromatography–mass spectrometry [49–54] and gas chromatography–mass spectrometry [55–62] are the most widely used methods for nitrosamine analysis. However, while these methods are commonly used for identifying illicit drugs, they tend to be both expensive and time-consuming. Additionally, these techniques are not portable, which limits their use for fast, in situ, point-of-care, and field opioid analysis. Electrochemical biosensors and optical sensors are viable analytical approaches that may address some current challenges of opioids and nitrosamine drug impurity analysis. We have provided

a detailed review of the attractive properties of electrochemical and optical sensors for accurate, sensitive, low-cost, and rapid sample analysis elsewhere [63–66]. In particular, electrochemical sensors are well known for their applicability in analyzing drugs during pharmaceutical, clinical, and forensic investigations because of their sensitivity, specificity, and short response time. They can produce strong electrical impulses that are directly proportional to the measured drug concentration at the electrode–solution interface. For these reasons, electrochemical sensors are excellent for instantaneous observations, point-of-care examinations, emergency settings, and quantitative analyses. Furthermore, electrochemical sensors have proven to be selective, inexpensive, simple, rapid, and user-friendly. These devices operate by measuring the electrical response of an electrochemical reaction between an electrode and the target analyte. Based on the electrical properties measured during such a reaction, these sensors can be generally divided into conductometric, potentiometric, amperometric, and voltametric types. Another advantage of electrochemical sensors is that they can be easily miniaturized and, therefore, are usable as portable devices for on-the-scene investigations. Optical sensors, such as Fourier transform infrared (FTIR), Raman, colorimetric, and fluorescence sensors, are low-cost methods to expedite the identification of opioids drugs. Optical sensors cater to the rapid detection of popular illicit substances, such as cocaine, cannabis, methamphetamine, fentanyl, morphine, heroin, and benzodiazepines.

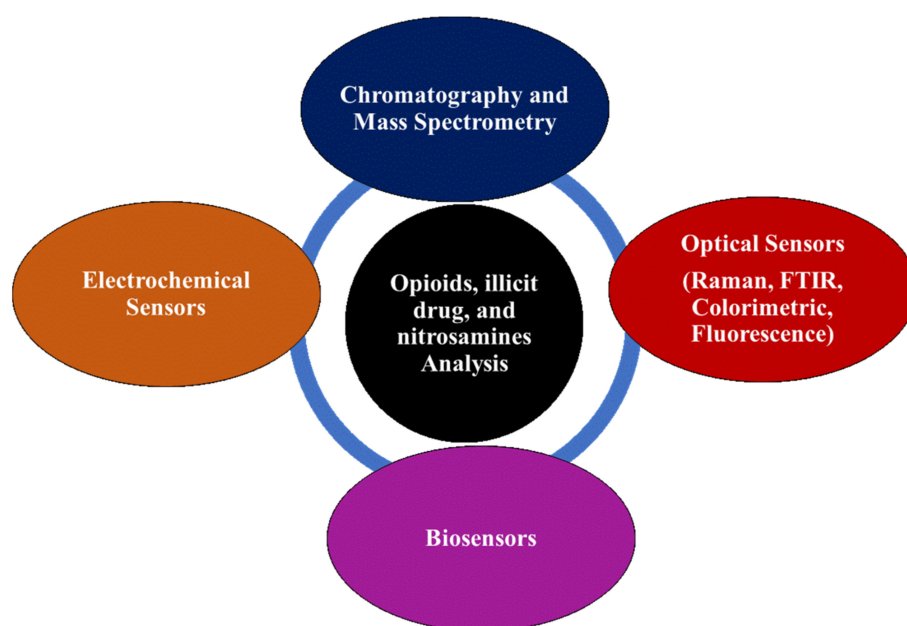


**Figure 2.** Detection methods of opioids, illicit drugs, and nitrosamines drug impurities.

This review highlights the recent advances in electrochemical, optical (Raman, FTIR, fluorescent, and colorimetric), and biosensors to detect opioids and nitrosamine impurities in pharmaceutical products. The review emphasizes the detection of pharmaceutical and illicit opioids and analogs and their metabolites in biological (urine, blood, and saliva) samples for therapeutic drug monitoring, in vitro cellular assay for clinical diagnoses, and community drug monitoring for forensic applications. The challenges and prospects of electrochemical, optical, and biosensors for pharmaceutical analysis and clinical diagnosis are discussed in promoting point-of-care and forensic applications. Figure 3 shows the selected chemical structures of opioids and their detected analogs highlighted in this review.

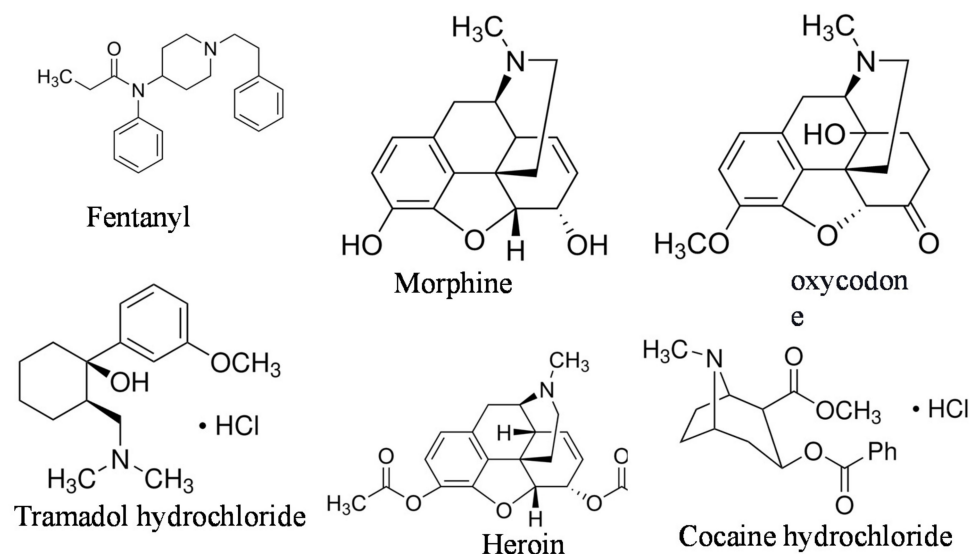


**Figure 3.** Selected chemical structures of opioids and their analogs that are covered in this review.

## 2. Biosensors Detection

### 2.1. Biosensors Detection of Pharmaceutical Opioids, Illicit Opioids, and Analogs in Biological Samples

The development of biosensors plays a pivotal role in the detection and monitoring of opioids due to their widespread use as prescription pain medications and recreational analogs. The effectiveness of their use as a method of pain management is counteracted by the narrow therapeutic window of use, which widens the threshold of abuse. Compared to traditional detection methods, such as spectroscopic methods, biosensors offer rapid, simple, sensitive, and specific analyte detection. The fast production of analogs necessitates continual development of detection methods to keep up with the rapidly increasing number of newly emerging variants. Additionally, the increase in opioid overdoses worldwide pointedly marks the need for sensors that both researchers and the general public can use for a wide range of applications, which include but are not limited to assessing evidence in drug-related deaths or crimes, tools needed for users to test their product for unwanted additions, the ability of first responders to determine the safety of a drug-related emergency, or for TSA workers to test the safety of incoming cargo as the potency of some of the opioid analogs pose significant health risks upon exposure. This section of the review offers a brief survey of novel efforts in developing biosensors for detecting pharmaceutical and illicit opioids in biological samples, pharmacological, forensic, and clinical applications, as presented in Figure 4.

The detection of the spectrum of opioid drugs in biological samples is essential in that the need for quantification varies. The effectiveness of opioids as analgesics supports their continued use in surgical procedures. However, it can be difficult for health workers to manage the patient's pain without a standard protocol for the use of these potentially highly addictive drugs. Uezozo and coworkers [67] recently published their work, which highlights this problem. Remifentanyl (REM) and fentanyl (FEN) are used during surgical procedures. However, little is understood about the best practices of switching from one to the other during surgical procedures to optimize effectiveness, as REM concentrations can be maintained during surgery, but FEN offers more optimal pain relief. The issue stems from the fact that the pain relief of both is accompanied by adverse side effects, the most problematic of which being desensitization of the opioid receptors, which increases the subject's tolerance. This, in turn, can increase the probability of dependence.



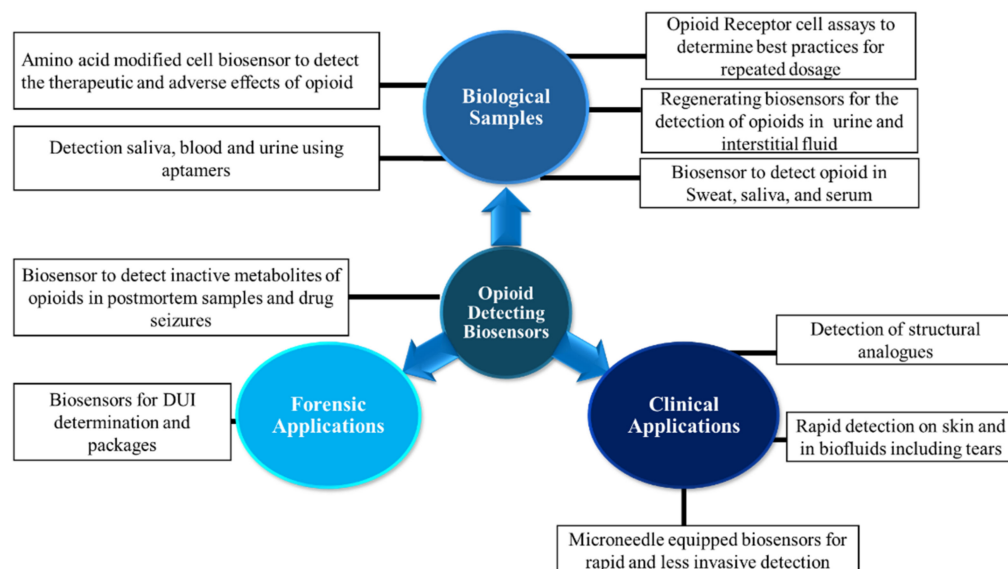


**Figure 4.** Schematic presentation of opioids analysis using biosensors.

To determine best practices for using these two drugs, the author conducted cell studies with the m-opioid receptor (MOR)-expressing HEK293 cells, which they used to perform an opioid-switching assay. This assay allowed the authors to assess the drug concentrations over time with multiple administrations. Specifically, this assay determined the response when various concentrations of the drugs were administered concurrently. They found that the second administration of FEN at a concentration of  $10^{-9}$  M gave a response equivalent to the first administration of REM, which was given at  $3 \times 10^{-9}$  M. Contrarily, the response was not accomplished when switching from FEN to REM. This finding suggests that switching from REM to FEN during surgical procedures may be effective as a lower concentration FEN would need to be used to achieve sufficient pain-relieving effects. The authors also performed visualization assays of opioid receptors (ORs) in human embryonic kidney cells that expressed Halotag® ORs. This assay explored the beta-arrestin mediated signaling pathway components. In this assay, the Halotag®-tagged ORs were previously stained with a pH-sensing ligand, which exhibits red fluorescence when the pH is decreased. Fluorescence of the internalized MOR is induced by each compound's uptake. These results showed an increase in both the number and intensity of the response upon the cell's uptake of REM when compared to the assays using FEN. The authors postulate that this observation could be attributed to the two conformational styles of beta-arrestin when activated by MOR, but this was not further investigated in this study and should be investigated to lend further insight into the binding interaction. This work highlights the need to develop standard administration protocols to determine best practices for this family of drugs. Suboptimal protocols can contribute to the epidemic of dependence and abuse. Other researchers have made efforts towards understanding the effects of opioid drugs at the cellular level.

Kroning and coworkers engineered an opioid biosensor in 2021 and then went on to publish a second paper in the same year in which they presented their improvements on the device [68,69]. In their most recent work, they detailed a new construct that is structurally differentiated from the previous iteration due to the addition of YNSH amino acids at the N-terminus. The importance of the addition of these four amino acids is that they allow full encapsulation of the fluorophore which does not occur in their absence. The complete encapsulation helps to increase the quantum yield. This theory is supported by the observed  $11 \times$  increase in fluorescence observed in HEK293T cells and the  $2.7 \times$  brighter fluorescence observed in neuronal cells. The N-terminal addition was also postulated to increase the stability of the structure. Future work includes the improvement of the background fluorescence of the sensor, which will aid in its applicability for high-throughput screening

and the detection of endogenous and exogenous opioids in animal brains at a cellular resolution [69]. The authors wished to compare the limit of detection of the new and improved modified version of the sensor to the previously prepared version, which they accomplished through titration of fentanyl. They observed similar levels of detection between the new and old preparations, both of which have the advantage of being able to detect the analyte at cellular resolution which is an improvement in comparison to other detection methods which can either only detect large quantities or are limited when it comes to the detection of other analytes. Selectivity studies demonstrated that the newly improved sensor is more selective to MOR antagonists, such as fentanyl, morphine, loperamide, oxycodone, and buprenorphine. The device presented could prove to be an integral tool in helping researchers to gain a more comprehensive understanding of the mechanism of opioid addictions, side effects of opioid use, such as respiratory suppression, and the therapeutic act of pain modulation as it pertains to opioid signaling.

Some researchers have opted to focus on developing modalities to detect opioids in various biofluids. One example of this is work recently published by Canoura and coworkers [70], which describes the development of a biosensor fabricated using a library-immobilized aptamer-based sensor for the detection of fentanyl in saliva, urine, and serum under biological-like conditions. Using aptamers for biosensors has several advantages over antibody-based sensors in that they are affordable and easily modified, tunable, simple to create, and possess reversible denaturation. This team optimized their sensor by conducting high-throughput screening to identify aptamer candidates via systematic evolution of ligands by exponential enrichment (SELEX) where 1 nmol of the concentrations of the aptamer library was used to assess binding to 100  $\mu$ M of fentanyl in the first round of selection. This pool was further refined a second and third time using a 350 pmol concentration of the library and 100 mM of fentanyl with counter SELEX to screen for a variety of cutting agents, adulterants, pharmaceuticals, and other illicit drugs. This screening continued through round 13. The resulting pool demonstrated a greater affinity to bind to fentanyl than to the other targets. The binding affinity was confirmed using a gel elution assay. The employed screening process resulted in the identification of a family of structurally related aptamer families that exhibited high analyte specificity. High-throughput screening was conducted on pools 10–13 to assess sequence abundance, which resulted in seven sequences that were divided into two families. The  $K_D$  values for fentanyl using ITC which were determined to range between 49–426 nM. The resulting electrochemical aptamer-based sensor was a folding sensor in which the attached aptamer is modified at one end with a thiol group and with a methylene blue redox tag at the other end. The aptamer is initially unfolded, and the redox tag is far from the surface of the gold electrode. Binding with the target analyte induces a change in conformation which brings the redox tag closer to the electrode which in turn increases the current in a concentration-dependent manner. The prepared aptamer performance highlights the device's potential to be employed as a point-of-care device as it was demonstrated to provide rapid analysis, having the ability to detect fentanyl within seconds with a limit of detection of 10 nM, which mimics the typical concentration of the drug in biological samples. The author also suggested that the conversion of the sensor to a paper-based device could combine the superior analytical function with a low-cost device that could be used in real-time to monitor levels of the analyte during surgical procedures [70].

A second manuscript was published by this same authors in 2023, where they present their work on the fabrication of two additional assays—a colorimetric dye-displacement assay and a strand-displacement-based fluorescence assay [71]. The colorimetric assay was shown to have the ability to detect low concentrations of fentanyl through visualization of the purple-to-blue color change and employed the use of three aptamers, which were determined to have varying levels of affinity for fentanyl to aid in the quantification of the analyte upon binding. The colorimetric aptamer-based dye displacement was developed to address the limitations of previously used spot tests by making the analysis faster and eliminating the need for highly trained technicians for data interpretation. The

dye used, 3,3'-di(3-sulfopropyl)-4,5,4',5'-dibenzo-9-methyl-thiacarbocyanine (MTC), was chosen because of its water solubility properties, its broad optical properties in its bound and unbound state, and because it demonstrated applicability in the development of assays. This is important because the initial complexation of the dye and the aptamer is disrupted by the target. The released dye produced a color change that can be observed with the naked eye. The specificity and selectivity of this method can also be tuned using high-quality aptamers. The authors were able to identify an aptamer that demonstrated high specificity for fentanyl, which also had an affinity to several fentanyl analogs. It was determined that the aptamer had a dissociation constant (KD) of  $212 \pm 15$  nM and displayed minimal binding affinity to other common additives found in drug mixtures, such as other drugs, adulterants, and cutting agents. The strand-displacement-based fluorescence assay addressed the limitations of the lateral-flow immunoassays, as they are also semiquantitative, by introducing a method that allows for the acquisition of easily quantifiable data over a dynamic range of 10 nM to 10 mM. This was accomplished using short complementary DNA (cDNA) that is initially bound to the aptamer, and this binding interaction is displaced by the target, which is quantifiable. In all, the three sensors developed have a potential utility for in-home testing usage for detecting fentanyl in drug samples.

In 2023, Nah and coworkers [72] fabricated an optical sensor functionalized with one-dimensional photonic crystals (1D PhCs), comprised of two dielectric materials with low and high refractive indexes. This property allows for band gaps, which are capitalized upon by targeted layering patterns, the addition of an absorbing layer at the bottom, and the incident angle of light. The combination of these elements in the fabrication allows for the bandgaps created by the material to reflect light at each wavelength, resulting in the acquisition of a single resonance peak and facilitating the detection of the antibody–antigen binding through shifts in the resonance peaks. The sensor was demonstrated to have a broad working range of 10 ng/mL to 1 mg/mL. The minimum effective plasma concentration of morphine is 20–40 ng/mL, and the lethal dose is 0.5 mg/mL, which means that the sensor can effectively detect relevant points on concentration in the blood. Fentanyl dosage is much more potent, as the lethal dose is about 7 ng/mL, but the LOD of the fentanyl sensor is just below that threshold at 6 ng/mL, which is an improvement over previous work. Therefore, future work is needed to improve the detection of fentanyl. The authors also demonstrated the sensor's ability for multiplexing when multiple fluidic channels were functionalized with the prepared antibodies. They could subtract the background signals to quantify the concentrations of the two analytes in the sample, highlighting the device's applicability in analyzing unknown mixtures.

Additionally, the authors conducted studies assessing the ability of the sensor to be regenerated and the efficacy of the sensor in detecting morphine and fentanyl in artificial interstitial fluid and human urine samples. It was determined that the sensor could be regenerated with up to 93.66% recovery after five cycles at pH 2.5, which is not optimal. Future work entails determining how the sensor could be regenerated under physiological conditions. Optimization of this would make the sensors suitable for use in a wearable sensor, which could be useful for real-time monitoring. Results from the detection of the fentanyl in the biological samples determined that the sensor could detect it at sample concentrations from 5 to 1000 ng/mL. Overall, the sensor shows promise for several applications but needs further optimization to improve several performance features [72].

Methadone has been used since the 1960s to treat opioid abuse by preventing the onset of withdrawal symptoms without producing the euphoric high associated with opioid use. However, its therapeutic usage is limited by the variation in how it metabolizes from one individual to the next, and the metabolic stage is typically measured through the collection of a blood sample. However, this method is laborious and invasive to the patient. Muthusamy and coworkers [73] presented their work in the development of a reagentless, intensity-based, S-methadone fluorescent sensor which sought to address the limitations of the standard detection tools that would enable real-time monitoring of the

methadone in biological fluids to promote effective opioid weaning. Their work is novel in that it highlights the first genetically encoded fluorescence protein biosensor to be used to detect an opioid drug. The fabrication of the sensor was achieved through mutations to the binding pocket of the iNicSnFR3a. These mutations resulted in an abundance of aromaticity within the binding pocket that can easily bind to the protonated amines while other areas can bind to other functional groups and the steric bulk of the ligand. The development of this sensor allows for real-time quantification, and the sensor was shown to be selective, stable, and sensitive. In their work, they screened each methadone enantiomer against previously reported nicotine biosensors, which were chosen because several had been previously identified to have weak fluorescence responses to the S-methadone enantiomer. The biosensors were mutated three times with a W436F, N11V, and L490A, which helped to create space, volume, and flexibility within the overall structure. These mutations were postulated to allow S-methadone to potentially have better access to the aromatic residues within the binding pocket. The resultant biosensors were tested in human sweat, human saliva, and mouse serum samples, and the responses were within the pharmacologically relevant concentrations [73].

Urine testing for opioids serves as a valuable tool for monitoring drug use, ensuring compliance with prescribed therapies and promoting public safety. Thus, urine is also a critical body fluid to target and utilize in developing robust opioid detection methods. In 2022, Gonzalez-Hernandez and colleagues [74] highlighted a novel voltametric enzymatic biosensor to detect fentanyl in urine samples. The function of the sensor was based on the usage of cytochrome c as the enzyme, which helped to improve the analytical response compared to the function of other electrodes. The selectivity of the method was evaluated by using several spiked fentanyl solutions with caffeine, pseudoephedrine, and cocaine at four different ratios, and it was determined that the advantage of this technique is that it can be used to test mixtures so long as the ratios of the analyte and other interferents are not greater than 1:1 and that only small amount of the sample is needed for the analysis. The limit of detection of this method was determined to be 0.086 mg/mL, which is not as low as other electrodes, but this is offset by the fact that those electrodes are more laborious to prepare. These attributes also suggest the applicability of the sensor for rapid and reliable testing of biological samples of drug users [74].

Cortade and coworkers [75] detailed their work on developing a giant magnetoresistive nanosensor array (GMR) for the dual-use detection of morphine and hydromorphone in saliva, blood, and plasma. The fabricated array was comprised of an array of 80 independent sensors on a square  $5 \times 5$  mm chip that was bound to a printed circuit board with wire. The fabricated sensor could fit into a reusable cartridge. Signals from the chip arise from the translation of in the local magnetic fields of the sensors up to 150 nm. These fluctuations can be translated into quantifiable changes in resistances that occur because of binding events between biotinylated proteins and superparamagnetic nanoparticles (MNPs) that were functionalized with streptavidin. The resultant device was not only easy to manufacture but also multiplexable, supported the point-of-care quantification needs over a wide range of concentrations, and allowed for detecting the analytes in saliva, whole blood, and plasma. In addition, less than 200 mL of sample is needed for analysis, which is essential because a limiting factor for accurate analysis may be sample size [75]. Biological samples are essential targets for ever-developing screening tools, which can help researchers gain an understanding of the metabolic impact of opioid use and allow for greater variation in the types of samples that can be tested to determine opioid concentrations or to confirm drug presence.

## 2.2. Biosensors: Clinical Applications

The rapid development of analogs of opioids poses a significant challenge to existing detection methods. While structurally similar to their parent compounds, these analogs often exhibit subtle differences that can evade detection by conventional means. This poses a serious concern, as detecting these analogs is crucial for effective drug monitoring,

forensic analysis, and public health efforts. Traditional detection methods for opioids rely on the specific binding of the analyte to a recognition element, such as an antibody or enzyme, which is designed to target a particular molecular structure. However, the structural similarities between opioids and their analogs mean that these new compounds may bind to the recognition element at a site different from the original analyte, leading to false negatives or inaccurate results. Therefore, there is an urgent need for the development of new detection methods that can effectively distinguish between closely related opioid analogs. These methods must be able to detect the presence of these analogs even when they do not correspond with the original binding site of the analyte. Such advancements in detection technology are essential for ensuring the accuracy and reliability of drug testing, as well as for combating the growing opioid crisis.

To keep up with the ever-increasing number of analogs, Liu and coworkers [76] report on their work on a sensor fabricated for the detection of butyrylfentanyl, which is a new designer drug whose use has been linked to a growing number of fatal overdoses. Because of its novelty, there are few methods to detect the analyte, a problem that is the inspiration for this project. The fabrication of a fiberoptic sensor that measures carboxyl fentanyl, a metabolite of the designer drug that can be detected in the blood, was presented. The developed fiberoptic sensor arose from the combination of molecularly imprinted polymeric nanoparticles (nanoMIPs), which have been shown to be effective alternatives to antibodies in many diagnostic techniques useful in detecting a wide variety of analytes, and an optical fiber long-period grating (LPG) sensor. These sensors couple an electric field into the fiber itself which allows for an extension of the electric field, which results in the sensitivity of the fiber to changes in the refractive index, which correspond to changes in the resonance wavelengths which can be quantified. The nanoMIPs functionalized LPG sensor operates against a reference LPG sensor which helps to compensate for temperature cross-sensitivity. This is an important aspect of the design in that detection with LPG sensors has been demonstrated to be strongly dependent on temperature variations, which is addressed by the configuration of the array. The sensor they developed was demonstrated to have a wide range of detectable concentrations and could detect the analyte down to 50 ng/mL because of shared similarities in binding sites; this sensor could also be used to detect carboxyl-fentanyl, which would allow for the detection of fentanyl due to the two analytes having identical binding sites. Additionally, this array is selective in that it has negligible binding to other analytes or biological molecules which may be present in collected samples [76]. This project further emphasizes the need for detection tools in these areas in that structural similarity does not guarantee binding behavior, and without testing, it remains unknown if new analogs can be detected with old tools. Wang and colleagues wrote of their developed point-of-care assay for fentanyl monitoring. To achieve this, they began with a gold working electrode coated with an L-arginine-PANI layer which serves as an anchor for adsorption of fentanyl and which has been demonstrated to have high sensitivity to analytes with the chain conformation that arises from pi-orbital structures. These binding interactions occur as a result of the combination of intermolecular interaction-enabled small molecule recognition (iMSR) coupled with differential impedance analysis of conjugated polymers. The binding interaction, which produces an elective signal, can provide rapid and quantifiable data, and can be measured using electrochemical impedance spectroscopy (EIS). The developed assay demonstrates high analyte selectivity and the ability to analyze body fluids on the skin or using testing strips. The presented device was demonstrated to be sensitive over a wide concentration range in serum (0.1 to 1000 nM), tears (0.5 to 500 nM), and artificial sweat (1 to 200 nM). Future work includes adapting the device for use with mobile devices to increase its functionality as a POC analysis method [77].

Recently, Joshi and coworkers [78] published their novel work on developing a 3D-printed microneedle array to detect fentanyl in biofluids. The use of a microneedle in small-scale detection tools has revolutionized the function of these devices by improving their overall performance and allowing for transdermal biosensing with less pain overall. The 3D-printed version of the hollow needles made from E-Shell 200 presented in this



work addresses the limitations of the traditional fabrications, which are typically made from Si and are brittle; as such, they have yet to see the widespread use predicted by their small functional size. E-Shell 200 is a Class IIa biocompatible, water-resistant material stronger than Si. The hollow needle was filled with a graphene ink that was modified with 4 (3-butyl-1-imidazolium)-1-butananesulfonate) ionic liquid which helped to improve the conductivity of the device. The needle was also filled with platinum and silver electrodes, which acted as the counter and reference electrodes. The biosensor not only provided a minimally invasive detection method in serum, but it could do so over a dynamic range, between 20 and 160  $\mu\text{M}$ , and was shown to have an LOD of 27.8  $\mu\text{M}$ . The development of this device is critical to the never-ending battle of combatting the opioid epidemic that is affecting the world. This work offers an up-and-coming platform that has the potential to be used by first responders and clinicians [78]. Tools that can be used as point-of-care devices are pivotal to the landscape of combating and optimizing opioid overuse. Rapid and straightforward analysis tools will help extend the plausible applications further and broaden the variety of users equipped to utilize the devices.

### 2.3. Biosensors: Forensic Applications

The detection of opioids in forensic applications is critical for law enforcement, health-care providers, and regulatory agencies to combat drug abuse, overdose incidents, and criminal activities. Traditional detection methods, such as immunoassays and chromatography, have been instrumental in this regard. However, the emergence of new opioid analogs with subtle structural modifications poses a significant challenge to current detection methods. Opioid analogs, designed to mimic the effects of traditional opioids while evading legal restrictions, are increasingly prevalent in illicit drug markets. These analogs often have chemical structures that are very similar to their parent compounds, making them difficult to detect using conventional techniques. This presents a severe problem for forensic scientists and law enforcement agencies tasked with identifying and monitoring these substances. The need for new detection methods for opioids in forensic applications is obvious. These methods must detect a wide range of opioid analogs, including those with structural differences that may not correspond to the original binding site of the analyte.

Furthermore, these methods should be sensitive, selective, and reliable, allowing for the accurate identification and quantification of opioids in various sample matrices. In response to this need, researchers are actively developing innovative detection technologies that can address the challenges posed by new opioid analogs. These advancements hold great promise for enhancing the capabilities of forensic laboratories in detecting and identifying opioids, thereby aiding in the prevention and investigation of opioid-related crimes and public health threats. Recent work published by Shao and coworkers [79] described an ultrasensitive norfentanyl sensors on a semiconductor-enriched (sc)-single-walled carbon nanotube (SWCNT)-based field-effect transistor (FET) to detect fentanyl exposure. Norfentanyl is the product of the rapid metabolism of fentanyl by the liver. It can be detected in body fluids, such as blood and urine, and has a longer and more reliable detection window than the analyte in the case of analyte degradation or suboptimal conditions in the biological matrix.

The developed biosensor is functionalized with a norfentanyl antibody, the primary inactive metabolite to detect fentanyl in samples. Figure 5 illustrates the structure and the working principle of the device. Figure 5a displays that the developed chip has eight interdigitated gold source and drain electrodes and is fixed on a chip carrier to aid analysis by FET. The semiconductor enriched SWCNTs were then deposited between the gold electrodes as platforms for antibody immobilization. The sensing antibodies were attached to the device via two different approaches, as shown in Figure 5b,d, i.e., using direct bonding or using an Au nanoparticle, respectively. The direct coupling decreased conduction following the addition of a blocking buffer, which was not observed in the devices that were functionalized with the Au nanoparticle. This decrease or lack thereof are shown in Figure 5c,e, respectively. However, when studies were conducted to detect the

analyte or fentanyl, the direct immobilization preparation was used. While both versions of the device developed were shown to be sensitive and selective for the detection of norfentanyl, the Au nanoparticle offered 69.6% more sensitivity than the device in which the antibody was bound directly. The presented sensors were demonstrated to have an LOD on the order of fg/mL [79]. Angelini and coworkers [80] detailed their work on developing two different lateral flow immunoassay (LFI) configurations—dipsticks and cassettes. LFIs function on the premise that antibodies are directed against a target analyte. The binding interaction between the analyte and target is incorporated into the surface of the assay, which allows detection. The authors sought to compare the effectiveness of both configurations in detecting fentanyl in seized drug samples and in samples of postmortem urine samples. For both types of samples, both configurations demonstrated 100% sensitivity. When testing the seized drug samples, the cassettes displayed a specificity and efficiency of 100% in the seized drug samples. However, the dipstick reported false positives with samples containing cocaine and cocaine-containing mixtures, and it was determined to have a specificity of 75% and 93% efficiency, respectively. False positives were also reported with the cassettes when testing urine containing cocaine, resulting in a specificity and efficiency of 75 and 92.9, respectively. The observance of the false positive may be potentially linked to differences in the pH or the presence of acetone in the samples, which may have been able to remove the fentanyl bound on the test line. Overall, their work demonstrated that LFIs are useful, practical, and low-cost tools for detecting fentanyl. These immunoassays can be valuable tools for a variety of applications, including preliminary screenings in death investigations, field testing for DUI cases, and homeland security applications by testing packages and containers for illicit drug [80].

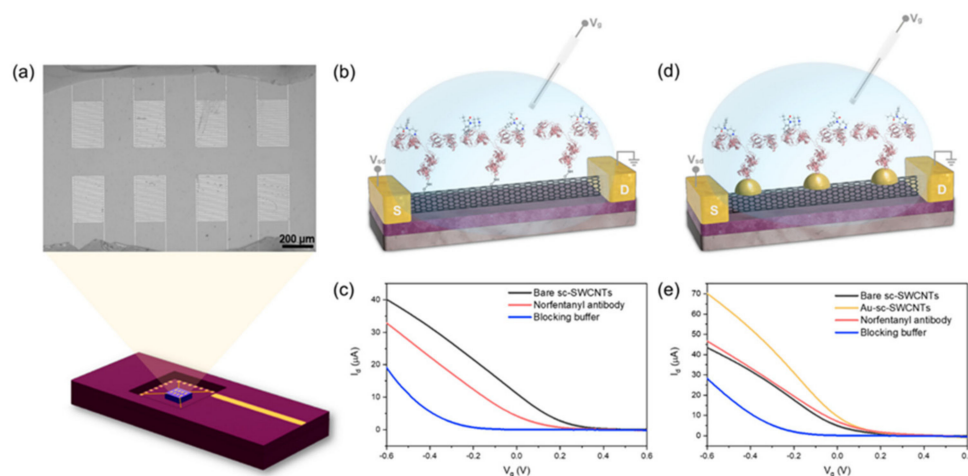


**Figure 5.** Norfentanyl antibody-functionalized SWCNT-based FET biosensor. (a) Top: optical image of the sensing chip with 8 devices. Bottom: the sensing chip was wire-bonded in a package for measurements. (b) Schematic illustration of a norfentanyl antibody-functionalized SWCNT-based FET biosensor via direct coupling approach. (S: source; D: drain.) (c) FET transfer characteristics of each functionalization step using a direct coupling approach. (d) Schematic illustration of a norfentanyl antibody functionalized SWCNT-based FET biosensor via the AuNP approach. (e) FET transfer characteristics of each functionalization step using the AuNP approach. Published with permission from Ref [79].

This brief overview of novel works focused on biosensor development for detecting opioids dually highlights the urgency of creating tools for use in various applications and the lack of optimized tools to keep up with the growing number of analogs. Great strides have been made to this end. Nonetheless, more studies are needed to give researchers concrete data and a comprehensive understanding of how to navigate the current state of the opioid usage epidemic.

### 3. Electrochemical Detection

This review section highlights recent innovations in electrochemical sensors for opioid analysis and pharmaceutical, clinical, and forensic applications. Table 1 gives a summarized overview of figures of merits, including the electrode type, electrode modification, electrochemical method, target analyte, linear range, limit of detection (LOD), and the square correlation of the calibration curve of the electrochemical sensors reviewed. Figure 6 displays a general scheme of current electrochemical sensors developed for detecting pharmaceutical and illicit opioids in biological samples and medications. In addition, Figure 7 shows a schematic description of how an electrochemical sensor functions.

**Table 1.** Overview of the types and figures of merit of the electrochemical sensors reviewed.

Electrode Type	Electrode Modification	Electrochemical Method	Target Analyte	Linear Range	LOD	R <sup>2</sup>	Ref.
Biological Applications							
Glassy carbon	PMF/GO nanocomposite	Differential pulse voltammetry	Oxycodone	0.01–45 $\mu\text{mol}\cdot\text{L}^{-1}$	2.0 $\text{nmol}\cdot\text{L}^{-1}$	0.994	[81]
Glassy carbon	(Gr/AgNPs) <sub>2</sub> /GCE nanocomposite	Differential pulse voltammetry	Methadone	1.0–200 $\mu\text{M}$	0.18 $\mu\text{M}$	0.998	[82]
Glassy carbon	GCE/CMK-5	Square wave voltammetry	Methadone and morphine	0.1 to 4 $\mu\text{M}$	0.027 $\mu\text{M}$	0.948 and 0.990	[83]
Glassy carbon	Poly(CTAB)/GO	Differential pulse voltammetry	Morphine	50 nM–60 $\mu\text{M}$	0.36 $\mu\text{M}$	0.990	[84]
Graphite screen printed	GO/Fe <sub>3</sub> O <sub>4</sub> @SiO <sub>2</sub>	Differential pulse voltammetry	Morphine	1.0–100 $\mu\text{M}$	$7.5 \times 10^{-7}$ M	0.9986	[85]
Screen printed glassy electrode	Graphene–Co <sub>3</sub> O <sub>4</sub> nanocomposite	Differential pulse voltammetry	Morphine and diclofenac	2.5–550 $\mu\text{M}$ and 2.5–700 $\mu\text{M}$	0.007 $\mu\text{M}$		[86]
Screen printed electrode	La <sup>3+</sup> /ZnO nanoflowers and MWCNTs	Differential pulse voltammetry	Tramadol	0.5–800 $\mu\text{M}$	0.08 $\mu\text{M}$	0.9992	[87]
Platinum (Pt) electrode	Pt/PEDOT/FC1/PEDOT...SDS	Cyclic voltammetry	Tramadol	7–300 $\mu\text{M}$ and 5–280 $\mu\text{M}$	18.6 nM and 16 nM		[88]
Laser carbonized polyimide electrode (LCE)	None	Square-wave voltammetry	Fentanyl	20–200 $\mu\text{M}$	1 $\mu\text{M}$		[89]
Glassy carbon	CoO@f-CNTs nanocomposite	Amperometry	Tramadol	1–300 mM	6 nM	0.9998	[90]
Pharmaceutical Applications							
Screen-printed	MWCNTs	Potentiometric	Pholcodine	$5.5 \times 10^{-6}$ to $1.0 \times 10^{-2}$ M	$2.5 \times 10^{-7}$ M	0.9980	[91]
Glassy carbon electrode	MWCNTs	Differential pulse adsorptive stripping voltammetry	Fentanyl	$5 \times 10^{-7}$ to $1 \times 10^{-4}$ M	$1 \times 10^{-7}$ M		[92]
Carbon paste electrode	Au/NPs/BMTCB/CPE	Square-wave voltammetry	Tramadol	0.01–400 $\mu\text{M}$	6 nM	0.993	[93]
Glass carbon electrode	UiO-66-NH <sub>2</sub> MOF/G3-PAMAM nanocomposite	Differential pulse voltammetry	Tramadol in acetaminophen	0.5–500 $\mu\text{M}$	0.2 $\mu\text{M}$	0.9997	[94]

Table 1. Cont.

Electrode Type	Electrode Modification	Electrochemical Method	Target Analyte	Linear Range	LOD	R <sup>2</sup>	Ref.
Pharmaceutical Applications							
Screen-printed electrode	Yb <sub>2</sub> O <sub>3</sub> nanoplate	Cyclic voltammetry and differential pulse voltammetry	Acetaminophen and tramadol—mixed and separate	0.25–654 $\mu\text{mol}\cdot\text{L}^{-1}$ and 0.50–115 $\mu\text{mol}\cdot\text{L}^{-1}$	55 and 87 $\text{nmol}\cdot\text{L}^{-1}$		[95]
Activated screen-printed electrode	aSPCE/SDS	Voltammetry	Paracetamol (PA), diclofenac (DF), and tramadol (TR)	$5.0 \times 10^{-8}$ – $2.0 \times 10^{-5}$ $\text{mol}\cdot\text{L}^{-1}$ for PA; $1.0 \times 10^{-9}$ – $2.0 \times 10^{-7}$ $\text{mol}\cdot\text{L}^{-1}$ for DF; $1.0 \times 10^{-8}$ – $2.0 \times 10^{-7}$ $\text{mol}\cdot\text{L}^{-1}$ and $2.0 \times 10^{-7}$ – $2.0 \times 10^{-6}$ $\text{mol}\cdot\text{L}^{-1}$ for TR	14.87, 0.21, and 1.71 $\text{nmol}\cdot\text{L}^{-1}$		[96]
Boron-doped diamond (BDD) electrode	None	Square wave voltammetry	Tramadol	0.25–50 $\mu\text{g}\cdot\text{mL}^{-1}$	0.072 $\mu\text{g}\cdot\text{mL}^{-1}$		[97]
Clinical Applications							
Microneedle sensor array platform	4-(3-butyl-1-imidazolio)-1-butanedisulfonate	Square wave voltammetry	Fentanyl	0–160 $\mu\text{M}$	27.8 $\mu\text{M}$		[78]
Disc electrode with a Pt-Ir wire	None	Amperometry	Heroin and cocaine	0–20 $\mu\text{M}$	Not reported		[98]
Forensic Applications							
Carbon screen-printed electrode	MoWS <sub>2</sub> nanopetals	Differential pulse voltammetry	Morphine in tramadol	$4.8 \times 10^{-8}$ M– $5.05 \times 10^{-4}$ M	$1.44 \times 10^{-8}$ M		[99]
Carbon paste electrode	CuO nanostructures and MWCNTs	Square wave voltammetry	Tramadol	0.05–200 $\mu\text{M}$	0.025 $\mu\text{M}$		[100]
3D-printed support	None	Electrified liquid–liquid interface (eLLI) miniaturization	Heroin (by itself and with cutting agents)	0–50 $\mu\text{M}$	1.3 $\mu\text{M}$		[101]

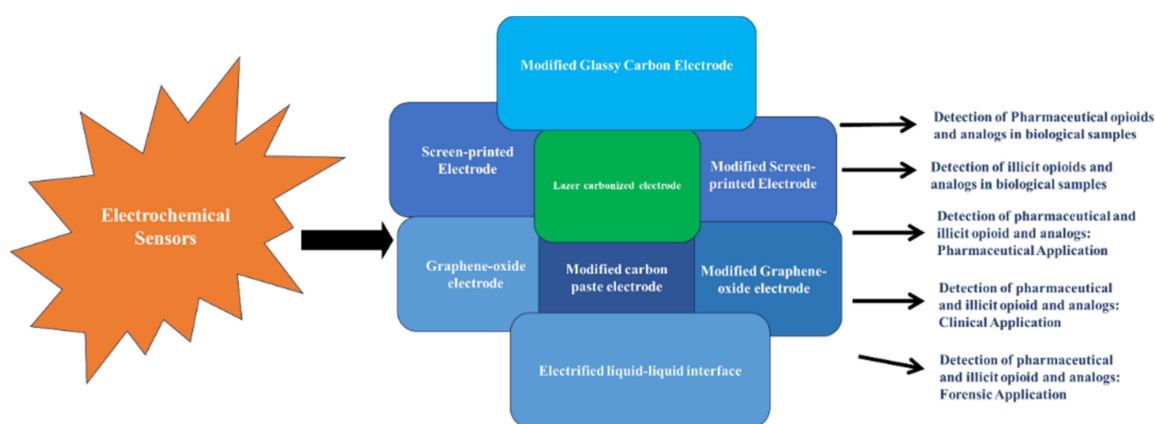
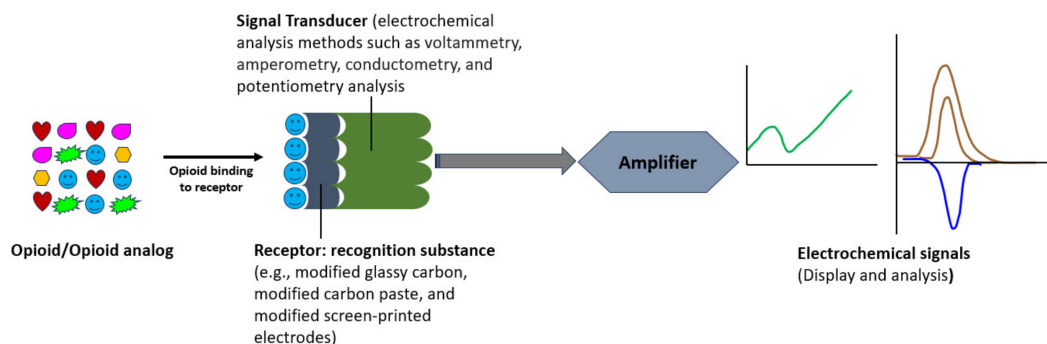


Figure 6. Scheme of select recently developed electrochemical sensors for the detection of opioids.



**Figure 7.** Schematic illustration of an electrochemical sensor.

### 3.1. Electrochemical Sensors Detection of Pharmaceutical Opioids, Illicit Opioids, and Analogs in Biological Samples

Khosropour et al. [81] fabricated a modified glassy carbon electrode (GCE) using a poly-melamine formaldehyde/graphene oxide (PMF/GO) nanocomposite. They demonstrated its application in the determination of oxycodone. They anchored PMF onto prepared graphene oxide, and then this nanocomposite was cast onto the surface of glassy carbon electrodes. Various characterization studies were used to examine the PMF/GO nanocomposite morphology. Cyclic, linear sweep, and differential pulse voltammetry studies revealed increased oxycodone oxidation peak currents when the modified GCE (PMF/GO/GCE) sensor was compared to the bare GCE or to the GCE that had been modified with graphene oxide alone. Under optimized conditions, differential pulse voltammetry (DPV) gave increased oxidation peak currents (+0.71 V (vs. Ag/AgCl)) for oxycodone. The improved electrocatalytic ability of the PMF/GO/GCE is due to an increased electroactive area on the GCE that PMF provided. Furthermore, the PMF/GO/GCE sensor detected oxycodone under optimal experiment conditions in the linear range of 0.01–45  $\mu\text{mol}\cdot\text{L}^{-1}$ , with a limit of detection (LOD) of 2.0  $\text{nmol}\cdot\text{L}^{-1}$ . The capability of the proposed PMF/GO/GCE sensor was investigated by direct analysis of human urine (from two healthy volunteers, one of whom used the 5 mg oxycodone tablet provided by the laboratory) and human blood (provided by two healthy volunteers). The results from standard addition methods were acceptable in illustrating the use of this sensor in efficiently detecting oxycodone in real samples [81].

Baghayeri and coworkers [82] fabricated an electrochemical nanosensor based on a glassy carbon electrode modified with a double layer of graphene and Ag nanoparticles. This resulted in a (Gr/AgNPs)<sub>2</sub>/GCE nanocomposite, which was used to detect methadone in bodily fluids. The sensor's morphological, structural, and electrochemical characteristics were examined using scanning electron microscopy with energy dispersive spectroscopy (SEM/EDS) analysis. The electrocatalytic activity of (Gr/AgNPs)<sub>2</sub>/GCE for methadone oxidation using cyclic voltammetry (CV) gave a 1.9-fold increase toward the oxidation current of the bare GCE, with a peak potential at +0.79 V (vs. Ag/AgCl). The designed sensor was shown to be selective in the detection of methadone in human blood samples. The linear range for methadone was 1.0–200.0  $\mu\text{M}$ , with an LOD of 0.18  $\mu\text{M}$ . The authors conclude that this hybrid nanocomposite electrochemical sensor is suitable for clinical and forensic applications [82].

Habibi et al. [83] designed a sensitive electrochemical sensor for the simultaneous detection of morphine and methadone, utilizing a glassy carbon electrode functionalized with CMK-5 mesoporous carbon (GCE/CMK-5). In this study, CMK-5 mesoporous carbon was used because of its high porosity and its enormous surface area. Furthermore, compared with carbon nanotubes, the electron transfer resistance of mesoporous carbon was lower. The authors used chemical and thermal treatment methods to synthesize CMK-5 mesoporous carbon in an Al SBA-15 rigid template. Subsequently, the synthesized CMK-5 nanostructures were subjected to characterization and morphological studies. The acquired CMK-5 nanostructures were then used to modify the GCE surface (GCE/CMK-5).



The electrochemical features of the CMK-5 surface and the GCE/CMK-5 sensors were assessed using EIS and CV. These examinations demonstrated the electrocatalytic activity of CMK-5 nanostructures to oxidize morphine and methadone. Moreover, the data of all these characterization studies indicated that CMK-5 mesoporous carbon could absorb both morphine and methadone in high amounts in its nanostructure. Quantitative multivariable analysis of the analytes using the GCE/CMK-5 sensor was performed using fast Fourier transform square-wave voltammetry (FFT-SWV) combined with the partial least-squares (PLS) method. The fabricated sensor showed to have good sensitivity, with an LOD of  $0.027\text{ }\mu\text{M}$  for morphine and  $0.029\text{ }\mu\text{M}$  for methadone. The linear range was reported for both analytes between  $0.1$  to  $4\text{ }\mu\text{M}$ . The authors also used the GCE/CMK-5 sensor to detect morphine and methadone in urine samples. They found the sensor to have high recoveries for the analytes, indicating its excellent functionality in complex sample matrices [83].

In another study, Abraham et al. [84] capitalized on the structural features (hydrophilic head and lipophilic tail) of the surfactant poly(cetyltrimethylammoniumbromide)-polyCTAB to enhance the conductivity of graphene oxide (GO) and then used this composite to modify a glassy carbon electrode (GCE). This constructed sensor, poly(CTAB)/GO/GCE, was used to determine morphine in real samples. Cyclic voltammetry revealed that when compared to the unmodified electrode, this novel sensor, with its larger surface area, enabled an increased electrochemical response of morphine. The analytical performance of the poly(CTAB)/GO/GCE sensor was assessed from pulse differential voltammetry studies, using optimum experimental conditions to electrochemically determine morphine. Linear relationships between the anodic peak currents and morphine concentration were observed in the  $50\text{ nM}$ – $60\text{ }\mu\text{M}$  concentration range, with an LOD of  $0.36\text{ }\mu\text{M}$ . In addition, this electrode showed good repeatability and stability in response to trace amounts of morphine. The interference effects of biological molecules, such as ascorbic and uric acid, on the sensor's ability to detect morphine revealed that the poly(CTAB)/GO/GCE electrode could still effectively detect morphine in the presence of these interferents. Lastly, the modified electrode was successfully used to detect morphine in human blood serum and urine samples with satisfactory recoveries [84].

Beitollahi and Nejad [85] developed a novel, graphite screen-printed electrode (SPE) modified with graphene oxide (GO)  $\text{Fe}_3\text{O}_4$ @ $\text{SiO}_2$  nanocomposites. This GO/ $\text{Fe}_3\text{O}_4$ @ $\text{SiO}_2$  nanocomposite was used to determine morphine in biological samples via CV, DPV, and chronoamperometry techniques. The modified electrode produced a higher anodic peak current for the oxidation of morphine, signaling improved electron transfer when compared to the unmodified SPE. Moreover, the DPV linear response for the determination of morphine using the GO/ $\text{Fe}_3\text{O}_4$ @ $\text{SiO}_2$  sensor was  $1.0$ – $100\text{ }\mu\text{M}$ , with a high correlation ( $0.9986$ ) and a detection limit of  $7.5 \times 10^{-7}\text{ M}$ . The analytical performance of the prepared sensor was assessed for morphine determination in morphine ampules and in urine-spiked samples, with good recovery and reproducibility. In addition, the sensor enabled sensing of morphine in the presence of frequently encountered interfering substances found with morphine in pharmaceuticals and or biological samples. Ascorbic acid in equimolar ratios was the only tested substance that showed interference. In these instances, the enzyme ascorbic oxidase would be introduced to selectively oxidize ascorbic acid and minimize this issue [85].

Beitollahi and coworkers [86] went on to synthesize a graphene– $\text{Co}_3\text{O}_4$  nanocomposite, which was used to coat the surface of a screen-printed graphite electrode (SPGE) for the creation of a modified graphene– $\text{Co}_3\text{O}_4$ /SPGE sensor. This sensor was used to determine morphine combined with diclofenac in biological samples and pharmaceutical preparations. Cyclic voltammetry revealed a higher electrochemically active surface area on the graphene– $\text{Co}_3\text{O}_4$ /SPGE sensor when compared to unmodified electrodes. DPV at optimum experimental conditions for analysis of morphine solutions using the graphene– $\text{Co}_3\text{O}_4$ /SPGE sensor demonstrated the linearity of peak currents with a wide range of morphine concentrations ( $0.02$ – $575.0\text{ }\mu\text{M}$ ), a sensitivity of  $0.4\text{ }\mu\text{M}$ , and an LOD of  $0.007\text{ }\mu\text{M}$ . To assess the ability of this modified sensor in co-detecting morphine and diclofenac, the

electrochemical activities of solutions containing varying concentrations of both analytes were analyzed under optimum experimental conditions. DPV curves revealed two distinct, non-interfering morphine and diclofenac peaks; the peak currents of both morphine and diclofenac oxidation were linear in the concentration ranges for morphine (2.5–550  $\mu\text{M}$ ) and diclofenac (2.5–700  $\mu\text{M}$ ), respectively. The selectivity of the graphene- $\text{Co}_3\text{O}_4$ /SPGE sensor for determining morphine in the presence of interferents was assessed. Interfering components, such as inorganic ions, essential and non-essential amino acids, acetaminophen, sugars, methyl dopa, ascorbic acid (after removal with ascorbic oxidase), etc., did not interfere with the sensor's ability to detect morphine. Finally, the practical application of this sensor was evaluated for the determination of morphine and diclofenac in morphine tablets, diclofenac tablets, and urine specimens using DPV with standard addition methods. Recovery results were satisfactory [86].

Mohammadi and colleagues [87] developed a sensitive, fast response, field-use appropriate, low-priced, electrochemical sensor by modifying a screen-printed electrode (SPE) with  $\text{La}^{3+}$ /ZnO nanoflowers ( $\text{La}^{3+}$ /ZnO/NFs) and multiwalled carbon nanotubes (MWCNTs). The sensor's design capitalized on the catalytic nature of the nanoflowers as well as the electronic nature of the MWCNTs. This refashioned sensor ( $\text{La}^{3+}$ /ZnO/NFs-MWCNTs/SPE) was used to electrochemically determine tramadol. Differential pulse voltammetry, chronoamperometry, and cyclic voltammetry methods revealed the sensor's ability to produce improved tramadol oxidation peak signals compared to the bare electrode. Differential pulse voltammetry experiments at optimal conditions showed a linear relationship between tramadol concentration and peak current (a linearity in the tramadol concentration range of 0.5–800  $\mu\text{M}$ , and an estimated LOD of 0.08  $\mu\text{M}$ ). Additionally, the analytical performance of the  $\text{La}^{3+}$ /ZnO/NFs-MWCNTs/SPE sensor for detecting tramadol in real samples was assessed in its capacity to determine tramadol in urine and tramadol tablets. The standard addition methods gave good recovery and reproducibility [87].

Atta et al. [88] evaluated the performance of composite sensors that utilized three different metal complexes for the electrocatalytic determination of tramadol. The modified platinum (Pt) electrode was constructed by applying two layers of the conducting polymer poly(3,4-ethylenedioxythiophene) (PEDOT) onto the surface of the electrode with a layer of one of three metallocenes/metal mediators, immobilized between the polymer layers. The metallocene or charge transfer mediators used were ferrocene carboxylic acid (FC1), ferrocene (F1), and cobaltocene (CC); thus, the order of the components in one of their modified electrodes would be Pt/PEDOT/FC1/PEDOT. The surface of the constructed sensor was further modified with successive additions of sodium dodecyl sulfate (SDS), which improved the aggregation of the target analyte at the electrode surface. The metal mediators assisted in increasing current response and charge transfer rate at the electrode surface during electrochemical oxidation and reduction. According to CV measurements, the Pt/PEDOT/FC1/PEDOT...SDS sensor produced a sharper and well-resolved tramadol peak for tramadol, a fast electron transfer rate, and the highest overall catalytic effect when compared to the other combinations of metallocene-modified electrodes, as well as the bare platinum electrode. Incidentally, the FC1-modified sensor gave no tramadol signal in the absence of SDS, indicating the role of the surfactant in pre-concentrating the tramadol analyte and aiding its accumulation at the electrode. Moreover, the structural features of the ferrocene carboxylic acid ( $\pi$  bonds and carboxyl functional groups) mediator resulted in increased electronic conduction of the PEDOT polymer. The practical performance of the Pt/PEDOT/FC1/PEDOT...SDS sensor was evaluated to analyze tramadol in real human urine and serum samples. Calibration curves showed linearity between the anodic peak current and dilute tramadol concentration in the ranges of 7–300  $\mu\text{M}$  and 5–280  $\mu\text{M}$ , and extremely low LODs of 18.6 nM and 16 nM for urine and serum samples, respectively. Furthermore, the sensor was shown to be selective in the simultaneous analysis of tramadol in the presence of its interfering substances. The real sample tests confirmed the ability of the Pt/PEDOT/FC1/PEDOT...SDS sensor to detect tramadol [88].

A one-step laser-carbonized polyimide electrode (LCE), fabricated for the rapid detection of fentanyl in remote, field, and non-ideal environments, was reported by Mishra and coworkers [89]. They reported their electrode as the first example of a disposable, strip-based sensor that could detect fentanyl concentrations in human blood serum. This electrochemical sensor was fabricated from commercially available polyimide sheets; a CO<sub>2</sub> laser machine was used to carbonize the polyimide sheets, resulting in a highly porous carbon structure. The final laser-carbonized pattern included three electrodes (working, reference, and auxiliary) with a sensing area of 0.36 cm<sup>2</sup> and a total length of 3.5 cm. A conductive silver/silver chloride paste was applied to one electrode for use as the Ag/AgCl reference. All electrical interconnections were passivated. The mechanism of fentanyl detection on the LCE was via square-wave voltammetry (SWV) techniques coupled with the specific electrochemical signatures of fentanyl. Briefly, the fentanyl detection mechanism involves an observed SWV electrochemical oxidation response ( $E^\circ \sim 0.56$  V) of fentanyl on the LCE surface when fentanyl's pyridine ring undergoes oxidative cleavage at the second position. A portable potentiostat was used for electrochemical detection, with the data being wirelessly transmitted to a smartphone. This mode of detection/data transmission is desirable since the device could find application in detecting fentanyl in the non-ideal locales of fentanyl abusers. The sensing performance of the LCE was assessed in increasing concentrations of fentanyl analyte in phosphate buffer solution (PBS). A linear current trend against fentanyl concentration, with a regression coefficient ( $R^2$ ) of 0.9960 from five trials and an RSD of less than 5%, was observed. Additionally, the sensor's linear range, sensitivity, and limit of detection (LOD) were found to be 20–200  $\mu$ M, 0.025  $\mu$ A  $\cdot$   $\mu$ M<sup>-1</sup>  $\cdot$  cm<sup>-2</sup>, and 1  $\mu$ M, respectively. The stability of the electrode from the SWV response over 30 days was calculated to be 93.65%. Furthermore, the selectivity of the sensor to fentanyl in the presence of interferents and cutting agents was assessed by recording the SWV of the electrode in the presence of theophylline, fentanyl, acetaminophen, ascorbic acid, uric acid, and caffeine. The oxidation peak corresponding to fentanyl was observed to be strong and not diminished, with no visual current drifts in the presence of the other interference analytes, thus proving this strip-based carbonized sensor to be effective for fentanyl detection with high selectivity. Finally, to illustrate the practical application of the LCE, diluted real human serum samples were spiked with fentanyl (40–200  $\mu$ M) and analyzed with electrochemical SWV techniques. Here, the sensor's performance was comparable to its detection of fentanyl in PBS solutions. Overall, this sensor is a promising, cost-effective, and easy-to-use device that can be used by first responders, drug enforcement agents, and other agencies that work to detect the over-usage of fentanyl [89].

Li and Wang [90] developed a stable, sensitive, and selective electrochemical sensor, fabricated from CoO nanoparticles functionalized with carbon nanotubes (CoO@f-CNTs) to detect tramadol in athletes' urine for application in doping investigations. The electrodeposition method was used to prepare the modified glass carbon electrode (GCE) CoO@f-CNTs nanocomposite. The preparation of the sensor was confirmed with SEM and X-ray diffraction (XRD) characterization. The performance and utility of the CoO@f-CNTs/GCE were determined from its identification of tramadol in urine samples from athlete volunteers. For comparison, tramadol ELISA kits were also used to analyze the urine samples before and after tramadol addition. The standard addition method was used for all analytical experiments. The RSD and recovery values from amperometric experiments at 0.62 V and those of the ELISA kits showed good agreement (3.33% and 4.18%; 98.50% and 100.50%, respectively). Furthermore, amperometry data at a potential of 0.62 V for the CoO@f-CNTs/GCE in the presence of increasing concentrations of tramadol (1–300 mM) resulted in a linear relationship between the electrocatalytic peak current and tramadol concentration. The correlation coefficient ( $R^2 = 0.99980$ ), sensitivity (0.4491  $\mu$ A/ $\mu$ M), and detection limit (6 nM;  $S/N = 3$ ) were, thus, determined. Based on the figures of merit obtained from the performance of their sensor, the researchers have illustrated a promising approach for practical application of urine sample analysis [91].

### 3.2. Electrochemical Sensors: Pharmaceutical Applications

Interest has grown toward developing electrochemical nanosensors for pharmaceutical applications because of their high selectivity, relatively low cost, and ease of use. Pholcodine (3-(2-morpholinoethyl)morphine), a derivative of morphine, is prescribed in some countries as an antitussive and is classified as an opioid cough suppressant [102]. Abd-Rabboh [91] and coworkers developed and presented a cost-effective, compact, portable, potentiometric monitoring device for analyzing pholcodine in dosage forms and in plasma. The sensors were designed from screen-printed electrodes modified with multiwalled carbon nanotubes (MWCNTs). Next, unique pholcodine molecular imprinted polymers (MIPs) were prepared, characterized, and used as the sensing receptors in these potentiometric sensing devices. The potentiometric analytical device integrated the pholcodine–MIP ion selective electrode with a Ag/AgCl reference electrode and a polyvinyl butyral (PVB) reference membrane. The potentiometric performance characteristics of the sensor were evaluated and tested in pholcodine solutions at pH 4, and the concentration ranged from  $1.0 \times 10^{-2}$ – $1.0 \times 10^{-8}$  M. The calibration curve gave a Nernst response with a slope of  $31.6 \pm 0.5$  mV/decade ( $n = 5$ ,  $R^2 = 0.9980$ ) in the range of  $5.5 \times 10^{-6}$  to  $1.0 \times 10^{-2}$  M, and a detection limit of  $2.5 \times 10^{-7}$  M. Furthermore, it was concluded that the observed responses of the sensor were mainly due to a specific interaction between pholcodine and the binding MIP particles, since a non-imprinted polymer-based sensor, when tested under the same conditions, gave a sub-Nernst response. In addition, the fabricated sensor showed potential stability at a pH range of 4–6. The device was also successfully used to determine pholcodine in different pharmaceutical formulations containing pholcodine (syrups and suspensions from two Egyptian pharmaceutical companies, both labeled 4 mg/mL). The data obtained from the tested pharmaceutical formulations were in good agreement with a suggested reference method, thus confirming the validity of using the presented sensor for routine assessment of pholcodine [91].

Although carbon-based electrodes are commonly used, they present disadvantages because the electron transfer is slow. However, these issues can be alleviated with modifications to the electrode surface. In this vein, Najafi et al. [92] modified glassy carbon electrodes (GCE) with multiwalled carbon nanotubes (MWCNTs) and analyzed the electrochemical behavior in the determination of fentanyl. The electrode was prepared using an abrasion immobilization method that involved rubbing the cleaned glass surface of the electrode with filter paper containing MWCNTs. The distribution of the carbon nanotubes on the surface of the electrode was confirmed by scanning electron microscopy. The electrodes with and without MWCNTs were then used to determine fentanyl using differential pulse adsorptive stripping voltammetry. A large enhancement of the fentanyl oxidation peak current (against a Ag/AgCl reference electrode) illustrated a significant catalytic ability of MWCNTs toward fentanyl oxidation. The linear range and detection limit were also determined via this method and revealed linear oxidation peak currents for fentanyl in the concentration range of  $5 \times 10^{-7}$  to  $1 \times 10^{-4}$  M. The LOD was estimated to be  $1 \times 10^{-7}$  M, using  $3s_b/m$  rules (where  $m$  is the slope;  $s_b$  is the standard deviation of the blank solution;  $n = 6$ ). Moreover, six independently prepared MWCNT-GC-modified electrodes gave good reproducibility and repeatability when used to measure the peak currents of  $1 \times 10^{-4}$  M fentanyl. To evaluate the analytical application of the presented sensor, the DPV method was used to measure fentanyl at the surface of MWCNT-GCEs in urine and protein-free, spiked human serum (three concentrations of fentanyl) samples. The average recovery of fentanyl added to the urine and plasma samples was 101% and 103%, respectively. In other tests, the response current of the sensor showed little deviation when testing for fentanyl in the presence of uric acid, ascorbic acid, and interfering ions ( $\text{Cl}^-$ ,  $\text{CO}_3^{2-}$ ,  $\text{PO}_4^{3-}$ ,  $\text{Na}^+$ ), illustrating the excellent selectivity of this modified electrode to fentanyl. In addition, the authors proposed and illustrated a mechanism of fentanyl oxidation that included the loss of an electron from the nitrogen on the fentanyl's piperidine ring, forming a carbocation radical, which loses a proton and an electron to form a quaternary Schiff base. The Schiff base then quickly oxidizes to a secondary amine [92].



The unique properties of nanoparticles have attracted attention for their potential use in various analytical investigations. Hojjati-Najafabadi et al. [93] presented a new analytical sensor for tramadol and serum tests. This sensor was fabricated by modifying a paste electrode with gold nanoparticles (Au/NPs) and 1-butyl-3-methylimidazolium tetrachloroborate (BMTCB). The AuNPs were biosynthesized from *Mentha aquatic* extract and then used as a conductive mediator along with the ionic liquid BMTCB to modify the tramadol electrochemical sensor. The Au/NPs/BMTCB/CPE showed high catalytic activity for determining tramadol in an aqueous solution. The modified electrode showed superiority compared to the unmodified electrode: the Au/NPs/BMTCB/CPE increased the tramadol oxidation current by a factor of 8.8 and lowered the drug oxidation potential by 20 mV. According to square-wave voltammetry measurements, the Au/NPs/BMTCB/CPE produced a linear dynamic range of 0.01–400  $\mu\text{M}$  for the determination of tramadol. The detection limit of 6.0 nM ( $\text{LOD} = 3\text{sb}/m$ ) for tramadol was obtained. In addition, this sensor enabled the sensing of tramadol in the presence of interfering components, such as ions ( $\text{Ca}^{2+}$ ,  $\text{Na}^{+}$ ,  $\text{Cl}^{-}$ ), biological interferents (alanine isoleucine, phenylalanine), and hormones (dopamine and epinephrine). Finally, the analytical performance of the developed sensor was assessed to detect tramadol in spiked injection and serum samples with an acceptable output [93].

While tramadol can be administered on its own as an analgesic, it also finds combination use with acetaminophen for pain management. Thus, the determination of the concentrations of these drugs individually or mixed is vital to researchers who want to limit overdose and any toxic effects that they may have. The traditional methods to determine the combinations of these two drugs have the disadvantages of being costly and complex procedures requiring large instrumentation. Scientists are interested in developing simple, sensitive, and selective analytical methods for detecting these analytes. Garkani Nejad et al. [94] took advantage of the properties of nanomaterials, such as dendrimers (e.g., poly(amido)amine-PAMAM) and molecular organic frameworks (MOFs, e.g., UiO-66- $\text{NH}_2$ ), and developed a novel electrochemical sensor for the detection of tramadol in the presence of acetaminophen. They reported that the MOFs enhance the conductivity of the dendrimer nanocomposite and, together, enhance the electrochemical active area and sensitivity of a glass carbon electrode (GCE). In this respect, a UiO-66- $\text{NH}_2$ MOF/G3-PAMAM nanocomposite was fabricated and anchored on a GCE to obtain an electrocatalytic and voltametric tramadol sensor (UiO-66- $\text{NH}_2$ MOF/G3-PAMAM/GCE). This sensor demonstrated a high degree of catalysis toward tramadol in acetaminophen co-existence. From differential pulse voltammetry quantitation results, the sensor demonstrated similar sensitivity (0.088  $\mu\text{M}/\mu\text{A}$ ) in the presence and absence of acetaminophen. An LOD of 0.2  $\mu\text{M}$  and a wide linear range (0.5–500  $\mu\text{M}$ ) for tramadol detection were reported. The sensor showed good selectivity for tramadol in the presence of potential interfering components, including a 1000-fold excess of  $\text{Na}^{+}$ ,  $\text{Mg}^{2+}$ ,  $\text{Ca}^{2+}$ ,  $\text{NH}_4^{+}$ ,  $\text{SO}_4^{2-}$ , and a 500-fold excess of starch, fructose, glucose, lactose, sucrose, L-lysine, L-serine, 100-fold excess dopamine, uric acid, epinephrine, and norepinephrine. However, ascorbic acid gave significant interference in equal concentrations of tramadol. The application of the sensor for the analysis of pharmaceutical formulations gave reasonable recoveries [94].

In another study, Khairy and Banks [95] modified screen-printed electrodes (SPEs) with nanostructured ytterbium oxide ( $\text{Yb}_2\text{O}_3$ ) nanoplates for the electrochemical analysis of acetaminophen and tramadol. Cyclic voltammetry revealed the higher electrocatalytic activity of the  $\text{Yb}_2\text{O}_3$  nanoplate-modified SPEs ( $\text{Yb}_2\text{O}_3$ -SPEs) compared to graphite SPEs. Additionally, electrochemical determination of acetaminophen and tramadol individually and as mixtures was achieved with cyclic voltammetry and differential pulse voltammetry using this modified sensor. Tramadol and acetaminophen gave distinct and non-overlapping voltametric signals at +0.3 V and +0.67 V against the Ag/AgCl reference electrode at pH = 9. Finally, the proposed sensor was used for the determination of spiked human fluids and pharmaceutical dosage forms at wide linear ranges of 0.25–654  $\mu\text{mol}\cdot\text{L}^{-1}$  and 0.50–115  $\mu\text{mol}\cdot\text{L}^{-1}$  tramadol and acetaminophen, with detection limits of 55 and



87 nmol·L<sup>-1</sup>, respectively. The development of portable, sensitive, and selective devices, such as these, is significant to diagnostic and analytical research [95].

Kozak et al. [96] proposed an electrochemically activated screen-printed carbon electrode modified with an anionic surfactant, sodium dodecyl sulfate (aSPCE/SDS), for the simultaneous determination of the pharmaceuticals paracetamol (PA), diclofenac (DF), and tramadol (TR). Their study was developed from previous investigations, which showed surfactants to be advantageous in increasing the buildup of some electroactive molecules on the electrode surface, leading to increased signal and selectivity of the analytical method. Voltammograms showed the superior performance of the modified sensor when compared to the bare (unmodified) electrode. The aSPCE/SDS electrode was used to determine PA, DF, and TR individually and simultaneously, under optimized conditions with the following results: the limits of detection (LOD) and limits of quantification (LOQ) for simultaneous analyses were 14.87, 0.21, and 1.71 nmol·L<sup>-1</sup>, and 49.46, 0.69 and 5.69 nmol·L<sup>-1</sup>, respectively. Good linear responses were obtained in the concentration ranges of  $5.0 \times 10^{-8}$ – $2.0 \times 10^{-5}$  mol·L<sup>-1</sup> for PA,  $1.0 \times 10^{-9}$ – $2.0 \times 10^{-7}$  mol·L<sup>-1</sup> for DF,  $1.0 \times 10^{-8}$ – $2.0 \times 10^{-7}$  mol·L<sup>-1</sup>, and  $2.0 \times 10^{-7}$ – $2.0 \times 10^{-6}$  mol·L<sup>-1</sup> for TR. The analytical usefulness of the modified electrode was assessed in its simultaneous determination of PA, DF, and TR in spiked human serum, river samples, as well as in pharmaceutical preparations, with good recoveries. The results verified the prospects of this sensor and associated procedures as a cheap and simple alternative to other methods, with the added advantage of portability, making it suitable for quick fieldwork [96].

Keskin et al. [97] investigated the electrochemical properties of unmodified boron-doped diamond (BDD) electrodes, in the presence of anionic surfactant sodium dodecyl sulfate (SDS), for the determination of tramadol. The unmodified BDD already possesses the characteristics of a reputable quality electrode in its ability to facilitate the analysis of substances that the traditional solid electrodes would not be able to determine. The unmodified electrode becomes even more sensitive in the presence of surfactants, which serve to increase the adsorption of the electroactive analyte onto the electrode surface. This study developed an SWV method for using the BDD to quantify tramadol. Under optimized experimental conditions and in a buffer solution containing SDS at 1.5 V, it was shown that an excellent correlation existed between oxidation peak current and tramadol concentration in the range 0.25–50 µg·mL<sup>-1</sup>, with a detection limit of 0.072 µg·mL<sup>-1</sup>. The BDD electrode was able to sense tramadol in the presence of most interfering compounds typically found in pharmaceutical formulations and biological samples (inorganic ions and carbohydrates in biological samples; cornstarch, microcrystalline cellulose, and magnesium in pharmaceutical samples) without any effect on the oxidation peak signal of tramadol. Also, the oxidation peak current of tramadol was unaffected by the individual peak currents of ascorbic acid, dopamine, and uric acid solutions. The results here indicate the potential use of the electrode in real samples. The analytical performance of this BDD was illustrated in its successful determination of tramadol in spiked human and pharmaceutical samples, with appreciable recoveries [97].

### 3.3. Electrochemical Sensors: Clinical Applications

Joshi and coworkers [78] designed a novel electrochemical microneedle sensor array platform using 3D printing to detect fentanyl in biofluids. The working, counter, and reference electrodes were integrated into the hollow polymeric microneedle structures. The working electrode was composed of graphene ink that was modified with an ionic liquid (4-(3-butyl-1-imidazolium)-1-butan-1-sulfonate)). Platinum was used as the counter electrode, and a silver wire was employed for the reference electrode. During this electrochemical detection, fentanyl was directly oxidized (oxidation peak of +0.55 V) using SWV. Experiments to determine the analytical functioning of the sensors were conducted with buffer solutions containing fentanyl. The linear range was reported to be 0–160 µM, and the LOD was 27.8 µM. The microneedle sensor was capable of detecting fentanyl in serum samples that were diluted. Moreover, the sensor device was highly selective and

sensitive ( $0.069 \mu\text{A}/\mu\text{M}$ ) toward detecting fentanyl in these diluted serum samples. The reproducibility was also shown to be good. Additionally, this sensor could sense fentanyl in the presence of its interferents (i.e., uric acid, caffeine, ascorbic acid, and acetaminophen) and, therefore, was found to be selective. The authors concluded that this microneedle sensor is a promising point-of-need method for detecting fentanyl in the field (e.g., in clinics and emergency rooms) [78].

Thomas et al. [103] investigated, in an animal study with rats, the correlation between oxygen alterations in the brain and periphery due to physiological stimuli, heroin, and cocaine treatment using two commercial electrochemical sensor recordings, which were joined with high-speed amperometry. Commercial pinnacle oxygen sensors comprise a disc electrode with a PT-Ir wire of  $180 \mu\text{m}$  containing an integrated Ag/AgCl reference electrode. The electrode's sensing area ( $0.025 \text{ mm}^2$ ) is on its tip. This oxygen sensor functions at a constant potential of  $-0.6 \text{ V}$  against the reference electrode. During in vivo studies, the amount of reduced dissolved oxygen on the sensor generates a current that can be measured by a potentiostat [98]. Pinnacle oxygen sensors were implanted in the rat brains' nucleus accumbens (NAc) and subcutaneous (SC) areas. The animals were then subjected to various gentle physiological activations and treatment with cocaine and heroin through intravenous injection (IV). The authors found that the produced physiological stimuli and cocaine increased the oxygen levels of NAc while decreasing the oxygen amount in the SC area. Heroin was found to have biphasic down-up oxygen variations in the brain, related to a monophasic oxygen reduction in the SC area. The linear range of the oxygen sensors was  $0\text{--}20 \mu\text{M}$ , and the sensitivity was between  $0.63$  and  $1.08 \text{ nA}/\mu\text{M}$ . The oxygen sensors were also found to be selective with respect to other electroactive compounds (i.e., dopamine and ascorbate) [103].

### 3.4. Electrochemical Sensors: Forensic Applications

Mohammadi et al. [99] fabricated MoWS<sub>2</sub> nanopetals to modify carbon screen-printed electrodes (CSPEs), MoWS<sub>2</sub>/CSPE, for the electrochemical detection of morphine and tramadol. The nanopetals were generated by synthesizing MoWS<sub>2</sub> nanocomposite using a one-pot hydrothermal method. Following the synthesis of the MoWS<sub>2</sub> nanocomposite, its surface morphology and elemental composition were studied using several characterization techniques. The obtained characterization data revealed the presence of closely and tidily packed nanopetals, which acted as active sites for the electrocatalytic oxidation of morphine and tramadol. The effectiveness of the generated MoWS<sub>2</sub>/CSPEs on the oxidation peak current and the concentration of the analytes was studied using differential pulse voltammetry. The investigators noticed a significant increase in the oxidation peak current (a 2.6-fold rise related to the bare CSPE) when the modified CSPE electrode was used. The oxidation potentials at the surface of the modified electrode for morphine and tramadol were  $275 \text{ mV}$  and  $920 \text{ mV}$ , respectively. The linear range for morphine was between  $4.8 \times 10^{-8} \text{ M}$  and  $5.05 \times 10^{-4} \text{ M}$ , and the LOD was  $1.44 \times 10^{-8} \text{ M}$ . In this study, the selectivity of the MoWS<sub>2</sub>/CSPE sensor was assessed by detecting the analytes in the presence of their interfering substances. Only ascorbic acid was found to interfere with the oxidation potential of morphine. However, the authors suggest using the ascorbic oxidase enzyme to decrease the interference. The researchers applied the newly developed MoWS<sub>2</sub>/CSPE to detect morphine and tramadol in clinical samples. This novel nanosensor is a fast, inexpensive, and simple method for the selective quantification of these analytes [99].

Razavi et al. [100] developed an electrochemical nanosensor to examine tramadol utilizing a modified carbon paste electrode (CPE) with CuO nanostructures. Copper(II)oxide nanoparticles (CuO NPs) were synthesized through co-precipitation using a water-based extract of the medicinal plant *Origanum majorana*, which functioned as a reducer and stabilizer. The generated CuO nanostructures functioned as the electrocatalyst during tramadol detection. Characterization studies by XRD, SEM, and FTIR revealed the presence of CuO NPs and multiwalled carbon nanotubes (MWCNTs). These nanostructures were then used to modify the carbon paste working electrode. This resulted in a CuONPs/MWCNT/CPE

sensor to analyze tramadol through the SWV technique. The nanosensor proved highly selective for the electrocatalytic oxidation of tramadol, with potentials of 230 mV and 700 mV. The linear range was 0.05–200  $\mu\text{M}$ , and the LOD was 0.025  $\mu\text{M}$ . Moreover, the CuONPs/MWCNT/CPE sensor was considerably sensitive toward detecting tramadol (0.0773  $\mu\text{A}/\mu\text{M}$ ). The authors used this modified electrode to detect tramadol in drug and biological samples [100].

Borgul and coworkers [101] used an electrified liquid–liquid interface (eLLI) miniaturization method to detect the interfacial behavior of heroin by itself and in the presence of two of its cutting agents. They employed an electrified water–1,2-dichloroethane interface using a 3D printed support containing a space for the Ag/AgCl electrode (which hosted 20  $\mu\text{L}$  of the aqueous phase and heroin) and a fused silica microcapillary in a micropipette tip (containing 5  $\mu\text{L}$  of the organic phase). The authors were able to examine the interfacial transfer of protonated heroin in the presence of a significantly high amount of caffeine and paracetamol. The linear range was 0–50  $\mu\text{M}$ , and the LOD was 1.3  $\mu\text{M}$ . The reproducibility of the developed eLLI sensing platform was good at extremely low sample volumes [101].

Electrochemical sensors have become crucial analytical techniques for opioid analyses with desirable advantages. Nevertheless, these sensors require accurate calibration to minimize interference from complicated sample matrices, and, sometimes, the potential can drift after a while. Moreover, the electrodes must often be modified to ensure specificity towards specific analytes [104].

#### 4. Main Optical Spectroscopy Sensors Detection Methods

This review section discusses and highlights the advances in the use of optical sensors for opioid analysis and pharmaceutical, clinical, and forensics applications. Figure 8 presents the primary optical sensors and their applications for biological sample analysis and clinical and forensic applications highlighted in this review section.

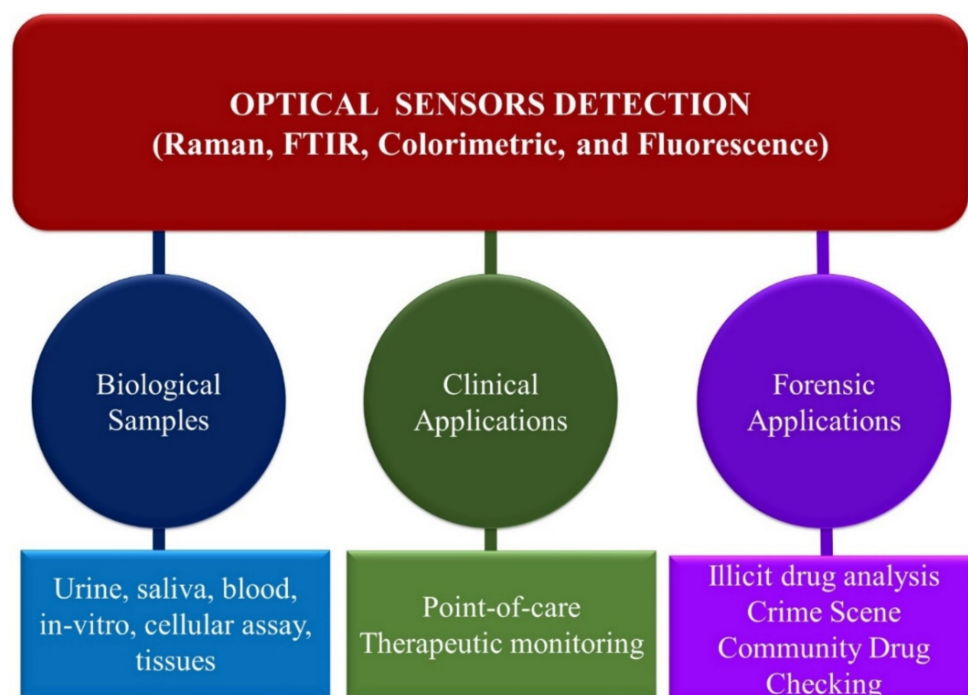


**Figure 8.** Optical sensors for opioid detection in biological samples and clinical and forensic applications.

##### 4.1. FTIR Detection Methods

Fourier transform infrared (FTIR) spectroscopy is a vibrational technique in which the spectrum is generated from molecular vibration of incident photons on a molecule that changes in a dipole moment. The typical FTIR region of the spectrum has a wavenumber

from  $4000\text{ cm}^{-1}$  to  $400\text{ cm}^{-1}$ . In IR measurements, an interferometer is used to improve the signal-to-noise ratio, and Fourier transformation is performed to convert the identified signal into a spectrum. The detection principle in FTIR relies on the fingerprint wavelength spectra obtained from the interaction of light with an IR-active molecule. The IR spectrum is the characteristic fingerprint of a specific molecular structure, including the opioids covered in this review. The development of portable IR systems makes it convenient for the onsite screening of drugs, including opioids. FTIR has several advantages: it requires minimal sample preparation, exhibits sensitivity, and it is nondestructive and fast. The advances in FTIR with chemometric analysis enable simultaneous identification of multiple drug components. We note that IR has some disadvantages, such as a strong interference signal from moisture, and does not work for opaque samples.

The minimal or no sample preparation, small sample size, nondestructive nature, rapidity, and versatility of FTIR spectroscopy allow for the detection of opioids and illicit drugs in samples of varying matrices. The attractive properties of FTIR spectroscopy make it ideal for the rapid detection of opioids and illegal drugs at point-of-care drug-checking and community services drug analysis. McCrae et al. demonstrated the potential use of FTIR spectroscopy in combination with immunoassay strips for the detection of fentanyl at a point-of-care drug-checking in Canada [105]. The study analyzed 283 volunteer drug samples and analyzed fentanyl using FTIR spectroscopy. The drug samples were further sent for quantitative nuclear magnetic resonance (qNMR) analysis and immunoassay strip testing for laboratory confirmatory testing. A total of 173 out of 283 (or 61.1%) of the samples tested positive for fentanyl. qNMR detected fentanyl concentrations ranging from 1% to 91% by weight. However, FTIR could not detect fentanyl in 30/173 (or 17.3%) samples containing fentanyl concentrations  $\leq 10\%$ . In addition, the immunoassay strip testing failed to detect fentanyl in 4 out of 173 (or 2.3%) samples containing fentanyl concentrations  $\leq 5\%$ . In addition, the study reported the ability of FTIR spectroscopy to detect fentanyl in liquids, pebbles, powders, granules, and crystal samples, showing the versatility of FTIR spectroscopy for drug detection.

Nonetheless, the application of FTIR spectroscopy for opioids and fentanyl detection has some significant drawbacks. For instance, FTIR spectroscopy is applicable for determining opioid concentrations at a minor to major % weight concentration range but is less effective for fentanyl detection at lower (trace or ultra-trace) concentrations. This limitation is problematic for detecting synthetic opioid analogs, such as carfentanil, that have high potency and toxicity at relatively low concentrations [106,107]. Furthermore, the sample must be dried to prevent the moisture FTIR spectra from overlapping with the FTIR spectra analyte band. Combining FTIR spectroscopy and complementary analytical techniques, such as immunoassay strips, may address these challenges. Most street drugs contain diluents or adulterants, such as caffeine, phenacetin, sucrose, starch, and glucose additives, which could limit the use of FTIR spectroscopy for opioids or fentanyl drug detection. For instance, carbonyl (C=O) from caffeine overlaps with fentanyl drug C=O FTIR spectra band around  $1700\text{ cm}^{-1}$ . In addition, lab technicians' interpretations of FTIR spectral data may be subjective, leading to different outcomes, conclusions, and false negative rates [108]. This is a major FTIR spectroscopy flaw, raising doubts about the validity of FTIR spectroscopy for fentanyl community drug-checking sample analysis.

Combining chemometrics and multivariate analyses with Raman or FTIR spectroscopy may resolve these challenges. Accordingly, the combined use of FTIR and various multivariate analysis strategies, such as artificial neural networks (ANN), principal component analysis (PCA), principal component regression (PCR), linear discriminant analysis (LDA), hierarchical clustering analysis (HCA), K-nearest neighbors (k-NN), partial-least-square (PLS) regression, support vector machine (SVM), linear fitting analysis (LFA), and many more for the detection, profiling, classifications, and pattern recognition of illicit drugs with excellent accuracy and precision has been exploited and widely reported [109–112]. The FTIR fingerprint ( $1800\text{--}650\text{ cm}^{-1}$ ) region is of interest and is the most widely used region for illicit drug analysis.

For instance, Ti et al. [113] employed a combined use of FTIR spectroscopy and a neural network model for the detection and prediction of fentanyl in community drug samples in British Columbia, Canada, where the prevalence of opioid overdoses is rampant and is a public health safety challenge [113]. Approximately 5 mg of suspected drug samples were donated anonymously by drug users to a trained drug-checking technician at the harm reduction sites. The drug samples were analyzed on sites using FTIR spectroscopy and immunoassay strips. The results of the drug testing were provided to the donating drug users instantaneously. Table 2 shows the properties of the study sample, including the sample numbers, colors, textures, physical state, and fentanyl immunoassay strip results. According to the report, fentanyl, heroin, and methamphetamine are the most abundant active ingredients detected in the samples. Figure 9 shows typical FTIR spectra for an illicit opioid mixture containing fentanyl drug samples showing the characteristic FTIR profiles and peaks of fentanyl hydrochloride. Importantly, FTIR demonstrated the capability to detect fentanyl at  $\geq 5\%$  by weight concentration. The sample's FTIR absorbance spectra and the fentanyl concentration data set were divided into two sets (training and validation sets). The training data set was subjected to neural network modeling. The developed neural network model's capability for predicting fentanyl was validated by independent samples. Table 3 was the figure of merit of the validated study, showing the FI score, accuracy, precision, and recall of the neural network model and the drug-checking technician's results. The obtained neural network model F1 score of 96.4% and accuracy of 96.4% were better than the corresponding F1 score of 78.4% and accuracy of 82.4% obtained with the drug-check technician. An F1 score is defined as the neuron network model's accuracy that accounted for the precision, i.e., samples that were correctly identified as positives among test positives. Recall is defined as the ability to correctly identify positives among true positives. Notably, the neural network model demonstrated positive sample identification and detection of low fentanyl concentrations in the 0.0–4.6% weight range, which was not achievable by the drug-check technician.

**Table 2.** Characteristics of the study sample, stratified by fentanyl immunoassay strip results ( $n = 12,684$ ). Reprinted with permission from reference [113].

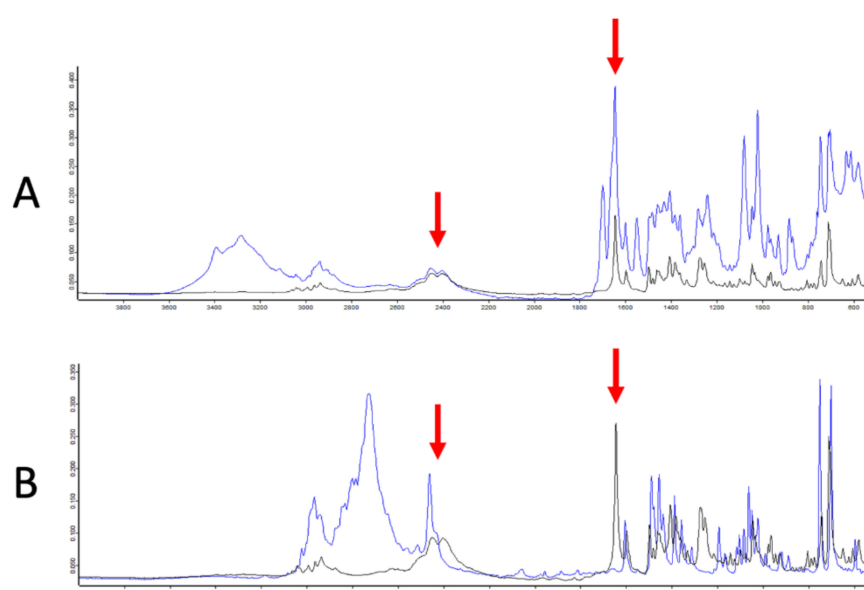
	Fentanyl Immunoassay Strip Result	
	Positive ( $n = 6099$ )	Negative ( $n = 6585$ )
Year		
2018	519 (8.5)	394 (6.0)
2019	2473 (40.5)	1718 (26.1)
2020	2723 (44.6)	3960 (60.1)
2021	384 (6.3)	513 (7.8)
Health Authority Region		
Fraser	533 (8.7)	194 (2.9)
Interior	359 (5.9)	445 (6.8)
Vancouver Coastal	5161 (84.6)	5931 (90.1)
Vancouver Island	46 (0.8)	15 (0.2)
Color		
Black	72 (1.2)	28 (0.4)
Blue	413 (6.8)	138 (2.1)
Brown	1173 (19.2)	769 (11.7)
Colorless	25 (0.4)	1009 (15.3)
Green	1229 (20.2)	143 (2.2)



Table 2. Cont.

Fentanyl Immunoassay Strip Result		
	Positive (n = 6099)	Negative (n = 6585)
Grey	292 (4.8)	195 (3.0)
Orange	217 (3.6)	116 (1.8)
Pink	368 (6.0)	175 (2.7)
Purple	1400 (23.0)	167 (2.5)
Red	140 (6.2)	34 (0.5)
White	380 (5.8)	3552 (53.9)
Yellow	351 (5.8)	227 (3.4)
Other	5 (0.1)	0 (0.0)
Not reported	34 (0.6)	32 (0.5)
Texture		
Chunk	1471 (24.1)	567 (8.6)
Crystal	48 (0.8)	2264 (34.4)
Flake	18 (0.3)	68 (1.0)
Granules	533 (8.7)	151 (2.3)
Liquid	20 (0.3)	110 (1.7)
Paste	145 (2.4)	49 (0.7)
Pebble	3010 (49.4)	271 (4.1)
Powder	704 (11.5)	2483 (37.7)
Pressed tablet	7 (0.1)	170 (2.6)
Residue	65 (1.1)	19 (0.3)
Tablet (pharmaceutical)	65 (0.4)	368 (5.6)
Other	3 (0.05)	28 (0.4)
Not reported	23 (0.9) 37	37 (0.6)

Note: Categories where cells were less than 5 were recategorized as ‘Other’.



**Figure 9.** Sample drug-checking FTIR spectra. Drug-checking samples (blue) are overlaid with the fentanyl hydrochloride spectrum (black). The drug sample in (A) is an illicit opioid mixture containing

fentanyl, caffeine, and mannitol. The drug sample in (B) is methamphetamine with no fentanyl present. The red arrows indicate characteristic peaks of fentanyl hydrochloride that are recognizable when present in drug mixtures. Reprinted with permission from reference [113].

**Table 3.** Comparing the performance of different methods for detecting fentanyl. Reprinted with permission from reference [113].

	F1 Score	Accuracy	Precision	Recall
Neural network model	96.4	96.4	95.7	97.1
% (95%CI)	(95.6–97.1)	(95.6–97.1)	(94.5–96.7)	(96.1–98.0)
Drug-checking technician	78.4	82.4	99.4	64.7
% (95%CI)	(76.4–80.3)	(80.9–83.9)	(98.8–99.9)	(62.1–67.3)
CI: confidence interval				

He et al. [114] also reported the combined use of attenuated total reflection (ATR) FTIR and a radial basis function neural network (RBFNN), multilayer perceptron neural network (MLPNN), and linear fitting analysis (LFA) for successful classification of mixtures of heroin and its additives (caffeine, phenacetin, sucrose, starch, and glucose) in various samples with a classification accuracy ranging between 66.67% for heroin hydrochloride and glucose mixtures and 100% for heroin hydrochloride and caffeine mixtures [114]. The samples contained 10–90% heroin chloride by mass, in which there were five characteristic absorption peaks of heroin chloride that were unaffected by the additives. These characteristic peaks are at 1759, 1735, 1369, 1179, 1157, and 911  $\text{cm}^{-1}$  [114]. A multivariate analysis was used for the accurate determination and classification of the different mixtures containing heroin hydrochloride. The ATR-FTIR and multivariate analysis methods provide a low-cost, effective, and nondestructive method for characterizing heroin samples for forensic applications [114].

According to the report, the use of ATR-FTIR spectroscopy and multivariate analysis allowed for small sample analysis and rapid classification of the heroin hydrochloride additive. However, the sample's classification accuracy was model-type-dependent, with better accuracy reported for quadratic polynomial function models than with a linear model. This study has a potential practical application for rapid forensic classification of heroin and other illicit drugs in the mixture of common caffeine, phenacetin, sucrose, starch, and glucose additives and adulterants. In a related study, Kranenburg et al. [115] demonstrated the combined use of a handheld near-infrared spectrometer and machine learning algorithms for rapid on-site drug detection [115]. Figure 10 shows the handheld NIR spectrometer using a smartphone and the scanning procedure for the SCiO NIR sensor with the glass sample vial placed directly on top of the light source and detection window.

The initial process in cocaine detection by NIR spectra machine learning involves employing NIR spectra preprocessing using various strategies, including k-NN sub-models, spectra derivatives, and PCA, to remove outliers and enhance the detection of substances and the model's predictive ability for cocaine. In general, better cocaine detection was recorded using a small window (740–1070 nm) of NIR spectra wavelength regions. Figure 11 shows the preprocessed NIR spectra wavelength region corresponding to cocaine detection.



**Figure 10.** Handheld NIR spectrometer using a smartphone and scanning procedure for a SCiO NIR sensor with the glass sample vial placed directly on top of the light source and detection window. Reprinted with permission from reference [115].

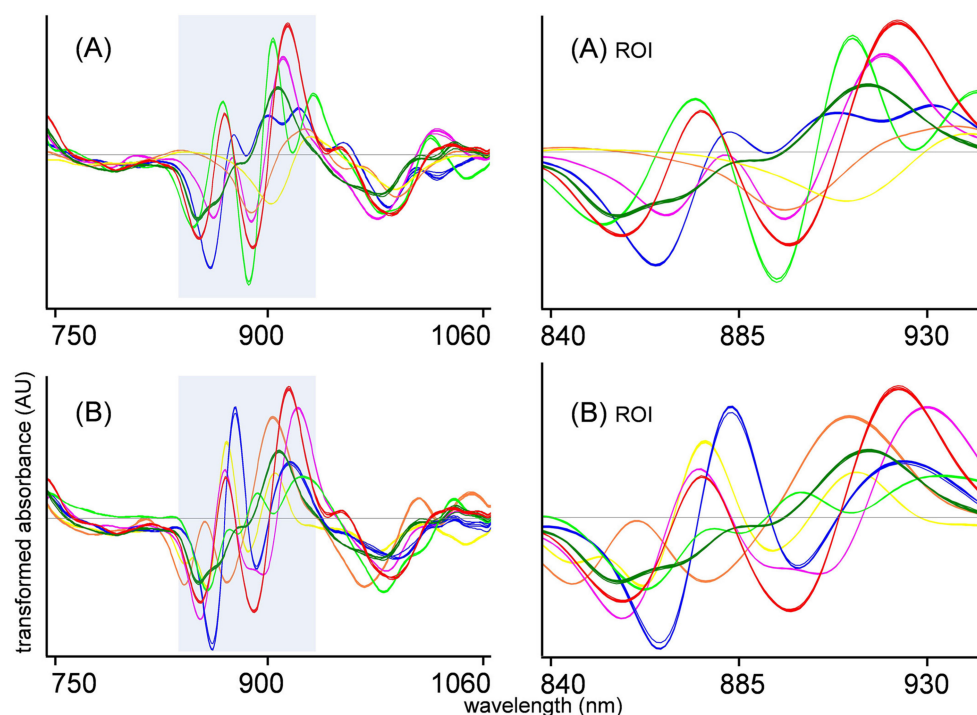


**Figure 11.** Near-infrared spectra after standard normal variate-first derivative preprocessing of cocaine HCl (dark green) and cocaine base (red) in comparison with (A) five common cutting agents, and (B) five common drugs, for both the full-wavelength range and the 839–939 nm region of interest (ROI). Cutting agents (A): levamisole (blue), phenacetin (light green), lidocaine (pink), inositol (yellow), and mannitol (orange). Drugs (B): amphetamine (blue); methylenedioxymethamphetamine (light green); ketamine (pink); acetaminophen (yellow); and caffeine (orange). Reprinted with permission from reference [115].

The developed models were used to predict the cocaine concentration of independent validation samples at known cocaine concentrations. Figure 12 shows the result of the validation study using the standard normal variate (SNV) first derivative full-spectrum preprocessing and SNV second derivative (740–1070 nm) region of interest preprocessing. Notably, the machine learning algorithms model yielded 97% true-positive and 98% true-negative results. In addition, the models demonstrated accurate detection of the cocaine types (base of HCl) in over 100 case-independent samples, demonstrating the

practical application of the protocols for on-scene drug detection. The use of chemometrics combined with various spectroscopy methods, including FTIR spectroscopy, has been extensively reviewed by Deconinck and coauthors [109]. Some of the drugs focused on in this review include cocaine, heroin, and MDMA (or ecstasy). Applying chemometrics to spectroscopy techniques has several advantages for analyzing and identifying various illicit drugs [109]. Although chemometrics require training and is often complex, it is useful for the determination of multiple drug compounds and identifying new illicit drugs that appear as outliers in the chemometric model [109]. In addition to its low cost and portability, this handheld NIR spectrometer is robust, easy to use, requires no extensive training, and requires limited sample preparation, allowing drug enforcement offices and community drug service technicians access to use it. In addition, easy access to Internet networks allows smartphones to rapidly disseminate and store NIR spectral data in a cloud environment via Bluetooth and WiFi/4G connections.

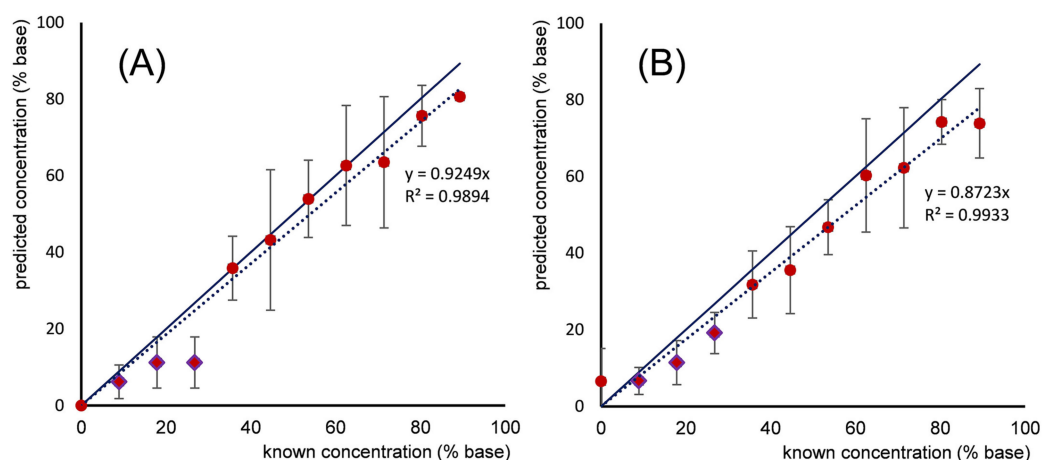


**Figure 12.** Predicted versus actual concentrations of external validation samples consisting of binary 0–100% cocaine HCl mixtures with levamisole, caffeine, and inositol, each scanned five-fold. (A), Results after standard normal variate (SNV) first derivative full-spectrum preprocessing; (B) after SNV second derivative region of interest preprocessing. Diamond-shaped datapoints originate from the ANN-treebag regression model; all other datapoints originate from the k-nearest neighbor model. Reprinted with permission from reference [109].

#### 4.2. Raman Detection Methods

Raman, like FTIR, is a vibrational technique that has proven useful for detecting various analytes, including opioids and their analogs. This technique has gained widespread use because it is rapid, sensitive, selective, nondestructive, and requires minimal to no sample preparation. The detection principle in Raman spectroscopy is based on inelastic light scattering by molecules that change polarizability. As a result, the frequency of incident light ( $\nu_i$ ) differs from that of scattered light ( $\nu_s$ ). In contrast, the frequency of incident and scattered light remains the same in Rayleigh scattering. Below is a schematic illustration of the difference between Raman and Rayleigh scattering (Figure 13). When the frequency of the incident light ( $\nu_i$ ) is higher than that of the scattered light ( $\nu_s$ ) due to the absorption of energy by a molecule, it results in a Raman Stokes shift. In contrast, Raman anti-Stokes scattering is generated when the frequency of the incident radiation is lower than that of the scattered light ( $\nu_i < \nu_s$ ) due to energy loss. Unlike FTIR, moisture is not a problem in Raman spectroscopy; however, Raman suffers from interference by fluorescence signals.

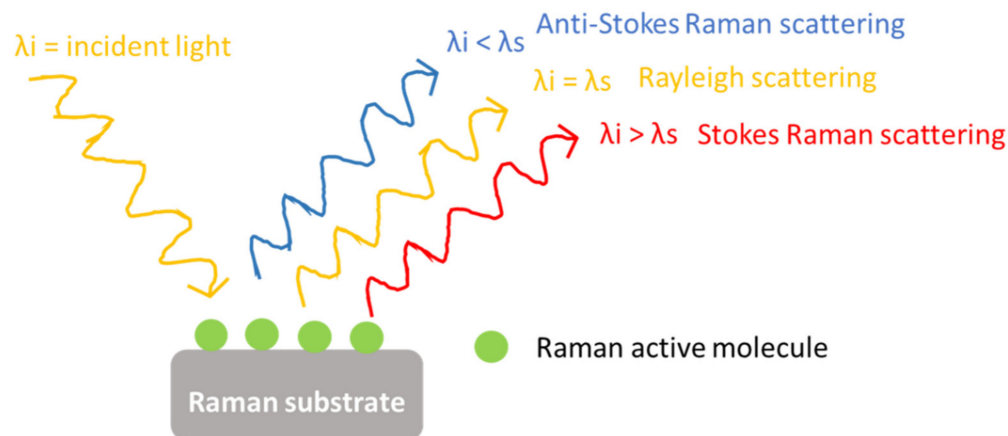


**Figure 13.** Schematic illustration of the Raman principle showing the difference between Raman and Rayleigh (Stokes and anti-Stokes) scattering.

Raman signals are generally weak because many more molecules undergo Rayleigh scattering compared to Raman scattering. Advances, such as surface-enhanced Raman scattering (SERS), have been used to improve the signal strength and sensitivity of this technique. In SERS, metal nanoparticles (e.g., silver and gold) are typically deposited on a surface to increase light scattering, enhancing the signal and resolution of the resulting Raman spectrum. The incident light interacts with the electrons on the surface of the substrate (e.g., nanoparticle electrons) to form a plasmon by the electromagnetic effect, i.e., the energy transfer from the plasmon to the adsorbed molecule results in enhanced light scattering (Figure 14).

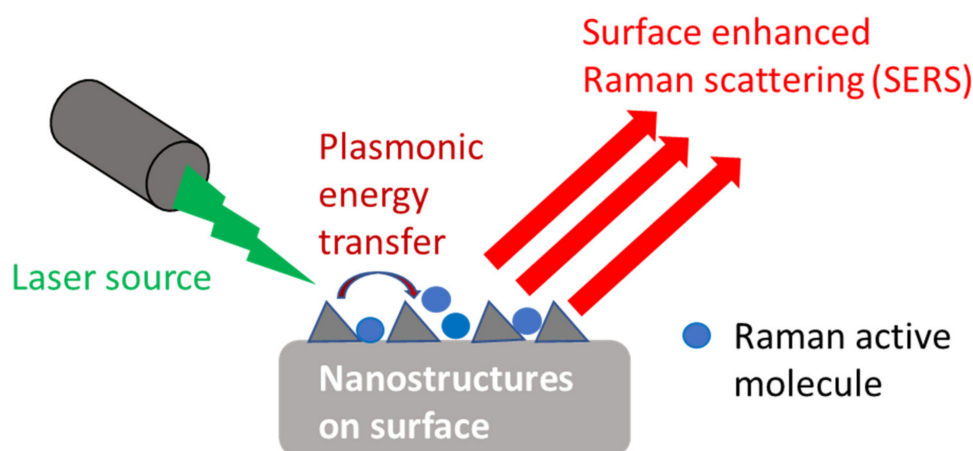


**Figure 14.** Schematic surface-enhanced Raman scattering (SERS) principle.

This review section highlights the developments in using Raman spectroscopy (including SERS) to detect opioids and their analogs relevant to pharmaceutical, forensic, and clinical screening applications.

Raman and Fourier transform infrared (FTIR) are vibrational techniques that have proven useful for detecting various analytes, including opioids and their analogs. These techniques have gained widespread use because they are rapid, sensitive, selective, nondestructive, and require minimal to no sample preparation. This review section highlights the developments in using Raman and FTIR spectroscopy to detect opioids and their analogs relevant to pharmaceutical, forensic, and clinical screening applications.



#### 4.2.1. Raman Spectroscopic Detection of Pharmaceutical Opioids, Illicit Opioids, and Analogs in Biological Samples

Substance abuse disorders affect several groups of people, and veterans are among a large group of those impacted. Farquharson et al. developed a method using liquid extraction followed by surface-enhanced Raman spectroscopy (SERS) to analyze the drugs in the saliva of military veterans [116]. Urinalysis was performed to validate the results from SERS. This method detected nicotine, buprenorphine, cannabinoids, codeine, and methamphetamine. The SERS technique detected opioids in three of the samples, but this was not supported by the urinalysis, which is attributed to different metabolites in saliva and urine [116]. This method can detect drug medications with acceptable accuracy, is noninvasive, and can help monitor substance abuse disorder treatment for military veterans [116]. The use of SERS for narcotics detection in biological fluids has been extensively reviewed by Markina et al. [117]. The review details the application of SERS for detecting medicines, drugs, and narcotics in body fluids, including saliva and urine. In addition, the approaches to improve the selectivity of SERS for drug detection in biological fluids by decreasing background signals are reviewed [117]. Overall, SERS effectively detects drugs in biological fluids and can still be optimized to achieve improved selectivity [117].

Dynamic surface-enhanced Raman scattering (D-SERS) was developed by drying colloidal gold nanoparticles on a surface to generate 3D optimal hotspot structures with a strong signal for the sensitive detection of fentanyl (Figure 15). The internal standard (IS) used was 4-mercaptopyridine.

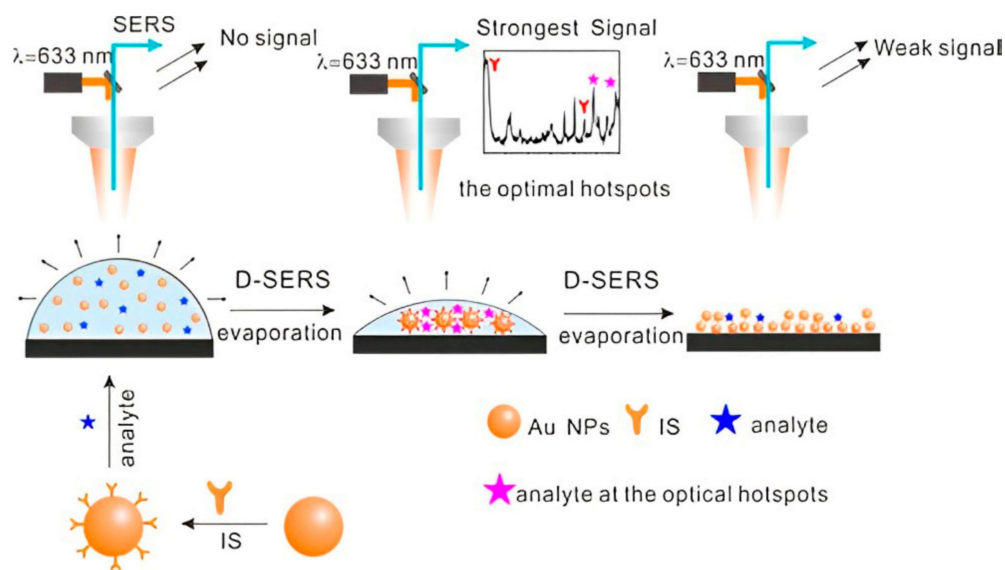


**Figure 15.** Schematics showing the optimum hotspots formed during D-SERS combined with the use of internal standard (IS) for the detection of fentanyl. Sketches on the surface represent Au solution, 3D hotspots, and aggregates of Au nanoparticles, respectively (i.e., from left to right). Reprinted with permission from ref [118]. Copyright MDPI.

The use of saliva samples provides a noninvasive approach for the screening of illicit drugs. Akcan and coworkers developed a SERS method to analyze heroin and its metabolites in saliva [118]. To achieve this goal, the authors evaluated various surfaces to determine the most effective surface for SERS measurements of heroin and its metabolites. The surfaces evaluated for SERS measurements include thin layer chromatography (TLC), gold nanorods (AuNRs), gold nanorods/polyaniline (AuNRs/polyaniline), and gold nanorods/nanocellulose (AuNRs/nanocellulose) [118]. The results from screening the surfaces using morphine as a model drug indicated that gold nanorods (AuNRs) were the most effective surface sensor for SERS measurements regarding the number of identifiable peaks and relatively low background signal (Figure 16) [118].

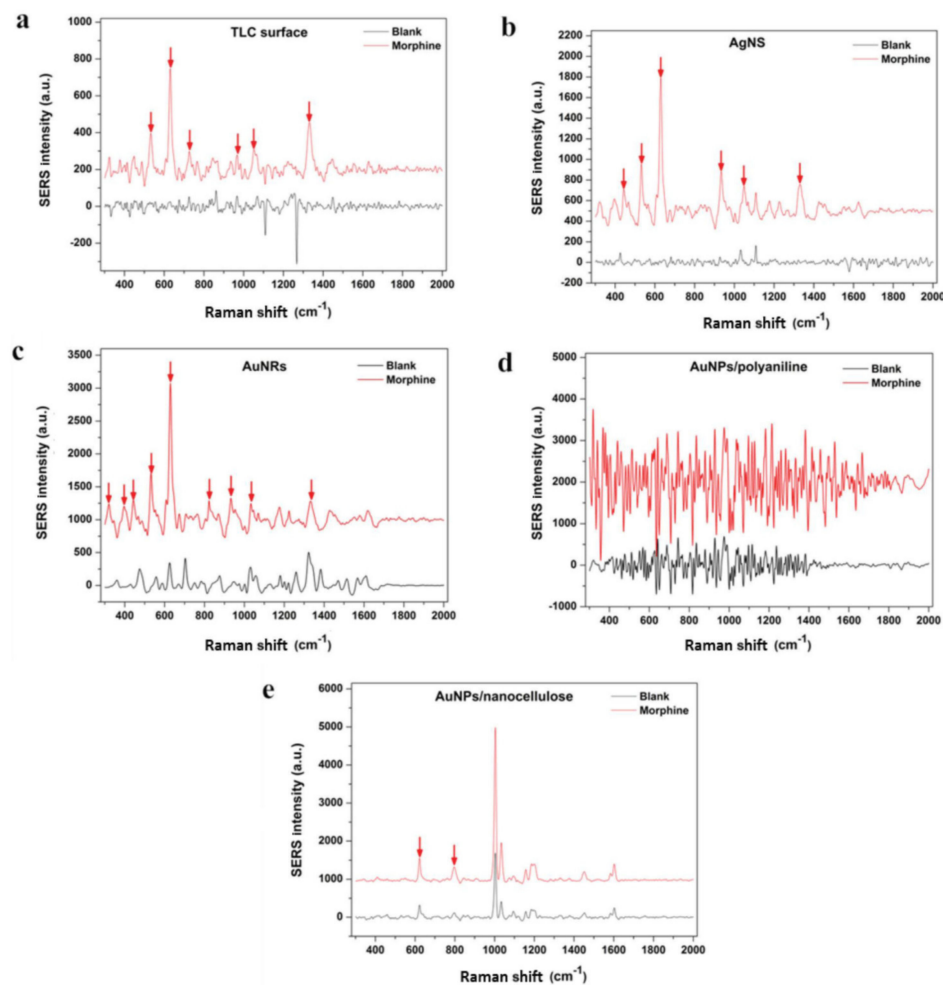


**Figure 16.** (a) SERS spectra of morphine and blank on TLC; (b) AgNS; (c) AgNRs; (d) AgNPs/polyaniline; (e) AgNPs/nanocellulose (red arrows show strong bands of morphine spectra). Reprinted with permission from ref [118]. Copyright *Turkish Journal of Medical Sciences*.

Having established the best SERS surface, the authors found that samples in saliva with concentrations ranging from 20 ppb–125 ppm can be detected using SERS. The limit of detection (LOD) for heroin in saliva is 31.69 ppb, while the LOD of its metabolites ranged from 17.01–20.91 ppb (Figure 17) [118]. As depicted in Figure 17, the band at 627 cm<sup>-1</sup> is the most consistent with the highest intensity compared to the bands at 443, 531, 1107, 1245, and 1338 cm<sup>-1</sup>. Therefore, the band at 627 cm<sup>-1</sup> was used to construct a calibration curve for determination of the LOD for heroin and metabolites. Saliva was chosen for developing the SERS method because it consistently showed stable bands with the highest intensity compared to other biological matrices. The findings from this study demonstrate, for the first time, that the SERS technique can detect heroin and its metabolites at low concentrations in saliva [118].

The use of SERS for detecting and identifying illicit drugs in biological fluids, including saliva, urine, and blood, has been reviewed [119]. The authors note that SERS signals are greatly influenced by the substrates used, and some of the most optimal substrates are silver and gold nanoparticles. Other techniques, such as thin-layer chromatography and artificial neural networks combined with SERS, have been found to increase their effectiveness. The use of both conventional and portable SERS for fast, sensitive detection of illicit drugs in biofluids is highlighted [119].

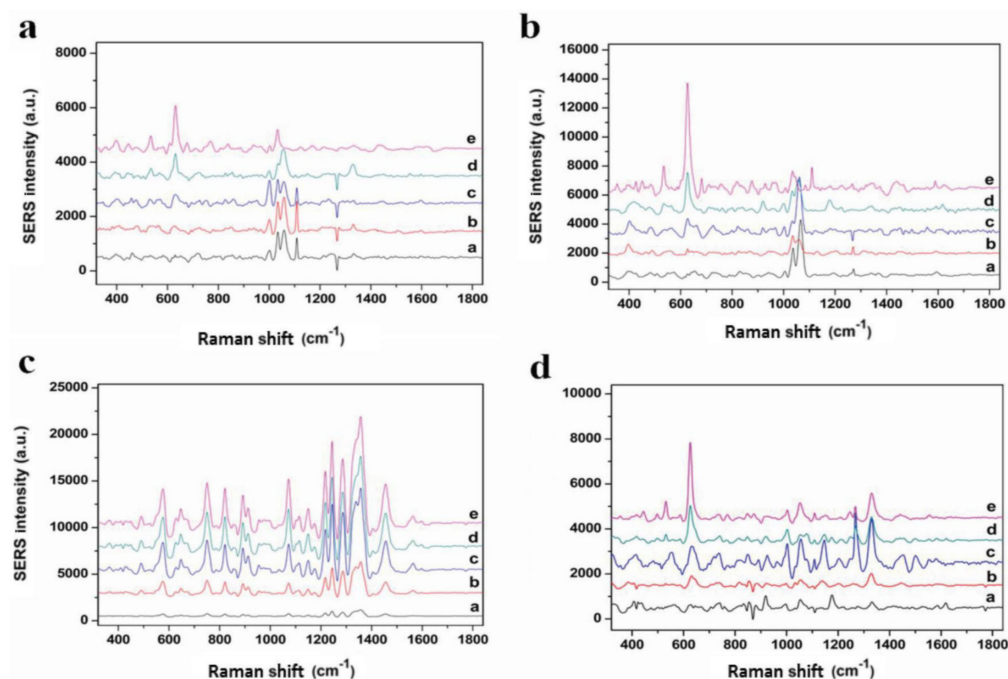


**Figure 17.** C-C alicyclic–aliphatic bands at  $627\text{ cm}^{-1}$  of (a) MM; (b) M3B; (c) 6MAM; (d) heroin from 20 ppb to 125 ppm in saliva. (a) 20 ppm; (b) 1 ppm; (c) 5 ppm; (d) 25 ppm; (e) 125 ppm. Reprinted with permission from ref [118]. Copyright *Turkish Journal of Medical Sciences*.

#### 4.2.2. Raman Spectroscopy: Forensic Application

One of the leading causes of death in drug overdose is the presence of fentanyl used as an adulterant in other drugs of abuse. Detection of trace amounts of fentanyl in these drugs would save lives. Haddad et al. [120] loaded silver nanoparticles onto a paper-based substrate for the detection of fentanyl in cocaine using SERS. Although there are several similarities in the SERS spectra of cocaine and fentanyl, there are some differences from the C-C bending stretch [120]. This Raman technique allowed the detection of fentanyl with a limit of detection of 500 ng (65 ppm). In addition, there is a linear correlation between the intensities of concentration of the characteristic peaks of fentanyl and cocaine. The result from this study provides a useful qualitative method for forensic detection of traces amount of fentanyl in cocaine [120].

Wang et al. [121] synthesized gold–silver nanostars for use with a handheld SERS method for the detection of fentanyl-laced cocaine and heroin samples. The spectra of heroin and cocaine with decreasing concentration are shown (Figure 18) [121]. SERS with multivariate analysis was used for the detection of trace amounts of fentanyl in cocaine and heroin. Aggregated colloidal nanostars were synthesized and used to interact with the drug samples. The detection of fentanyl adulterated in cocaine was achieved using a handheld Raman spectrometer (Figure 19). The detection limit for fentanyl was determined using a multivariate analysis and was found to be  $0.20 \pm 0.06\text{ ng/mL}$  [121]. For samples of heroin and cocaine laced with fentanyl, the detection limit was in the lower nanogram to microgram level. The handheld Raman sensor demonstrated excellent sensitivity and detection of trace amounts of fentanyl in both heroin and cocaine for forensic applications.

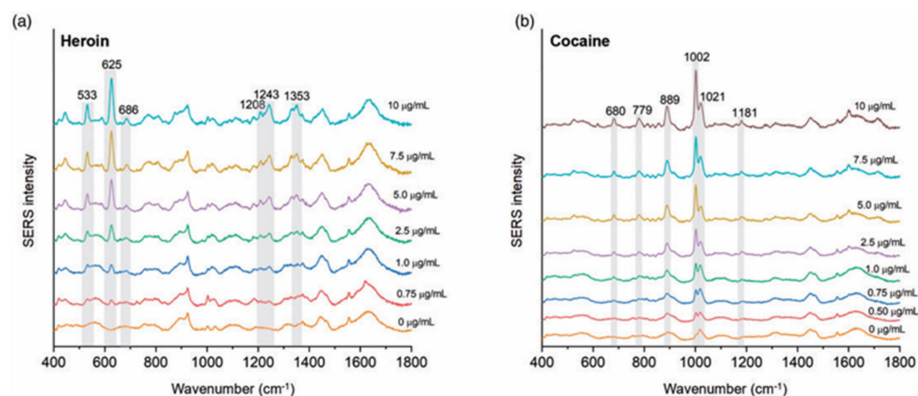


**Figure 18.** SERS spectra of (a) decreasing concentration of heroin and labeled characteristic bands, and (b) decreasing concentration of cocaine and labeled characteristic bands. Reproduced with permission from ref [121]. Copyright the authors.

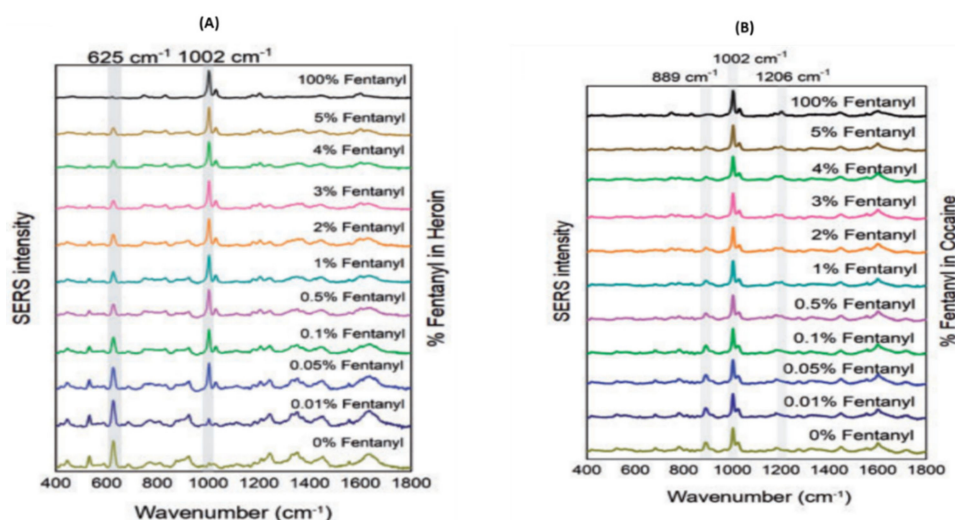


**Figure 19.** Handheld Raman detection of fentanyl in (A) heroin and (B) cocaine with different mixture ratios and their characteristic peaks. Reproduced with permission from ref [121]. Copyright the authors.

Wilcox et al. [122] used Raman spectroscopy measurements to determine five prevalent fentanyl analogs (including alfentanil hydrochloride, cartefanil oxalate, fentanyl citrate, remifentanyl hydrochloride, and sufentanil hydrochloride) [122]. Raman cross-sections were used with density functional theory (DFT) to evaluate the analogs in different adulterants and to determine the fentanyl detection limit. The Raman spectra of the fentanyl analogs show that these compounds have a strong ring-breathing aromatic signal near  $1000\text{ cm}^{-1}$  upon laser excitations at 532 nm and 785 nm (Figure 20) [122]. This peak was used to calculate the Raman cross sections of the compounds, which is beneficial in determining the detection limit of fentanyl and its analogs for varying Raman sensors [122]. This method has the potential to be used in the field by law enforcement agencies to detect fentanyl and its analogs in a mixture of drugs.

Shende and coworkers used gold nanoparticles with SERS active pads to detect both fentanyl and codeine at various concentrations [123]. Using this technique, the detection limits for fentanyl and codeine were found to be 5 ng/mL and 6 ng/mL, respectively. This study's findings indicate that using SERS pads would be advantageous for situations where illicit substances are often seized, such as for forensic analysis and airport security [123]. Qin et al. used porous structured silver crystals for SERS [124]. It was found that the granular-shaped silver crystals were most optimal as Raman substrates. Using the silver crystals, five methamphetamine analogs were identified at concentrations as low as 1 mg/L.



Applying density functional theory (DFT), each methamphetamine analog was successfully discriminated from one another. The results of this study suggest that the use of SERS with porous silver crystals can detect and identify methamphetamine and its analogs [124].

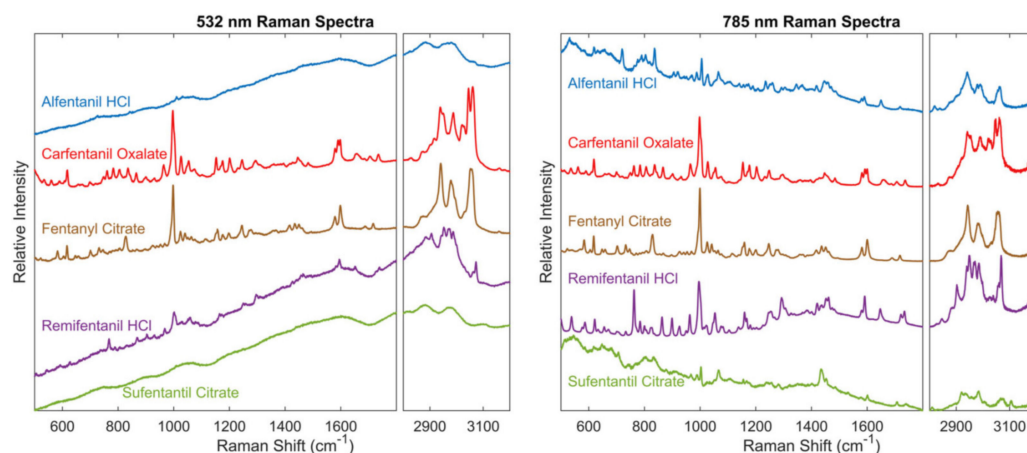


**Figure 20.** Measured Raman spectra of fentanyl compounds using 532 nm (left) and 785 nm (right) laser excitations. The data has been intensity corrected to account for the relative efficiency of the Raman spectrometers as a function of Raman shift. Reproduced with permission from ref [122]. Copyright the authors.

#### 4.2.3. Raman Spectroscopy: Clinical Applications

Wang et al. [125] synthesized silver nanoparticles as substrates for the detection of fentanyl in 27 different sample types using SERS [125]. The samples were analyzed by handheld SERS system, and it was determined that the limit of fentanyl detection using this technique is 0.1–25 ppb. Compared to a standard desktop Raman spectroscopy method, the portable technique demonstrated higher sensitivity and selectivity for fentanyl detection. The results of this study show that differential Raman spectroscopy can be used at the point-of-care for accurate detection and practical screening of fentanyl [125].

A novel program allowing a local hospital to be in contact with law enforcement and first responders to fight against the opioid epidemic was developed by Grover and coworkers [126]. A handheld Raman spectrometer was used to analyze seized drugs by law enforcement at the hospital, and patients could then be treated at the hospital. Using this technique, 27 substances were identified, including fentanyl and etizolam, that were obtained in the community. The authors found that a partnership between the hospital, law enforcement, and first responders is very beneficial for identifying illicit substances in the community and should be considered for use in other communities [126].

Mullin et al. conducted a point-of-care service that would allow pharmacists to analyze drug samples using a handheld Raman spectrometer [127]. Drug samples were provided anonymously from individuals who use drugs in the community. A total of 13 samples were obtained and analyzed in this study. After on-site analysis with a handheld Raman spectrometer, the samples would undergo confirmatory analysis at a laboratory (using techniques, such as high-performance liquid chromatography–mass spectrometry, gas chromatography–mass spectrometry, and proton nuclear magnetic resonance) [127]. The handheld Raman spectrometer was able to detect several drugs, including stimulants, depressants, and opioids. Despite the limitation of a small sample size from this study, the results show potential for future use of this pharmacist-led point-of-care service for screening psychoactive substances and providing treatments in the community [127].

Gerace and coworkers used a portable Raman spectroscopy device to analyze various drug samples from individuals during nightlife events [128]. For this study, a total of 472 samples were analyzed, and various drugs were detected in 304 samples, including methamphetamine, cocaine, psychoactive substances, ketamine, heroin, and 3,4-methylenedioxymethamphetamine (MDMA). Surprisingly, new psychoactive substances



were also detected in 9 samples, highlighting the risks of fatal overdose from these new illicit substances at nightlife events. The results from this study demonstrate that the portable Raman device with an updated library database is useful for drug detection and identification in nightlife events where new illicit drugs are often used [128].

#### 4.3. Colorimetric Detection

Colorimetric sensors for the detection of opioids utilize various mechanisms, including nanoparticle aggregation, polymeric micelles, sensor arrays, ligand–receptor binding, immunoassays, and mimetic enzymes, to detect the presence of these substances (Figure 21). Nanoparticles, such as gold or silver nanoparticles, can aggregate in the presence of opioids. This aggregation causes a shift in the color of the solution, which can be visually observed or measured using spectrophotometry. The aggregation is induced by the interaction between the opioids and functional groups on the surface of the nanoparticles, leading to changes in the nanoparticles' stability and, thus, their aggregation state. Polymeric micelles are nanoscale structures formed by the self-assembly of amphiphilic block copolymers in solution. These micelles can encapsulate hydrophobic compounds, such as opioids, within their cores. Functionalization of the micelles' surface with specific receptors or ligands enables selective binding to opioids. This binding can induce changes in the micelles' structure or stability, resulting in a measurable color change. In addition, ligands specific to opioid receptors can be immobilized onto a surface, such as a sensor chip or nanoparticles. When opioids are present in the sample, they bind to these receptors, leading to a change in the optical properties of the system. This change can be detected colorimetrically, providing a qualitative or quantitative measure of opioid concentration. Immunoassays rely on the specific binding between antibodies and antigens, such as opioids. In a colorimetric immunoassay, opioid-specific antibodies are immobilized onto a surface or conjugated with nanoparticles. When opioids are present in the sample, they bind to the antibodies, leading to the formation of antibody–antigen complexes. This complex formation triggers a colorimetric signal, either through a direct change in color or through the aggregation of nanoparticles. Mimetic enzymes are synthetic compounds that mimic the activity of natural enzymes. Some mimetic enzymes can catalyze colorimetric reactions in the presence of opioids. For example, a mimetic enzyme may catalyze the oxidation of a colorless substrate to a colored product in the presence of opioids. The intensity of the color change is proportional to the concentration of opioids in the sample, allowing for their detection and quantification. Sensor arrays consist of multiple sensing elements, each with different selectivity towards various target molecules, including opioids. Each sensing element may utilize different mechanisms, such as nanoparticle aggregation or ligand–receptor binding, to detect the presence of opioids. The pattern of responses from the array can provide a unique fingerprint that allows for the identification and quantification of opioids in a sample. These sensors offer advantages, such as simplicity, rapidity, and sensitivity, making them valuable tools for opioid detection in various applications, including medical diagnostics and forensic analysis.

Over the past few years, colorimetric sensors have demonstrated significant promise in advancing point-of-care diagnostic applications due to their notable advantages, such as easy preparation, simple readout, cost-effectiveness, and their ability to be visually interpreted without requiring specialized equipment [129]. Colorimetric sensors have emerged as essential tools in the detection of opioids and analogs across various applications, ranging from pharmaceutical and clinical to forensic settings. This review explores the recent developments and applications of colorimetric sensors in identifying pharmaceutical opioids, illicit opioids, and their analogs in diverse biological samples, and their utilization in pharmaceutical, clinical, and forensic scenarios. Earlier colorimetric sensors were susceptible to interference from other substances in the sample, leading to inaccurate results. Environmental factors and the composition of the sample matrix (e.g., blood, urine, saliva) influenced the sensor's performance and limited its ability to detect opioids accurately. Ongoing research and development efforts focusing on integrating innovative sensing

materials have improved the sensitivity, specificity, reliability, and usability of colorimetric sensors for opioid detection [129–132]. This advancement effectively addresses the challenges of identifying illicit drugs in intricate biological samples, presenting enhanced functionality and dependability.

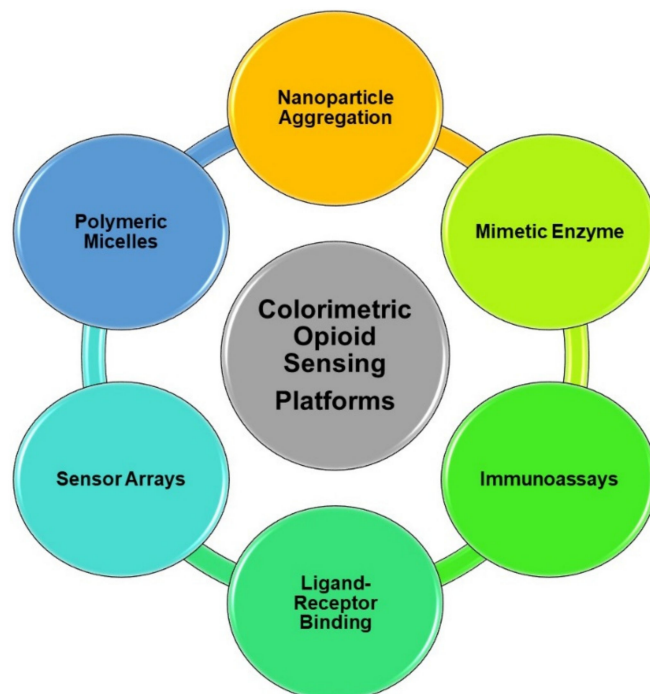


**Figure 21.** Schematic representation of colorimetric opioid sensing platforms.

Incorporation of nanomaterials, such as metal nanoparticles [133–135], carbon nanomaterials [136,137], and quantum dots [138], has dramatically enhanced the sensitivity of colorimetric sensors. Nanomaterials provide a large surface area for interactions with target analytes, leading to increased signal amplification and improved sensor response at lower concentrations of opioids. Novel sensing materials [139–141] often involve surface functionalization of nanomaterials with specific ligands or receptors [142] that selectively bind to opioid molecules, as seen in the schematic in Figure 22. This functionalization improves the sensor's selectivity by ensuring that it responds predominantly to the target opioids and minimizes interference from other substances present in biological samples.

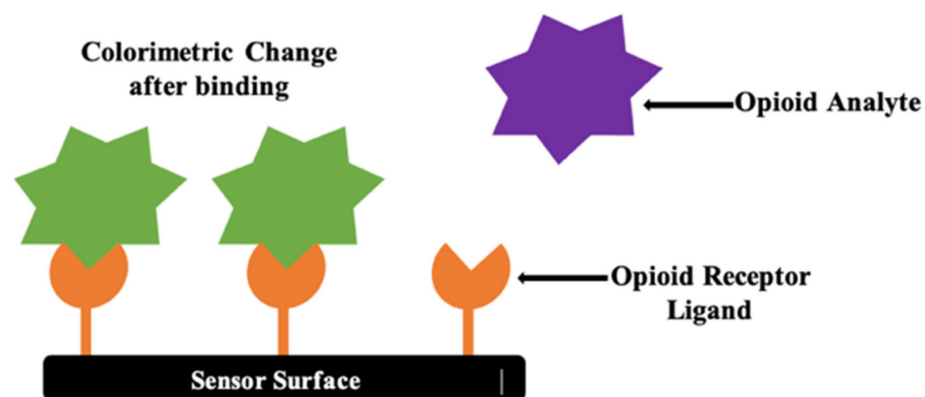


**Figure 22.** Opioid analyte and ligand interaction.

Advanced molecular recognition elements, such as aptamers [143–145], metal–organic frameworks (MOFs) [146], and molecularly imprinted polymers (MIPs) [147,148], have

enhanced the selectivity of colorimetric sensors. Aptamers are synthetic, single-stranded DNA or RNA sequences designed to bind specifically to target opioids. MIPs are artificial receptors with selective binding sites for target molecules, contributing to improved sensor specificity. Integrating responsive polymers and smart materials [149] that undergo conformational changes and controlled release of color indicators in the presence of opioids contributes to improved sensitivity. These materials enhance sensitivity and selectivity by providing a visual and measurable response to the binding of opioids, enabling easy detection and differentiation from other compounds.

Plasmonic resonance-based strategies [150], where noble metal nanoparticles interact with incident light, have enhanced the sensitivity of colorimetric sensors. The changes in the plasmonic resonance properties result in observable color shifts, providing a sensitive and specific response to the presence of opioids. Enzyme-assisted colorimetric reactions [151], where enzymes catalyze specific reactions leading to a color change, have been integrated into sensors for opioid detection. Enzymatic reactions increase sensitivity and specificity, enabling the detection of opioids at lower concentrations and reducing false positives. Incorporating these materials has significantly advanced the field of colorimetric sensors for opioid detection, improving sensitivity and selectivity. Furthermore, these innovations contribute to developing robust and reliable sensor systems for detecting opioids in diverse and complex biological matrices.

#### 4.3.1. Colorimetric Detection of Pharmaceutical Opioids, Illicit Opioids, and Analogs in Biological Samples

Significant advances have been made in developing colorimetric sensors for precisely detecting pharmaceutical opioids and their analogs in biological matrices [72,152], such as urine, saliva, blood, in vitro cellular assays, and tissues. The development of multiplexed colorimetric sensors [153,154], which can detect multiple opioids simultaneously, has broadened their utility. This advancement allows for a more comprehensive analysis of complex biological samples, offering a holistic view of opioid composition and concentration. Integration of colorimetric sensors with portable and handheld devices [155–158] has facilitated point-of-care testing. This progress is particularly beneficial in clinical settings, enabling rapid and on-site detection of pharmaceutical opioids in bodily fluids, like urine and saliva.

Improvements in the biocompatibility and biostability of colorimetric sensor components ensure the sensor's reliable performance in biological samples. This is critical for maintaining the sensor's accuracy over extended periods, making it suitable for applications in therapeutic drug monitoring and clinical diagnostics [159]. The designed cell-based biosensor used for biological samples can screen for ligands specific to cell surface receptors using an opioid-binding opioid receptor. These collective advancements showcase the evolving nature of colorimetric sensors, making them increasingly robust tools for precisely detecting pharmaceutical opioids and their analogs across diverse biological matrices.

Examining the detection of illicit opioids and analogs using colorimetric sensors reveals their potential in combatting the opioid epidemic. By effectively screening biological samples, including urine, saliva, blood, in vitro cellular assays, and tissues, these sensors contribute to the early detection and identification of illicit drugs, allowing for intervention [160–164] and thereby aiding in public health efforts to curb opioid abuse. The detection of the presence of illegal drugs in oral fluid has become increasingly popular as a non-invasive method to detect drug use. Several devices are now available to screen oral fluid for the presence of recreational and illicit drugs. The abused drugs of most interest are amphetamines, ecstasy, cocaine, opiates (morphine, codeine), benzodiazepines, and cannabis. Advancements in these devices aim to improve sensitivity, selectivity, and applicability in diverse settings.

In a comparative study by Cao [165], the colorimetric immunoassay correlated well with the conventional gas chromatography–mass spectrometry method. The high specificity of the sensor for methamphetamine determination was proved by four different illicit

drugs, including pseudoephedrine. Additionally, the sensor surface showed stable regeneration capacity throughout 100 binding-regeneration cycles. The sensor was proven to be simple, sensitive, rapid, and robust for the forensic determination of methamphetamine in human serum. As shown in the research of Dagar et al. [166], the portability and user-friendly nature of colorimetric sensors make them suitable for point-of-care testing. Various electrochemical and optical nanosensors have been developed for the analysis of the most common drugs of abuse and their metabolites, such as tetrahydrocannabinol, cocaine, opioids, amphetamines and methamphetamine, and benzodiazepine. Progress in these sensors has markedly enhanced the sensitivity and selectivity of diverse sensing methods, accompanied by the evolution of factors, such as real-time monitoring and measurement facilitated through a smart user interface. This enables healthcare professionals, law enforcement agencies, and outreach workers to conduct on-site screenings, facilitating quick identification of individuals at risk of opioid abuse or overdose, since illicit opioids are often involved in accidental exposures and poisonings. Colorimetric sensors for drugs of abuse [167–169], by providing a quick and reliable means of identifying these substances, help to reduce the likelihood of accidental exposure and subsequent harm to individuals, including children who might encounter opioids unknowingly.

Colorimetric sensors can be designed and customized to detect specific analogs of illicit opioids, as seen in the work of Cho et al. [153]. Using a chromogenic ring-opening mechanism upon reaction with secondary amines in illegal drugs, this reaction produces a red-shifted absorption band resulting in a distinct color change from colorless to red. This specificity is crucial, as illegal formulations of medications can vary, and new analogs may emerge.

#### 4.3.2. Colorimetry Sensors: Pharmaceutical Applications

This review section underscores the versatility of colorimetric sensors in pharmaceutical applications. Their ability to provide rapid and reliable detection of opioids facilitates quality control processes during drug development [143]. Colorimetric sensors are valuable tools for monitoring drug release kinetics and ensuring that pharmaceutical formulations meet stringent regulatory standards. The application of these sensors in pharmaceutical research and development offers several advantages in optimizing drug formulations and ensuring the safety and efficacy of medications [170].

By providing a visual and measurable response to changes in concentration, these sensors offer a dynamic and continuous assessment of the drug release profile [171]. This real-time capability allows researchers to gather detailed information on how drugs are released over time. The sensitivity of colorimetric sensors is crucial for accurately detecting even low concentrations of drugs in the release medium, ensuring that the monitoring process is precise and capable of capturing subtle variations in drug release kinetics. Unlike some traditional methods of monitoring drug release, colorimetric sensors often allow for non-destructive analysis, like in the work of Alonzo et al. [156]. This means that the same sample can be monitored continuously over an extended period without compromising the integrity of the formulation. Non-destructive analysis is particularly beneficial in long-term studies and helps to minimize the need for multiple samples. Colorimetric sensors can be tailored to specific drugs or classes of compounds. This customization ensures that the sensor's response is optimized for the pharmaceutical formulation under investigation [172,173]. Researchers can design sensors that selectively respond to the released drug, providing specificity in monitoring. During the formulation development phase, colorimetric sensors contribute to quality control by assessing the consistency and reliability of drug release profiles [174]. Any deviations from the expected release kinetics can be promptly identified and addressed, ensuring the final formulation meets the required specifications and standards.

The insights gained from colorimetric sensor data have aided in optimizing drug delivery systems. Researchers have used this information to refine pharmaceutical formulations, enhance drug stability, and adjust release profiles to meet specific therapeutic

needs [175–179]. For example, enzyme-responsive colorimetric sensors are designed to detect enzymatic activity within pharmaceutical formulations. These sensors help monitor drug degradation or metabolic processes, influencing release profiles and optimizing drug stability. At the same time, oxygen-sensitive colorimetric sensors are utilized to assess the oxygen permeability of pharmaceutical packaging. In contrast, sensors responsive to hydrogen peroxide levels are valuable for evaluating oxidative stress within pharmaceutical formulations [178]. Polymeric micelles and nanoparticles with colorimetric properties are employed to encapsulate and deliver drugs. Colorimetric sensing relies on a color change due to the breakdown of polymeric micellar systems by analyte recognition [179]. Integrating these colorimetric sensors in pharmaceutical development facilitates the refinement of formulations, ensures drug stability, and enables the adjustment of release profiles. Their ability to provide real-time, sensitive, and specific data contributes to developing high-quality medications that meet regulatory standards and deliver therapeutic benefits to patients.

#### 4.3.3. Colorimetry Sensors: Clinical Applications

Colorimetric sensors have demonstrated efficacy in clinical settings, particularly therapeutic drug monitoring and point-of-care delivery [166]. These sensors' real-time, on-site detection capabilities empower healthcare professionals to make informed decisions regarding opioid therapies, thereby enhancing patient care and safety [180]. The opioid epidemic provides unprecedented opportunities for point-of-care drug testing, with significant clinical needs. According to the Centers for Disease Control and Prevention, the leading cause of death from poisoning in the United States is opioid overdose. Opioid overdose, often involving prescription painkillers or illicit opioids, like heroin and fentanyl, has been a significant public health concern. Opioid-related deaths have risen dramatically in recent years, contributing to the overall increase in poisoning fatalities.

Limitations for commercially available opioid point-of-care testing include lower analytical sensitivity, specificity, and cross-reactivity. With the rise in abuse of certain opioids, like fentanyl, currently spreading around the world, there is an urgent need for on-site and rapid analytical methods for detection [181–184]. Lin et al. [183] used a synergistic recognition strategy for fast, cost-effective, selective, sensitive, and visual colorimetric detection of opioids, specifically fentanyl, by using Rose Bengal as the colorimetric probe. Their sensor assay works based on halogen- and hydrogen-bonding interactions, generating a charge transfer, and accompanying a red shift in the Rose Bengal absorption band and a naked-eye color change from red to purple.

#### 4.3.4. Colorimetry Sensors: Forensic Applications

Outside of therapeutic and clinical applications, it is also helpful to determine the presence and concentration of controlled substances for law enforcement. In forensic applications, colorimetric sensors play a crucial role in the rapid and sensitive identification of opioids and analogs. Their utility in analyzing diverse forensic samples contributes to law enforcement efforts, aiding in investigating opioid-related crimes and providing valuable evidence in legal proceedings. Color tests remain the most used screening technique for testing seized material in a forensic drug laboratory. In contrast, identification and confirmation of drugs are typically performed using gas chromatography–mass spectrometry [156]. These color reagent test sensors can detect specific chemical components of drugs, leading to color changes that help law enforcement quickly determine the presence of controlled substances. Additionally, they can be tailored to differentiate between classes of drugs [160–164], such as opioids, stimulants, and hallucinogens. This capability allows law enforcement to categorize substances accurately, aiding in classifying seized samples during investigations. For example, the dye eosin Y has been used to detect the presence of fentanyl in recent studies. The detection method involves a charge transfer interaction between eosin Y and fentanyl, leading to changes in visible color and fluorescence intensity [181,182]. See Figure 23 for the interaction between fentanyl and eosin Y. Also, since



illicit drugs are often adulterated with cutting agents, colorimetric sensors can assist in identifying these additional compounds [163], providing insights into the composition of seized drugs and potential trends in drug trafficking.

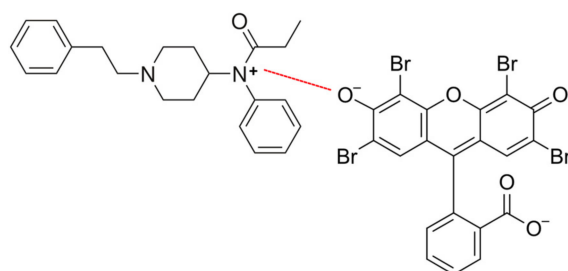


**Figure 23.** Charge transfer interaction (-----) between (+) charge of fentanyl and (-) charge of eosin.

Colorimetric sensors are used as presumptive field tests for the rapid and preliminary identification of substances [160]. Table 4 summarizes the most common illicit drug color tests used in presumptive field screening. Law enforcement can conduct these on-site tests to quickly assess whether a substance is likely an illicit drug, guiding further investigation and appropriate actions. On-site chemical color test reagents are often employed in a predetermined sequence to allow analysts to presumptively identify the drug of interest using a minimum number of tests.

**Table 4.** Presumptive color tests used in colorimetric sensing platforms.

Type	Color Test Name	Target Compounds
General Screening	Marquis	Alkaloids and other compounds (e.g., opiates, amphetamines, and phenethylamines)
	Liebermann's	Alkaloids and other compounds (e.g., amphetamines, and some synthetic cathinones)
	Mandelin's	Alkaloids and other compounds (e.g., amphetamines, some phenethylamines, and ketamine)
	Mecke	Alkaloids and other compounds (e.g., amphetamines, and some synthetic cathinones)
	Froehde's	Alkaloids and other compounds (e.g., opiates, and some synthetic cathinones)
Drug Class Selective	Duquenois–Levine	$\Delta$ -9Tetrahydrocannabinol (THC) and other cannabinoids
	Scott's	Cocaine
	Dille–Koppanyi	Barbiturates
	Chen-Kao	Ephedrine
	Ehrlich's	Ergot alkaloids, indoles, aromatic amines, and LSD
	Fast Blue B salt	$\Delta$ -9 Tetrahydrocannabinol (THC) and other cannabinoids
	Zwicker	Barbiturates
Functional Group Selective	Simon's	Secondary amines (e.g., methamphetamine)
	Zimmermann	Ketones (e.g., synthetic cathinones and benzodiazepines)

Some detection methods for drugs of abuse [104,185–187] allow for quantitative analysis, providing law enforcement with information about the concentration of a specific drug in a sample. They are also deployed at border checkpoints and customs to aid in the rapid screening of incoming shipments for illicit drugs [188]. This facilitates the interception of illegal substances and helps prevent the cross-border trafficking of narcotics. The versatility, rapidity, and specificity of colorimetric sensors make them valuable tools in the forensic analysis of diverse drug samples, contributing to law enforcement efforts to combat drug-related crimes and protect public safety. This comprehensive section of the review highlighted the multifaceted applications of colorimetric sensors in opioid detection, spanning pharmaceutical, clinical, and forensic domains. The advancements in sensor technology discussed herein underscore their potential as indispensable tools in the ongoing fight against opioid abuse and misuse, offering promising avenues for future research and development.

#### 4.4. Fluorescence Detection

Emergent technologies in fluorescence sensors development have found applications in several research areas, particularly for industrially manufactured pharmaceuticals and forensic applications [189]. This review section highlights the novel innovation of fluorescence-based detection of opioids and illicit drugs in biological, forensic, and clinical applications.

##### 4.4.1. Fluorescence Sensors: Detection of Pharmaceutical Opioids, Illicit Opioids, and Analogs in Biological Samples

Nanobiosensors have found applications for opioid detection in biological samples due to the versatility of nanoscale materials. These materials are advantageous for use in applications that would otherwise be limited by cost and portability, while also providing increased sensitivity due to their large surface areas (i.e., that these materials can afford. As opioid overdose deaths increase nationwide with an additional burden caused by the COVID-19 pandemic increasing these rates [190], there is a great need for the development of fast screening methods with accurate results that can be generated into reports that can be easily interpreted by clinicians and healthcare staff of all levels [191].

Though there have been advancements in the field for both mass production and small-scale tools for fluorescent quantification of opioids in samples, the mass production of portable devices that can afford the properties previously mentioned above is still years away from fruition [13]. Recent advancements in cost efficiency have led to more green or environmentally friendly synthesis methods sourced from readily available natural products, such as synthesizing quantum dots derived from carrots [192], resulting in increased sensitivity of the analytical method of detection [192]. Quantum dots (QDs) are exemplary materials that often exhibit enhanced fluorescence properties and are relatively small at <10 nm in size [193]. These materials have proven advantageous in many different applications, such as in drug delivery or trace element detection in water sources. In this manner, Meng et al. [192] fabricated a QD-based sensor using lidocaine as the target opioid. Lidocaine, also known as lignocaine, is a common pharmaceutical synthetic, often present in OTC drugs, that is primarily used as a local anesthetic in dental procedures or to alleviate chronic and acute pain [192,194]. The QDs in this study were synthesized via a hydrothermal reaction, a commonly used method for nanomaterial preparations performed under low or high pressure conditions, allowing for controlled morphology of the synthesized material [195]. In a hydrothermal reaction, reagents are placed inside a Teflon-lined autoclave pressure vessel where the mixture is heated above water's boiling point at a high pressure, thus forcing the reagents into solution and often forcing them to react. This strategy allows for the efficient combination of reagents in ways that would not be achievable at room temperature, resulting in faster reaction times more consistent results. The quantum dots solution probe described in this report was utilized to detect lidocaine in real blood samples through a fluorescence quenching mechanism with the inner filter effect [192]. The results of the sensor demonstrated that QDs synthesized from

a common vegetable could effectively *detect* the presence of lidocaine evident for RSDs ranging from 1.2–2.5% and lidocaine spiked recovery rates of 82.7–101.3% in real samples with minimal interference from other biological molecules in the blood samples. Figures of merit for the developed method included a low limit of detection at 20.52 nM and a linear dynamic range of 0.25–50 mM, with minimal QD degradation at 60 h of storage, and efficiency at pH 8, which results in very low cell toxicity.

Blood is not the only biological fluid collected to test for the presence of opioids in human samples. Urine is another specimen commonly used for drug testing; it is more favorable due to the relatively high concentrations of drugs and their metabolites, ease of collection, and extended drug detection window found in urine compared to blood [196]. However, a few limitations in urinalysis are that urine is an acidic substance, that it contains a high water content and high concentrations of other biological molecules and ions, and that it provides no correlation between drug concentrations in the samples with dosage taken or toxicity level [72]. Thus, the development of a different approach protocol for the detection of opioids in urine is imperative, and one is critically needed to assist in resolving the opioid crisis. One solution proposed by Nah et al. [197] is to harness the advantages provided by the combined use of inorganic–organic biological interfaces to assist in overcoming current challenges. In this recent report, the authors synthesized a highly sensitive photonic crystal (PhC)-based sensor implemented for the quantitative detection of fentanyl, in addition to detecting the concentration of fentanyl in the presence of other pharmaceutical opioids without the need for a *pre-tagging step* or labeling of the sensor. This sensor demonstrates great performance, indicated by a low limit of detection close to the clinical limit for fentanyl (LOD = 6 ng/mL) and well below the clinical limit for morphine (LOD = 7 ng/mL). The fabricated sensor displayed high selectivity for fentanyl present in fentanyl/morphine combinations, with recovery rates of over 93% over five cycles at a fast regeneration rate of 2 min. The device was constructed in a multi-layer fashion in several steps, resulting in titanium dioxide and silicon dioxide bilayers, with an exposed silicon cavity, and BK7 glass as the PhC substrate. The BK7 glass was cleaned with a piranha solution ( $\text{H}_2\text{SO}_4\text{:H}_2\text{O}_2$ ) at a 3:1 ratio and sonicated with several reagents to form the layers in a highly controlled stepwise manner. BK7 is one of the most common standard glass types used to produce high-quality optics, mainly for the visible spectrum. The relatively hard borosilicate crown material consists of the purest raw ingredients. It contains very few inclusions and is almost free of bubbles. The high material quality is a primary technical reason why N-BK7 glass is often the number one choice for optical windows, lenses, and prisms. Its smooth transmission and low absorption in the entire visible wavelength range are crucial features for numerous optical applications and sensor technologies.

The glass was subjected to sputtering with a  $\text{SiO}_2$  layer, following deposition of the  $\text{SiO}_2/\text{Si}$  defect layer through plasma-enhanced chemical vapor deposition. The device was functionalized by attaching opioid antibodies to the defect layer to enable detection properties. The thickness of the material was found to significantly affect the opioid detection ability of the developed sensors. The attached antibodies function as a monolayer substrate, enabling selective detection of analytes. The remaining reaction sites were shielded by a bovine serum albumin (BSA) solution employed in the experiment. A secondary antibody served as a control to enhance selectivity testing. Functionalized materials underwent analysis using a fluorescent microscope, revealing a faint green glow indicative of unbound secondary antibodies on the glass surface. This confirmed the proper functionalization of the material with the desired antibody. To further assess selectivity, a mixture of fentanyl and morphine was introduced to the sensor, yielding results comparable to those obtained by introducing only fentanyl. Consequently, it was deduced that the sensor exhibited excellent selectivity. Figure 24 summarizes results from the study, where it must be highlighted that the devices were tested under predetermined conditions and in “real life” scenarios for the detection of opioids in urine. The devices also showed the probe’s potential for the simultaneous detection of multiple opioids present

in the same sample to further investigate the robustness of the sensors. By preparing an organic/inorganic interface, the group demonstrated that the described device could dynamically monitor the levels of morphine in blood, among other opioids [197].

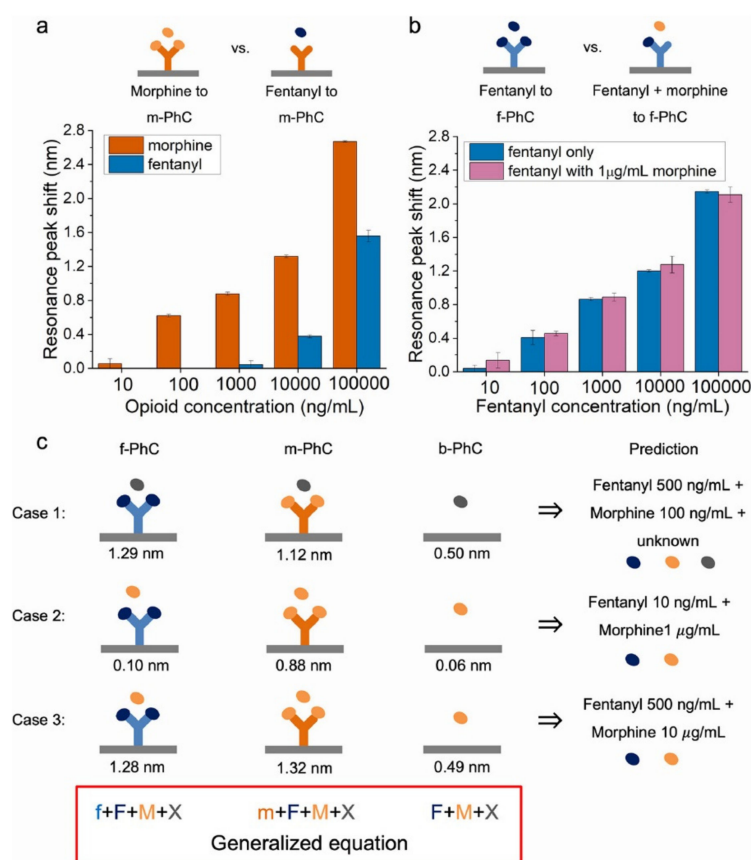


**Figure 24.** Shows the selectivity of the sensor and its promise in carrying multiple sensing antibodies in one device. (a) Comparison of a morphine (m-PhC) sensor and a fentanyl (m-PhC) sensor, (b) comparison of a fentanyl (f-PhC) sensor and fentanyl/morphine (f-PhC), (c) relation between the thickness of the film and prediction of results. Reprinted with permission from reference [197].

Like urine, saliva is also another common target for opioid detection due to the noninvasive nature of the sample collection process. However, urine and saliva as sample matrixes differ in both their chemical nature and composition. Although both saliva and urine are both composed of water, proteins, and salts, they differ by the types of proteins and salts present and their concentrations [197]. The detection of opioids in saliva has been extensively used and widely reported, especially for use in drug screenings of potential job applicants or for post-employment routine drug testing [198]. However, detection of opioids in saliva can be challenging for various reasons, including saliva sample quality, the speed at which the results are obtained, and the fact that not all opioids are detectable in saliva due to inference caused by other components found in saliva at higher concentrations. Nonetheless, due to the ease of sample collection of the biological fluid, the analysis of saliva remains the most routinely used biological sample matrix for opioid testing. For instance, the US Department of Transportation has recently adopted two methods for opioid testing in saliva [199]. Recent advancements in the area include increasing device detection limits, reducing the cost of processing samples, and producing improved devices that are simple to use and provide rapid, accurate results [200]. It is known that use of opioids generates detectable biomarkers in various bodily components of the human body, creating a greater interest in the field of advanced engineering of tissues for drug in vitro testing, an area which is growing due to recent discoveries. The field has grown from

initial *in vitro* studies conducted in a test tube and is progressing to real-time tissue/organ testing. Overall, the future of detection, quantification, safety, and overdose prevention of pharmaceutical opioids remains promising [201].

In addition to the detection of pharmaceutically prescribed opioid drugs, the development of sensors for the accurate detection of illicit opioids is equally essential. Detection of illicit drugs, such as heroin, cocaine, and methamphetamine, in human biological samples could potentially save lives and provide critical insights into community harm drug reduction. The detection of illicit drugs (narcotics) is also a research interest in fluorescence sensor development. The increased use of opioids has resulted in an epidemic nationwide, further confirmed by the detection of trace opioids, such as codeine and morphine, in wastewater and runoff water, particularly near highly densely populated urban areas [202]. Recently, sensors were developed to detect free-base illicit drugs using four compounds that exhibit enormous ionization potentials, thus making them effective in the photoinduced electron transfer process [203]. The authors reported the possibility of preparing thin films of these free base compounds which could detect (+)-methamphetamine vapors, cocaine analogs, and other similar compounds via the presence of chromophores, stressing the need for sensors that afford a high degree of selectivity.

Rapid detection of illicit opioids in bodily fluids is of great importance for law enforcement agencies, and the criminal justice and legal system. Inconclusive or invalid data is unacceptable in these fields as any bias or misinterpretation of results will heavily influence the difference between lawful or wrongful convictions. To this effect, some reports have evaluated metal–organic frameworks (MOFs) functionalized with fluorescent ligands to rapidly detect opioids in different fluids through a cost-effective synthesis method with results obtained at low detection limits. MOFs are supramolecular solids with applications in gas storage, molecular separation, and drug delivery [204–206]. MOFs are composed of a metal and an organic linker, where crystallization of the molecule results in a porous, three-dimensional, and infinite metal–organic material. The pore size indicates the captivity of these solids to store, separate, and detect specific molecules, making them attractive for these applications. One disadvantage to the use of these solids is that there is often no way to predict if the solids will exhibit porous properties. Therefore, there is an opportunity to tailor MOFs for selective and sensitive opioids [207].

Several studies have used fluorescent probes to detect illicit opioids in commonly tested bodily fluids, such as urine, blood, and saliva. For instance, a published article demonstrated a “mix and detect” strategy [208]. The authors of the study utilized the through binding of small-molecule Thioflavin-T (ThT) to a cocaine aptamer, resulting in a sensor which successfully detected cocaine in real samples composed of 2.5% urine and saliva over a range of cocaine concentrations. The probe also had an excellent lower limit of detection of 250 nM, demonstrating the strides made for the detection of illicit opioid substances via spectroscopic methods. Ju et al. [209] recently published an article on the application of computerized assistants and artificial intelligence for drug discovery/detection is currently at the forefront of new technologies in chemistry. The application of AI, in this case, assisted the research group in implementing fluorescent silver nanoclusters (AgNCs) to quantify the amounts of codeine and other related opioids [209]. Figure 25 shows the results reported in this paper, where AgNCs were the “sensing probe” and the standard for which the contour of the particles in the 3D spectra would change depending on the opioid detected. The experiments were divided into two primary components: (a) the development of a computational neural network GAN (generative adversarial network) classifier and (b) the integration of silver clusters in analyte detection. The GAN comprised a generator and a discriminator. The generator correlated the analyzed drugs with their spectral signatures. In contrast, the discriminator distinguished between drug classifications and their boundaries, mainly when they ceased to be classified as a specific narcotic. The generator generated data simulating synthesized species to deceive the discriminator into perceiving it as authentic. Subsequently, the discriminator endeavored to differentiate between actual and simulated spectra. Through generating examples, the GAN facilitated



the discriminator's refinement in distinguishing authentic spectra from simulated ones. Subsequently, silver clusters (AgNCs) were employed to ascertain whether the GAN could identify distinctive indicators from the opioids' fingerprints from the experimental data. Table 5 shows results comparative to traditional LC-MS techniques, demonstrating the promising capabilities of AI-assisted detection in this area of research. As can be seen, the relative detection of opioids in both cases is very favorable.

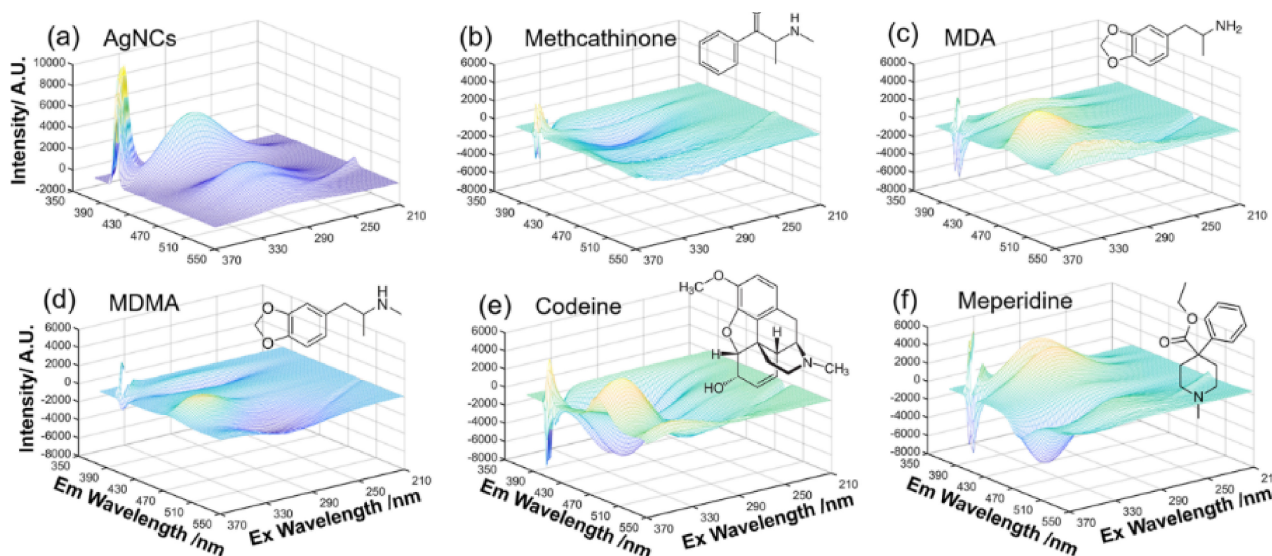


**Figure 25.** The AI-assisted deep learning 3D fluorescence spectra of opioids screening of (a) silver nanoclusters, (b) methcathinone, (c) MDA, (d) MDMA, (e) codeine, and (f) Meperidine. The differences in the contours of each sample indicate outputs related to the different functional groups in the opioids. Reprinted with permission of reference [209].

**Table 5.** Comparison of detection of illicit drugs LC-MS analysis vs. FL-DL analysis in urine samples. Reprinted with permission of reference [209].

Illicit Drugs	LC-MS Analysis: Concentration ( $\mu\text{g/mL}$ )	FL-DL Analysis: Concentration ( $\mu\text{g/mL}$ )
Codeine	$3.12 \pm 0.10$	$2.95 \pm 0.81$
MDA	$2.55 \pm 0.05$	$2.13 \pm 1.15$
MDMA	$6.96 \pm 0.11$	$8.91 \pm 4.47$
Meperidine	$2.13 \pm 0.08$	$3.24 \pm 1.39$
Methcathinone	$8.36 \pm 0.11$	$11.22 \pm 3.36$

#### 4.4.2. Fluorescence Sensors: Pharmaceutical Applications

An extraordinary increase in the number of prescriptions for opioids issued by general care providers for pain treatment has been seen since the early 1990s [210]. This increase in use initiated a wave of addiction which has rapidly become challenging to control. Opioid drugs are considered legal and approved by the FDA by prescription or OTC uses, making them readily available and prone to abuse due to euphoric effects, therefore causing the challenge of controlled use and making any reduction in overdoses extremely difficult. Over 643,000 opioid deaths were recorded and registered between 1999 and 2021 in the USA. Similarly, high deaths were recorded in other countries worldwide during the same time periods, necessitating the need for detection at the pharmaceutical development level, or screening of potentially addictive opioids for discontinued use without strict monitoring and regulation. Beatty et al. reported novel fluorescence screens utilizing genetically encoded drug biosensors (GEFIs) to target drugs of interest at the plasma and organelle

levels [211]. The biosensors could be tailored to detect specific drugs through “hit markers” and then further finetuned to enhance their sensitivity to the analyte target of choice. Over the span of three years (2017–2019), 176 drugs were tested with great hit/compatibility results, yielding just 1 example of research being conducted in the area of drug monitoring and screening, and similarly, using GEFIs allowed for creating an optogenetic microwell array screening system (Opto-MASS) [212]. In summary, the device involved the etching preparation of a silicon wafer using a deep reactive ion etching technique and modification through functionalization with polydimethylsiloxane (PDMS) to generate microwells and plasma treatment for a predetermined duration before being meticulously detached and pressed onto a dried bovine serum albumin substrate. Following this, the assembly was disassembled, and the microwells were meticulously excised and imprinted onto a 24-well glass bottom dish. This device is capable of high-throughput optical screening of monoamines and opioids. Figure 26 demonstrates a schematic diagram of the device, where the results indicate that the device is also reversible, with high-throughput capabilities for drug screening at shortened detection times, as is required for the analysis of dangerous substances.

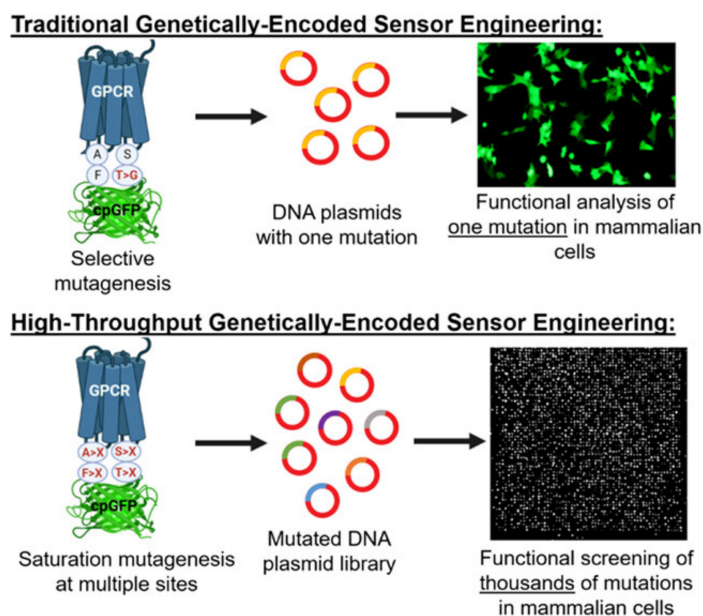


**Figure 26.** A diagram of the Opto-MASS device. Reproduced with permission of reference [212].

#### 4.4.3. Fluorescence Sensors: Clinical Applications

At the clinical level, the rapid detection of illicit/licit opiates can indicate the difference between life and death [213]. There is a critical need for user-friendly, simple-to-use, quick-output devices that provide legible results to the provider and the patient. Point-of-care testing has seen a rise in interest, as it allows a patient to go into an urgent care clinic and receive appropriate treatment in a timely manner by producing rapid, in-house results. Gozdziński et al. reported on the Vancouver Island Drug Checking Project in Victoria, Canada, where the authors utilized several quantitative spectroscopic methods to determine opioids in collected samples. Each spectroscopic technique has its advantages and disadvantages [42], which can be compared mostly based on portability, cost, detection limit, and sample environment/media interference. The challenge lies in finding a “perfect” method comprised of the advantageous features of the current methods for in situ detection while minimizing the disadvantages, as all the spectroscopic instruments compared differ in their capabilities and limitations.

A recently published review details the use of microneedle sensors that may help in point-of-care diagnostics and eliminate the need to transport bulky or inconvenient equipment while creating a minimally invasive sample collection procedure. Microneedle

sensors are comprised of materials, such as metals, inorganic components, hydrogels, and polymers commonly used for the fabrication of fluorescence sensors which are versatile and highly tunable. The authors proposed skin-embedded sensors that utilize electrochemical parameters, among others, to detect opioids in real-time analysis. Figure 27 demonstrates the proposed devices [77]. The skin-embedded sensors consist of an impedance-detecting material and an actual “strip” intended for placement on an individual’s skin, enabling the detection of concentrations through interaction with bodily fluids, like sweat. As depicted below, these sensors can assume diverse configurations and recognition factors.

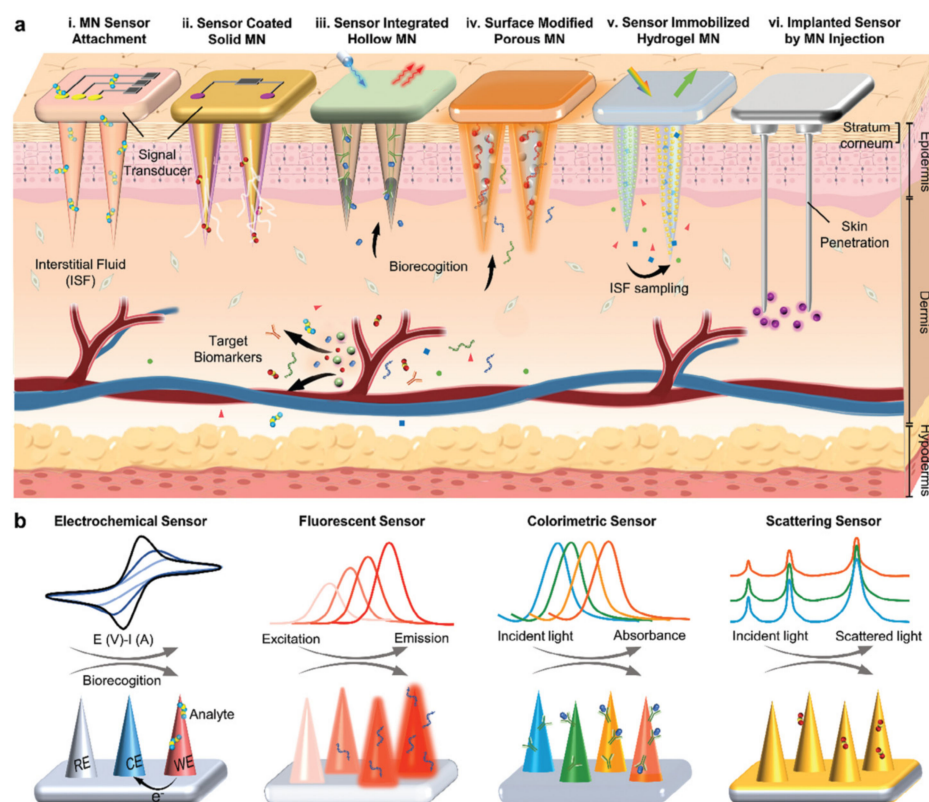


**Figure 27.** Multiple types of devices with types of detection. (a) Representation of the structure of the skin-embedded sensors, (b) generic representation of data from the sensors. Figure reproduced from reference [77] under a common share license (CC BY 4.0 DEE).

#### 4.4.4. Fluorescence Sensors: Forensic Applications

Law enforcement agencies and forensic scientists are highly aware of the opioid crisis. Hence, developing novel methods and technologies for opioid detection to combat the opioid challenge is an active research interest. For instance, in forensic chemistry, reports have shown that rapid detection of illicit substances used as evidence can be instrumental in solving a case [214]. In crime scenes where there are bodily fluids or human remains are discovered, the portable devices that can detect substances at low concentrations with efficacy are essential for onsite testing capabilities. Also, evidence waiting for analysis can suffer from environmental degradation during prolonged storage; therefore, having access to this type of portable yet accurate technology is critical to alleviate these current issues. The current gold standard technologies used for the detection of opiates are primarily lab-based, expensive, require specialized personal for operation and interpretation of results, and often do not have the ability to detect the low concentrations that these drugs can exist at in biological fluids. While these instruments serve their purpose well, there is always room for improvement to address the gaps present in the currently available technology.

Raman spectroscopy is a very versatile spectroscopic technique that is highly utilized for fluorescent sensor-based analysis. However, if the sample produces a strong fluorescent

signal, Raman becomes an inadequate technique for analysis as the sample can severely mask the IR and Raman signals, creating a selectivity issue. Additionally, evidence collection can be challenging, particularly in crime scenes where many environmental variables can cause a significant effect on data results leading to misidentifying a drug type. Several researchers have made various attempts at combating the issue of selectivity in Raman spectroscopy. For example, Wilke reported on the miniaturization of spectrometers for field study, where he stated that these spectrometers must be small enough to transport, user-friendly, and highly selective to avoid incorrect determinations, i.e., a “full-service lab” in a kit [215]. Dagar et al. described an extensive suite of instruments that could serve this purpose, delineating the advantages and disadvantages of each one [166].

Rapid increases in overdoses due to fentanyl use are on the rise in Canada and the United States. Fentanyl is one of the newest and most dangerous drugs on the market, with an LD<sub>50</sub> of 3.1 mg/kg in rats and 0.03 mg/kg in monkeys, while remaining an unknown variable in humans [216]. Since the amount of fentanyl required to be lethal is extremely low at 2 mg fentanyl, it is evident that low-detection limit devices are necessary. Canoura et al. [70] described the use of aptamer-based sensors that detected fentanyl and its analogs with excellent efficacy using a strand-displacement fluorescence assay where a single aptamer and a triple aptamer assay format revealed detection over a linear range from 10 µM–10 nM [70]. Initially, the target aptamers were isolated through a library-immobilized SELEX protocol. The aptamers then underwent PCR amplification for application. The sensors were fabricated on gold disks, employing a sophisticated electrode modification procedure to functionalize the disks for opioid detection. Notably, the sensors exhibited a pronounced affinity for fentanyl.

In conclusion, fluorescence sensors have made a significant mark in detecting harmful doses of opioids from various environments ranging from crime scenes to hospital/urgent care settings. These developed sensors show promise for increased use at the forefront of careful and measurable point-of-care management, with room for more work to be carried out in this area.

## 5. Conclusions and Prospects

Pharmaceutical opioids continue to be a significant treatment option for chronic and acute pain. However, the abuse, dependency, and overdose of opioids and illicit drugs are a global health safety epidemic. This review provides the innovations and recent advancements in using electrochemical sensors, biosensors, and optical sensors to detect pharmaceutical opioids, illicit drugs, and nitrosamine drug impurities. Electrochemical sensors provide the opportunity to selectively detect analytes at low levels at an affordable cost for laboratory and test tube testing. Nonetheless, electrochemical sensors suffer from challenges of reproducible electrode fabrication, stability, and aging of electrodes that may reduce the lifespan of the electrodes for large-scale sample analysis [217]. More studies will address this issue that will promote a large-scale use of electrochemical sensors for the analysis of opioids, illicit drugs, and nitrosamines. Biosensors offer specific and sensitive opioid detections. Nonetheless, biosensors are expensive and may hinder routine and wide applications of biosensors for opioid detection.

Among other desirable properties, optical sensors are cost-effective for sample analysis. Optical sensors, particularly colorimetric sensors, often lack the sensitivity for ultra-low analyte detections, limiting their practical applications in illicit drug analysis for clinical diagnosis and forensic studies. Additionally, multicomponent analysis of structurally related analytes with spectra overlaps and shifts is challenging for optical sensor detection. The use of spectra derivatives, machine learning, and multivariate analysis is an area of growth and offers the opportunity to address these challenges and facilitate multicomponent sample analyte analyses. FTIR sensors for opioids or nitrosamine detection in aqueous or biological samples are challenging due to FTIR water sensitivity. In addition, FTIR spectroscopy is generally adequate for determining opioid concentration at a minor to major concentration % weight range but is less effective at lower (trace or ultra-trace) concentrations. Combin-



ing FTIR and complementary analytical techniques, such as immunoassay, may address these challenges. Various new nanoparticles, carbon nanotubes, and nanomaterials are envisioned to be produced that will improve SERS detection, selectivity, and sensitivity for pharmaceutical opioids and illicit drug analysis. Raman spectroscopy may alleviate these challenges since Raman is water insensitive. Relatively poor Raman spectroscopy is a challenge that may be addressed using surface-enhanced Raman spectroscopy (SERS) to improve sensitivity and opioid drug detections. The research area that could be expanded includes the development of nanoparticles with better optical properties that will allow sensitivity and selectivity. Developing polymeric micelles, ligand receptors, immunoassays, and mimetic enzymes is another research area that can be expanded to promote selective opioid analysis. Moreover, developing microchip and microfluidic devices and sensor arrays that will promote low-cost, rapid, simultaneous, and selective multiple sensing of various opioid target molecules is an area of growth and opportunity in clinical, environmental, pharmaceutical, and forensic opioid analyses.

The US Food and Drug Administration is expected to continue to be proactive and provide oversight to ensure the safety of pharmaceutical products. Accountability and strong partnerships between health providers, drug manufacturers, local law enforcement authorities, the US Food and Drug Administration regulatory agency, and social workers and stakeholders are required to combat opioid and illicit drug overdose episodes to safeguard public health safety. The development of effective overdose intervention, rehabilitation schemes, and provision of adequate resources are recommended to help tens of thousands of people suffering from drug dependency globally. The use of non-pharmacological therapies, including chiropractic care, movement therapy, music therapy, yoga, and acupuncture [218] for chronic pain management, will gain more popularity. Effective drug quality control and on-site screening by governmental and law enforcement agencies will reduce access to illicit drug production, and street drug availability will reduce harm reduction. Using artificial intelligence, machine learning, drones, satellite imagery, and unmanned aerial vehicles for community drug monitoring of illicit drugs will also gain traction.

**Author Contributions:** Conceptualization, writing—original draft preparation, S.O.F.; P.N.B., writing—original draft preparation; C.G., writing—original draft preparation; V.F.N., writing—original draft preparation; P.R.F., writing—original draft preparation; C.H.L., writing—original draft preparation; D.K.B., writing—original draft preparation; P.N.B., writing—review and editing; C.G., writing—review and editing; V.F.N., writing—review and editing; P.R.F., writing—review and editing; C.H.L., writing—review and editing; D.K.B., writing—review and editing. All authors have read and agreed to the published version of the manuscript.

**Funding:** This research received no external funding.

**Conflicts of Interest:** The authors declare no conflict of interest.

## References

1. Breivik, H.; Collett, B.; Ventafridda, V.; Cohen, R.; Gallacher, D. Survey of chronic pain in Europe: Prevalence, impact on daily life, and treatment. *Eur. J. Pain* **2006**, *10*, 287–333. [[CrossRef](#)] [[PubMed](#)]
2. Eccleston, C.; Jordan, A.L.; Crombez, G. The impact of chronic pain on adolescents: A review of previously used measures. *J. Pediatr. Psychol.* **2006**, *31*, 684–697. [[CrossRef](#)] [[PubMed](#)]
3. Volkow, N.D.; McLellan, A.T. Opioid Abuse in Chronic Pain—Misconceptions and Mitigation Strategies. *N. Engl. J. Med.* **2016**, *374*, 1253–1263. [[CrossRef](#)] [[PubMed](#)]
4. An Hecke, O.; Torrance, N.; Smith, B.H. Chronic pain epidemiology and its clinical relevance. *Br. J. Anaesth.* **2013**, *111*, 13–18. [[CrossRef](#)] [[PubMed](#)]
5. Yong, R.J.; Mullins, P.M.; Bhattacharyya, N. Prevalence of chronic pain among adults in the United States. *Pain* **2022**, *163*, e328–e332. [[CrossRef](#)]
6. Singh, A.; Menéndez-Perdomo, I.M.; Facchini, P.J. Benzylisoquinoline Alkaloid Biosynthesis in Opium Poppy: An Update. *Phytochem. Rev.* **2019**, *18*, 1457–1482. [[CrossRef](#)]
7. World Health Organization. *WHO Model List of Essential Medicines—22nd List, 2021*; WHO: Geneva, Switzerland, 2021.



8. Chou, R.; Fanciullo, G.J.; Fine, P.G.; Adler, J.A.; Ballantyne, J.C.; Davies, P.; Donovan, M.I.; Fishbain, D.A.; Foley, K.M.; Fudin, J. Clinical guidelines for the use of chronic opioid therapy in chronic noncancer pain. *J. Pain* **2009**, *10*, 113–130.e22.
9. Fowler, T.O.; Durham, C.O.; Planton, J.; Edlund, B.J. Use of nonsteroidal anti-inflammatory drugs in the older adult. *J. Am. Assoc. Nurse Pract.* **2014**, *26*, 414–423. [\[CrossRef\]](#)
10. Reduce Overdose Deaths Involving Opioids—IVP-20. Available online: <https://health.gov/healthypeople/objectives-and-data/browse-objectives/injury-prevention/reduce-overdose-deaths-involving-opioids-ivp-20> (accessed on 16 December 2023).
11. National Institutes on Drug Abuse. Drug Overdose Death Rates. Available online: <https://nida.nih.gov/research-topics/trends-statistics/overdose-death-rates> (accessed on 16 December 2023).
12. Centers for Disease Control and Prevention. Drug Overdose Deaths in the U.S Top 100,000. Available online: <https://www.cdc.gov/drugoverdose/deaths/index.html> (accessed on 16 December 2023).
13. Lombardi, A.R.; Arya, R.; Rosen, J.G.; Thompson, E.; Welwean, R.; Tardif, J.; Rich, J.D.; Park, J.N. Overdose Detection Technologies to Reduce Solitary Overdose Deaths: A Literature Review. *Int. J. Environ. Res. Public Health* **2023**, *20*, 1230. [\[CrossRef\]](#) [\[PubMed\]](#)
14. Centers for Disease Control and Prevention; National Center for Health Statistics. Underlying Cause of Death 1999–2015 on CDC WONDER Online Database, Released 2017. Data are from the Multiple Cause of Death Files, 1999–2016, as Compiled from Data Provided by the 57 Vital Statistics Jurisdictions through the Vital Statistics Cooperative Program. 2017. Available online: <http://wonder.cdc.gov/ucd-icd10.html> (accessed on 16 December 2023).
15. American Psychiatric Association. *Diagnostic and Statistical Manual of Mental Disorders*, 5th ed.; American Psychiatric Association: Washington, DC, USA, 2013.
16. Campbell, C.I.; Bahorik, A.L.; VanVeldhuisen, P.; Weisner, C.; Rubinstein, A.L.; Ray, G.T. Use of a prescription opioid registry to examine opioid misuse and overdose in an integrated health system. *Prev. Med.* **2018**, *110*, 31–37. [\[CrossRef\]](#)
17. Centers for Disease Control and Prevention, Opioid Overdose: Opioid Data Analysis and Resources. Available online: <https://www.cdc.gov/drugoverdose/data/OD-death-data.html> (accessed on 3 February 2024).
18. Nuamah, J.K.; Sasangohar, F.; Erraguntla, M.; Mehta, R.K. The past, present and future opioid withdrawal assessment: A scoping review of scales and technologies. *BMC Med. Inform. Decis. Mak.* **2019**, *19*, 113. [\[CrossRef\]](#) [\[PubMed\]](#)
19. Birnbaum, H.G.; White, A.G.; Schiller, M.; Waldman, T.; Cleveland, J.M.; Roland, C.L. Societal costs of prescription opioid abuse, dependence, and misuse in the United States. *Pain Med.* **2011**, *12*, 657–667. [\[CrossRef\]](#) [\[PubMed\]](#)
20. Florence, C.S.; Zhou, C.; Luo, F.; Xu, L. The economic burden of prescription opioid overdose, abuse, and dependence in the United States, 2013. *Med. Care* **2016**, *54*, 901–906. [\[CrossRef\]](#) [\[PubMed\]](#)
21. McAdam-Marx, C.; Roland, C.L.; Cleveland, J.; Oderda, G.M. Costs of opioid abuse and misuse determined from a Medicaid database. *J. Pain Palliat. Care Pharmacother.* **2010**, *24*, 5–18. [\[CrossRef\]](#) [\[PubMed\]](#)
22. Krueger, A.B. Where have all the workers gone? An inquiry into the decline of the U.S. labor force participation rate. *Brook. Pap. Econ. Act.* **2017**, *2017*, 1–87.
23. Unfinished Business: Bipartisan Help for Child Victims of the Opioid Crisis. Retrieved September 17, 2018. Available online: <https://www.brookings.edu/opinions/unfinished-business-bipartisan-help-for-child-victims-of-the-opioid-crisis/> (accessed on 16 December 2023).
24. Strang, J.; Volkow, N.D.; Degenhardt, L.; Hickman, M.; Johnson, K.; Koob, G.F.; Marshall, B.D.L.; Walsh, S.L. Opioid use disorder. *Nat. Rev. Dis. Primers* **2020**, *6*, 4. [\[CrossRef\]](#) [\[PubMed\]](#)
25. Jones, C.M.; Baldwin, G.T.; Compton, W.M. Recent Increases in Cocaine-Related Overdose Deaths and the Role of Opioids. *AJPH Res.* **2017**, *107*, 3.
26. BC Coroners Service. *Illicit Drug Overdose Deaths in BC: January 1, 2008–December 31, 2018*; Ministry of Public Safety & Solicitor General: Victoria, BC, Canada, 2019.
27. Ahmad, F.B.; Rossen, L.M.; Spencer, M.R.; Warner, M.; Sutton, P. Provisional Drug Overdose Death Counts; National Center for Health Statistics: Centers for Disease Control and Prevention. Available online: <https://www.cdc.gov/nchs/nvss/vsrr/drug-overdose-data.htm> (accessed on 16 December 2023).
28. PHAC. Opioid- and Stimulant-Related Harms in Canada. Public Health Agency of Canada. 2022. Available online: <https://health-infobase.canada.ca/substance-related-harms/opioids-stimulants/> (accessed on 16 December 2023).
29. British Columbia Coroner's Service. Distribution of illicit Drug Toxicity Deaths (2015–2024): British Columbia Coroner's Service. Available online: <http://www.bccdc.ca/resource-gallery/Documents/Statistics%20and%20Research/Statistics%20and%20Reports/Overdose/Illicit%20Drug%20Toxicity%20Deaths%20by%20HSDA%20BC%20-%20No%20Counts.pdf> (accessed on 4 April 2024).
30. BC Coroners Service. *Illicit Drug Toxicity Deaths in BC*; BC Coroners Service: Victoria, BC, Canada, 2022.
31. Special Advisory Committee on the Epidemic of Opioid Overdoses. *National Report: Apparent Opioid-Related Deaths in Canada (January 2016 to December 2018)*; Web Based Report; Public Health Agency of Canada: Ottawa, ON, Canada, 2019.
32. Rudd, R.A.; Aleshire, N.; Zibbell, J.E.; Gladden, R.M. Increases in drug and opioid overdose deaths—United States, 2000–2014. *MMWR Morb. Mortal Wkly. Rep.* **2016**, *64*, 1378–1382. [\[CrossRef\]](#) [\[PubMed\]](#)
33. Peterson, A.B.; Gladden, R.M.; Delcher, C.; Spies, E.; Garcia-Williams, A.; Wang, Y.; Halpin, J.; Zibbell, J.; McCarthy, C.L.; DeFiore-Hyrmer, J.; et al. Increases in fentanyl-related overdose deaths—Florida and Ohio, 2013–2015. *MMWR Morb. Mortal Wkly. Rep.* **2016**, *65*, 844–849. [\[CrossRef\]](#) [\[PubMed\]](#)

34. American Medical Association. Physicians' Progress toward Ending the Nation's Drug Overdose Epidemic. 2022. Available online: <https://www.ama-assn.org/delivering-care/overdose-epidemic/physicians-progress-toward-ending-nation-s-drug-overdose-epidemic> (accessed on 11 December 2023).
35. Irvine, M.A.; Kuo, M.; Buxton, J.A.; Balshaw, R.; Otterstatter, M.; Macdougall, L.; Milloy, M.J.; Bharmal, A.; Henry, B.; Tyndall, M. Modelling the combined impact of interventions in averting deaths during a synthetic-opioid overdose epidemic. *Addiction* **2019**, *114*, 1602–1613. [CrossRef] [PubMed]
36. Wallace, B.; van Roode, T.; Pagan, F.; Phillips, P.; Wagner, H.; Calder, S.; Aasen, J.; Pauly, B.; Hore, D. What is needed for implementing drug checking services in the context of the overdose crisis? A qualitative study to explore perspectives of potential service users. *Harm Reduct. J.* **2020**, *17*, 29. [CrossRef] [PubMed]
37. Maghsoudi, N.; McDonald, K.; Stefan, C.; Beriault, D.R.; Mason, K.; Barnaby, L. Evaluating networked drug checking services in Toronto, Ontario: Study protocol and rationale. *Harm Reduct. J.* **2020**, *17*, 9. [CrossRef] [PubMed]
38. Larnder, A.; Saatchi, A.; Borden, S.A.; Moa, B.; Gill, C.G.; Wallace, B.; Hore, D. Variability in the unregulated opioid market in the context of extreme rates of overdose. *Drug Alcohol Depend.* **2022**, *235*, 109427. [CrossRef] [PubMed]
39. Beaulieu, T.; Wood, E.; Tobias, S.; Lysyshyn, M.; Patel, P.; Mathews, J.; Ti, L. Is expected substance type associated with timing of drug checking service utilization? A cross-sectional study. *Harm Reduct. J.* **2021**, *18*, 66. [CrossRef] [PubMed]
40. Tupper, K.W.; McCrae, K.; Garber, I.; Lysyshyn, M.; Wood, E. Initial results of a drug checking pilot program to detect fentanyl adulteration in a Canadian setting. *Drug Alcohol Depend.* **2018**, *1*, 242–245. [CrossRef] [PubMed]
41. Wallace, B.; van Roode, T.; Burek, P.; Hore, D.; Pauly, B. Everywhere and for everyone: Proportionate universalism as a framework for equitable access to community drug checking. *Harm Reduct. J.* **2022**, *19*, 143. [CrossRef] [PubMed]
42. Gozdziński, L.; Wallace, B.; Hore, D. Point-of-care community drug checking technologies: An insider look at the scientific principles and practical considerations. *Harm Reduct. J.* **2023**, *20*, 39. [CrossRef] [PubMed]
43. Harper, L.; Powell, J.; Pijl, E.M. An overview of forensic drug testing methods and their suitability for harm reduction point-of-care services. *Harm Reduct. J.* **2017**, *14*, 52. [CrossRef] [PubMed]
44. Barratt, M.J.; Kowalski, M.; Maier, L.J.; Ritter, A. *Global Review of Drug Checking Services Operating in 2017*; National Drug and Alcohol Research Centre: Sydney, QLD, Australia, 2018.
45. Pratiwi, R.; Noviana, E.; Fauziati, R.; Carrão, D.B.; Gandhi, F.A.; Majid, M.A.; Saputri, F.A. A Review of Analytical Methods for Codeine Determination. *Molecules* **2021**, *26*, 800. [CrossRef] [PubMed]
46. Shan, X.; Cao, C.; Yang, B. Analytical Approaches for the Determination of Buprenorphine, Methadone and Their Metabolites in Biological Matrices. *Molecules* **2022**, *27*, 5211. [CrossRef]
47. Musiał, J.; Czarny, J.; Gadzała-Kopciuch, R. Overview of analytical methods for determining novel psychoactive substances, drugs and their metabolites in biological samples. *Crit. Rev. Toxicol.* **2022**, *52*, 239–258. [CrossRef] [PubMed]
48. Guerrieri, D.; Kjellqvist, F.; Kronstrand, R.; Gréen, H. Validation and cross-reactivity data for fentanyl analogs with the immunoassay fentanyl ELISA. *J. Anal. Toxicol.* **2019**, *43*, 18–24. [CrossRef] [PubMed]
49. Abbott, D.L.; Limoges, J.F.; Virkler, K.J.; Tracy, S.J.; Sarris, G.G. ELISA screens for fentanyl in urine are susceptible to false-positives in high concentration methamphetamine samples. *J. Anal. Toxicol.* **2022**, *46*, 457–459. [CrossRef] [PubMed]
50. European Network of OMCLs, OMCLs Release. Determination of NDMA in Valsartan Active Substances and Finished Products by HPLC/UV. Available online: <https://www.google.com.hk/url?sa=t&source=web&rct=j&opi=89978449&url=https://www.edqm.eu/documents/52006/71923/Ad-hoc-projects-OMCL-Network-ansm-powdered-tablets-valsartan.pdf/a9bf0d81-f8da-9531-6de0-0268ab1614ad?t=1628667816207&ved=2ahUKEwjYvPCM7ayFAxWSsIYBHcYaD9AQFnoECB0QAQ&usq=AOvVaw2ft9Q3ITY49RCEAytE1dNV> (accessed on 22 February 2024).
51. French National Agency for Medicines and Health Products Safety; European Network of OMCLs, OMCLs Release. *Test Method for the Determination of NDMA by LC/MS/MS in Valsartan Finished Products*; Chemisches und Veterinäruntersuchungsamt: Karlsruhe, Germany, 2018.
52. Chang, S.; Chang, C.; Wang, L.; Chen, W.; Fan, S.; Zang, C.; Hsu, Y.; Lin, M.; Tseng, S.; Wang, D. A multi-analyte LC-MS/MS method for screening and quantification of nitrosamines in sartans. *J. Food Drug Anal.* **2020**, *28*, 98–107. [CrossRef] [PubMed]
53. Yang, J.; Marzan, T.A.; Ye, W.; Sommers, C.D.; Rodriguez, J.D.; Keire, D.A. A Cautionary Tale: Quantitative LC-HRMS Analytical Procedures for the Analysis of N-Nitrosodimethylamine in Metformin. *AAPS J.* **2020**, *22*, 89. [CrossRef] [PubMed]
54. Choudhary, S.; Sharma, A.; Chandrasekar, M.P.; Kotikalapudi, S. SCIEX, Gurgaon, India. LC-MS/MS Quantitative Analysis of NDMA in Ranitidine Active Pharmaceutical Ingredient (API) and Drug Product using the SCIEX 4500 QTRAP. Phenomenex India. Available online: <https://www.phenomenex.com/c68401a7-a7d2-4274-9dc1-0e1c88a9cb92> (accessed on 16 December 2023).
55. Guo, L.; Long, Z.; Leng, X.; Turner, J.; Rapid Analysis of Genotoxic Nitrosamines by HPLC-MS/MS. SCIEX APAC Applications Support Center, Beijing, China. Available online: <https://www.phenomenex.com/c04c6179-3a07-4864-bc03-0abdc16cc57c> (accessed on 16 December 2023).
56. Wichitnithad, W.; Sudtanon, O.; Srisunak, P.; Cheewatanakornkool, K.; Nantaphol, S.; Rojsitthisak, P. Development of a Sensitive Headspace Gas Chromatography–Mass Spectrometry Method for the Simultaneous Determination of Nitrosamines in Losartan Active Pharmaceutical Ingredients ACS Omega **2021**, *6*, 11048–11058. [CrossRef]
57. Parr, M.K.; Joseph, J.F. NDMA Impurity in Valsartan and Other Pharmaceutical Products: Analytical Methods for the Determination of N-Nitrosamines. *J. Pharm. Biomed. Anal.* **2019**, *164*, 536–549. [CrossRef] [PubMed]

58. Liu, J.; Xie, B.; Mai, B.; Cai, Q.; He, R.; Guo, D.; Zhang, Z.; Fan, J.; Zhang, W. Development of a Sensitive and Stable GC-MS/MS Method for Simultaneous Determination of Four N-Nitrosamine Genotoxic Impurities in Sartan Substances. *J. Anal. Sci. Technol.* **2021**, *12*, 3. [CrossRef]
59. US Food and Drug Administration. *Combined Headspace N-Nitrosodimethylamine (NDMA), N-Nitrosodiethylamine (NDEA), N-Nitrosoethylisopropylamine (NEIPA), and N-Nitrosodiisopropylamine (NDIPA) Impurity Assay by GC-MS/MS*; US Food and Drug Administration: Silver Spring, MD, USA, 2019; pp. 1–7.
60. Tsutsumi, T.; Akiyama, H.; Demizu, Y.; Uchiyama, N.; Masada, S.; Tsuji, G.; Arai, R.; Abe, Y.; Hakamatsuka, T.; Izutsu, K.; et al. Analysis of an Impurity, N-Nitrosodimethylamine, in Valsartan Drug Substances and Associated Products Using GC-MS. *Biol. Pharm. Bull.* **2019**, *42*, 547–551. [CrossRef] [PubMed]
61. New OMCL Method for Simultaneous Determination of NDMA and NDEA in Sartan. Available online: <https://www.edqm.eu/documents/52006/71923/Ad-hoc-projects-OMCL-Network-ranitidine.pdf/f775bf3-705e-ce82-d1e1-8eb3c06002d4?t=1628667875462> (accessed on 16 December 2023).
62. Lee, D.H.; Hwang, S.H.; Park, S.; Lee, J.; Oh, H.B.; Han, S.B.; Liu, K.-H.; Lee, Y.-M.; Pyo, H.S.; Hong, J. A Solvent-Free Headspace GC/MS Method for Sensitive Screening of N-Nitrosodimethylamine in Drug Products. *Anal. Methods* **2021**, *13*, 3402–3409. [CrossRef] [PubMed]
63. Fakayode, S.O.; Walgama, C.; Fernand-Narcisse, V.E.; Grant, C. Electrochemical and Optical Nanosensors for Detection of Heavy Metal Ions: A Review. *Sensors* **2023**, *23*, 9080. [CrossRef] [PubMed]
64. Fakayode, S.O.; Lisse, C.; Medawala, W.; Brady, P.M.; Bwambok, D.; Anum, D.; Alonge, T.; Taylor, M.E.; Baker, G.A.; Mehari, T.F.; et al. Fluorescent Chemical Sensors: Applications in Analytical, Environmental, Forensic, Pharmaceutical, Biological, and Biomedical Sample Measurement and Clinical Diagnosis. *Appl. Spectrosc. Rev.* **2023**, *59*, 1–89. [CrossRef]
65. Siraj, N.; Brady, N.P.; Elzey, B.; Taylor, T.; Baker, G.; Bwambok, D.; Bashiru, M.; Macchi, S.; Jaliha, A.; Denmark, I.; et al. Raman Spectroscopy and Multivariate Regression Analysis in Biomedical Research, Medical Diagnosis, and Clinical Analysis. *Appl. Spectrosc. Rev.* **2021**, *56*, 615–672. [CrossRef]
66. Fakayode, S.O.; Bwambok, D.; Suraj, N.; Baker, G.; Rodriguez, J.; Banerjee, S.; Perez, R.; Ayala, C.E.; Walgama, C.; Elzy, B.; et al. QCM Sensor Arrays, Electroanalytical Techniques and NIR Spectroscopy Coupled to Multivariate Analysis for Quality Assessment of Food Products, Raw Materials, and Ingredients and Foodborne Pathogen Detection: Challenges and Breakthroughs. *Sensors* **2020**, *20*, 6982. [CrossRef] [PubMed]
67. Uezono, E.; Mizobuchi, Y.; Miyano, K.; Ohbuchi, K.; Murata, H.; Komatsu, A.; Manabe, S.; Nonaka, M.; Hirokawa, T.; Yamaguchi, K.; et al. Distinct profiles of desensitization of  $\mu$ -opioid receptors caused by remifentanyl or fentanyl: In vitro assay with cells and three-dimensional structural analyses. *Int. J. Mol. Sci.* **2023**, *24*, 8369. [CrossRef] [PubMed]
68. Kroning, K.E.; Wang, W. Designing a single protein-chain reporter for opioid detection at cellular resolution. *Angew. Chem. Int. Ed. Engl.* **2021**, *60*, 13358–13365. [CrossRef] [PubMed]
69. Kroning, K.E.; Li, M.; Petrescu, D.I.; Wang, W. A genetically encoded sensor with improved fluorescence intensity for opioid detection at cellular resolution. *Chem. Commun.* **2021**, *57*, 10560–10563. [CrossRef] [PubMed]
70. Canoura, J.; Liu, Y.; Alkhamis, O.; Xiao, Y. Aptamer-based fentanyl detection in biological fluids. *Anal. Chem.* **2023**, *95*, 18258–18267. [CrossRef] [PubMed]
71. Canoura, J.; Liu, Y.; Perry, J.; Willis, C.; Xiao, Y. Suite of aptamer-based sensors for the detection of fentanyl and its analogues. *ACS Sens.* **2023**, *8*, 1901–1911. [CrossRef] [PubMed]
72. Nah, S.H.; Unsuhay, D.; Wang, P.; Yang, S. A highly sensitive and specific photonic crystal-based opioid sensor with rapid regeneration. *ACS Appl. Mater. Inter.* **2023**, *15*, 27647–27657. [CrossRef] [PubMed]
73. Muthusamy, A.K.; Kim, C.H.; Virgil, S.C.; Knox, H.J.; Marvin, J.S.; Nichols, A.L.; Cohen, B.N.; Dougherty, D.A.; Looger, L.L.; Lester, H.A. Three mutations convert the selectivity of a protein sensor from nicotinic agonists to s-methadone for use in cells, organelles, and biofluids. *J. Am. Chem. Soc.* **2022**, *144*, 8480–8486. [CrossRef] [PubMed]
74. González-Hernández, J.; Moya-Alvarado, G.; Alvarado-Gómez, A.L.; Urcuyo, R.; Barquero-Quirós, M.; Arcos-Martínez, M.J. Electrochemical biosensor for quantitative determination of fentanyl based on immobilized cytochrome c on multi-walled carbon nanotubes modified screen-printed carbon electrodes. *Mikrochim. Acta* **2022**, *189*, 483–495. [CrossRef] [PubMed]
75. Cortade, D.L.; Wang, S.X. Quantitative and rapid detection of morphine and hydromorphone at the point of care by an automated giant magnetoresistive nanosensor platform. *Anal. Bioanal. Chem.* **2022**, *414*, 7211–7221. [CrossRef] [PubMed]
76. Liu, L.; Grillo, F.; Canfarotta, F.; Whitcombe, M.; Morgan, S.P.; Piletsky, S.; Correia, R.; He, C.; Norris, A.; Korposh, S. Carboxyl-fentanyl detection using optical fibre grating-based sensors functionalised with molecularly imprinted nanoparticles. *Biosens. Bioelectron.* **2021**, *177*, 113002–113011. [CrossRef]
77. Wang, Z.; Nautiyal, A.; Alexopoulos, C.; Aqrabi, R.; Huang, X.; Ali, A.; Lawson, K.E.; Riley, K.; Adamczyk, A.J.; Dong, P.; et al. Fentanyl assay derived from intermolecular interaction-enabled small molecule recognition (imsr) with differential impedance analysis for point-of-care testing. *Anal. Chem.* **2022**, *94*, 9242–9251. [CrossRef] [PubMed]
78. Joshi, P.; Riley, P.R.; Mishra, R.; Azizi Macheckposhti, S.; Narayan, R. Transdermal polymeric microneedle sensing platform for fentanyl detection in biofluid. *Biosensors* **2022**, *12*, 198. [CrossRef] [PubMed]
79. Shao, W.; Zeng, Z.; Star, A. An ultrasensitive norfentanyl sensor based on a carbon nanotube-based field-effect transistor for the detection of fentanyl exposure. *ACS Appl. Mater. Interfaces* **2023**, *15*, 37784–37793. [CrossRef] [PubMed]



80. Angelini, D.J.; Biggs, T.D.; Prugh, A.M.; Smith, J.A.; Hanburger, J.A.; Llano, B.; Avelar, R.; Ellis, A.; Lusk, B.; Malik Naanaa, A.; et al. The use of lateral flow immunoassays for the detection of fentanyl in seized drug samples and postmortem urine. *J. Foren. Sci.* **2021**, *66*, 758–765. [[CrossRef](#)] [[PubMed](#)]
81. Khosropour, H.; Rezaei, B.; Alinajafi, H.A.; Ensafi, A.A. Electrochemical sensor based on glassy carbon electrode modified by polymelamine formaldehyde/graphene oxide nanocomposite for ultrasensitive detection of oxycodone. *Mikrochim. Acta* **2021**, *188*, 1. [[CrossRef](#)] [[PubMed](#)]
82. Baghayeri, M.; Nabavi, S.; Hasheminejad, E.; Ebrahimi, V. Introducing an electrochemical sensor based on two layers of Ag nanoparticles decorated graphene for rapid determination of methadone in human blood serum. *Top. Catal.* **2022**, *65*, 623–632. [[CrossRef](#)]
83. Habibi, M.M.; Ghasemi, J.B.; Badiei, A.; Narouzi, P. Simultaneous electrochemical determination of morphine and methadone by using CMK-5 mesoporous carbon and multivariate calibration. *Sci. Rep.* **2022**, *12*, 8270. [[CrossRef](#)] [[PubMed](#)]
84. Abraham, P.; Renjini, S.; Mary Nancy, T.E.; Kumary, V.A. Electrochemical synthesis of thin-layered graphene oxide poly-(CTAB) composite for detection of morphine. *J. App. Electrochem.* **2020**, *50*, 41–50. [[CrossRef](#)]
85. Beitollahi, H.; Nejad, F.G. Magnetic core-shell graphene oxide/Fe<sub>3</sub>O<sub>4</sub>@SiO<sub>2</sub> nanocomposite for sensitive and selective electrochemical detection of morphine using modified graphite screen printed electrode. *J. Anal. Chem.* **2020**, *75*, 127–134. [[CrossRef](#)]
86. Beitollahi, H.; Nejad, G.F.; Tajik, S.; Di Bartolomeo, A. Screen printed graphite electrode modified with graphene Co<sub>3</sub>O<sub>4</sub> nanocomposite: Voltametric assay of morphine in the presence of diclofenac in pharmaceutical and biological samples. *Nanomaterials* **2022**, *12*, 3454. [[CrossRef](#)] [[PubMed](#)]
87. Mohammadi, S.Z.; Jafari, M.; Jahani, M.P.; Ahmadi, S.A.; Mashayekh, R. Electrochemical determination of tramadol using modified screen-printed electrode. *J. Electrochem. Sci. Eng.* **2022**, *12*, 127–135. [[CrossRef](#)]
88. Atta, N.F.; Abdo, G.G.; Elzatahry, A.; Galal, A.; Hassan, S.H. Designed electrochemical sensor based on metallocene modified conducting polymer composite for effective determination of tramadol in real samples. *Can. J. Chem.* **2021**, *99*, 437–446. [[CrossRef](#)]
89. Mishra, K.R.; Krishnakumar, A.; Zareei, A.; Heredia-Rivera, U.; Rahimi, R. Electrochemical sensor for the rapid detection of fentanyl using laser-induced porous carbon-electrodes. *Microchim. Acta* **2022**, *189*, 198. [[CrossRef](#)] [[PubMed](#)]
90. Li, Q.; Wang, H. Fabrication of an electrochemical sensor based on a nanocomposite of CoO@f-CNTs for determination of tramadol narcotic drug in urine of athlete volunteers. *Int. J. Electrochem. Sci.* **2022**, *17*, 221018. [[CrossRef](#)]
91. Abd-Rabboh, H.S.M.; Amr, A.E.-G.E.; Almezahia, A.A.; Kamel, A.H. All-solid-state potentiometric ion-sensors based tailored imprinted polymers for Pholcodine determination. *Polymers* **2021**, *13*, 1192. [[CrossRef](#)] [[PubMed](#)]
92. Najafi, M.; Sohouli, E.; Mousavi, F. An electrochemical sensor for fentanyl detection based on multi-walled carbon nanotubes as electrocatalyst and the electrooxidation mechanism. *J. Anal. Chem.* **2021**, *75*, 1209–1217. [[CrossRef](#)]
93. Hojjati-Najafabadi, A.; Salmanpour, S.; Sen, F.; Asrami, P.N.; Mahdavian, M.; Khalilzadeh, M.A. A Tramadol drug electrochemical sensor amplified by biosynthesized Au nanoparticle using Mentha aquatic extract and ionic liquid. *Top. Catal.* **2022**, *65*, 587–594. [[CrossRef](#)]
94. Garkani Nejad, F.; Beitollahi, H.; Sheikhshoae, I. A UiO-66-NH<sub>2</sub> MOF/PAMAM Dendrimer Nanocomposite for Electrochemical Detection of Tramadol in the Presence of Acetaminophen in Pharmaceutical Formulations. *Biosensors* **2023**, *13*, 514. [[CrossRef](#)] [[PubMed](#)]
95. Khairy, M.; Banks, C.E. A screen-printed electrochemical sensing platform surface modified with nanostructured ytterbium oxide nanoplates facilitating the electroanalytical sensing of the analgesic drugs acetaminophen and tramadol. *Microchim. Acta* **2020**, *187*, 126. [[CrossRef](#)] [[PubMed](#)]
96. Kozak, J.; Tyszczyk-Rotko, K.; Wojciak, M.; Sowa, I. Electrochemically activated screen-printed carbon sensor modified with anionic surfactant (a SPCE/SDS) for simultaneous determination of Paracetamol, Diclofenac, and Tramadol. *Materials* **2021**, *14*, 3581. [[CrossRef](#)] [[PubMed](#)]
97. Keskin, E.; Allahverdiyeva, S.; Seyho, E.; Yardim, Y. Determination of tramadol in pharmaceutical forms and urine samples using a boron-doped diamond electrode. *J. Serb. Chem. Soc.* **2020**, *85*, 933–937. [[CrossRef](#)]
98. Solis, E., Jr.; Cameron-Burr, K.T.; Kivatkin, E.A. Rapid physiological fluctuations in nucleus accumbens oxygen levels induced by arousing stimuli: Relationships with changes in brain glucose and metabolic neural activation. *Front. Integr. Neurosci.* **2017**, *11*, 9. [[CrossRef](#)] [[PubMed](#)]
99. Mohammadi, S.; Taher, M.A.; Beitollahi, H. A hierarchical 3D camellia-like molybdenum tungsten disulfide architectures for the determination of morphine and tramadol. *Mikrochim. Acta* **2020**, *187*, 312. [[CrossRef](#)] [[PubMed](#)]
100. Razavi, R.; Amiri, M.; Divsalar, K.; Foroumadi, A. CuONPs/MWCNTs/carbon paste modified electrode for determination of tramadol: Theoretical and experimental investigation. *Sci. Rep.* **2023**, *13*, 7999. [[CrossRef](#)] [[PubMed](#)]
101. Borgul, P.; Sobczak, K.; Sipa, K.; Rudnicki, K.; Skrzypek, S.; Trynda, A.; Poltorak, L. Heroin detection in a droplet hosted in a 3D printed support at the miniaturized electrified liquid-liquid interface. *Sci. Rep.* **2022**, *12*, 18615. [[CrossRef](#)] [[PubMed](#)]
102. Chen, Z.R.; Bochner, F.; Somogyi, A. Pharmacokinetics of pholcodine in healthy volunteers: Single and chronic dosing studies. *Br. J. Clin. Pharmacol.* **1988**, *26*, 445–453. [[CrossRef](#)] [[PubMed](#)]
103. Thomas, S.A.; Curay, C.M.; Kiyatkin, E.A. Relationships between oxygen changes in the brain and periphery following physiological activation and the actions of heroin and cocaine. *Sci. Rep.* **2021**, *11*, 6355. [[CrossRef](#)] [[PubMed](#)]

104. Rosendo, L.M.; Antunes, M.; Simão, A.Y.; Brinca, A.T.; Catarro, G.; Pelixo, R.; Martinho, J.; Pires, B.; Soares, S.; Cascalheira, J.F.; et al. Sensors in the Detection of Abused Substances in Forensic Contexts: A Comprehensive Review. *Micromachines* **2023**, *14*, 2249. [CrossRef] [PubMed]
105. McCrae, K.; Tobias, S.; Grant, C.; Lysyshyn, M.; Laing, R.; Wood, E.; Ti, L. Assessing the limit of detection of Fourier-transform infrared spectroscopy and immunoassay strips for fentanyl in a real-world setting. *Drug Alcohol Rev.* **2020**, *39*, 98–102. [CrossRef] [PubMed]
106. United Nations Office on Drugs and Crime. United States: Rising Number of Deaths Involving Fentanyl and Fentanyl Analogues, Including Carfentanil. United Nations Office on Drugs and Crime. 2018. Available online: <https://www.unodc.org/LSS/Announcement/Details/b9ed5cee-8ab2-4c4c-a1d1-b34069eddf3> (accessed on 27 January 2024).
107. Misailidi, N.; Papoutsis, I.; Nikolaou, P.; Dona, A.; Spiliopoulou, C.; Athanaselis, S. Fentanyls continue to replace heroin in the drug arena: The cases of ocfentanil and carfentanil. *Forensic Toxicol.* **2018**, *36*, 12–32. [CrossRef] [PubMed]
108. Ti, L.; Tobias, S.; Lysyshyn, M.; Laing, R.; Nosova, E.; Choi, J.; Arredondo, J.; McCrae, K.; Tupper, K.; Wood, E. Detecting fentanyl using point-of-care drug checking technologies: A validation study. *Drug Alcohol Depend.* **2020**, *212*, 108006. [CrossRef] [PubMed]
109. Deconinck, E.; Duchateau, C.; Balcaen, M.; Gremeaux, L.; Courselle, P. Chemometrics and infrared spectroscopy—A winning team for the analysis of illicit drug products. *Rev. Anal. Chem.* **2022**, *41*, 228–255. [CrossRef]
110. Che, Z.; St Sauver, J.; Liu, H.; Liu, Y. Deep Learning Solutions for Classifying Patients on Opioid Use. *AMIA Annu. Symp. Proc.* **2018**, *2017*, 525–534. [PubMed]
111. Marcelo, M.C.A.; Mariotti, K.C.; Ferrão, M.F.; Ortiz, R.S. Profiling cocaine by ATR–FTIR. *Forensic Sci. Int.* **2015**, *246*, 65–71. [CrossRef]
112. Hespanhol, M.C.; Pasquini, C.; Maldaner, A. O Evaluation of a low-cost portable near-infrared spectrophotometer for in situ cocaine profiling. *Talanta* **2019**, *200*, 553–561. [CrossRef] [PubMed]
113. Ti, L.; Grant, C.J.; Tobias, S.; Hore, D.K.; Laing, R.; Marshall, B.D.L. Development of a neural network model to predict the presence of fentanyl in community drug samples. *PLoS ONE* **2023**, *18*, e0288656. [CrossRef]
114. He, X.; Wang, J.; Niu, F.; Fan, L.; Teng, X.; Zhang, C.; He, X. Characterization of Heroin and Its Additives by Attenuated Total Reflection (ATR)—Fourier Transform Infrared Spectroscopy (FTIR) and Multivariate Analysis. *Anal. Lett.* **2020**, *53*, 2656–2670. [CrossRef]
115. Kranenburg, R.F.; Verduin, J.; Weesepeel, Y.; Alewijn, M.; Heerschop, M.; Koomen, G.; Keizers, P.; Bakker, F.; Wallace, F.; van Esch, A.; et al. Rapid and robust on-scene detection of cocaine in street samples using a handheld near-infrared spectrometer and machine learning algorithms. *Drug Test Anal.* **2020**, *12*, 1404–1418. [CrossRef] [PubMed]
116. Farquharson, S.; Shende, C.; Newcomb, J.; Petrakis, I.L.; Arias, A.J. Analysis of drugs in saliva of US military veterans treated for substance use disorders using supported liquid extraction and surface-enhanced Raman spectral analysis. *Molecules* **2023**, *28*, 2010. [CrossRef] [PubMed]
117. Markina, N.E.; Goryacheva, I.Y.; Markin, A.V. Surface-enhanced Raman spectroscopy for the determination of medical and narcotic drugs in human biofluids. *J. Anal. Chem.* **2022**, *77*, 930–947. [CrossRef]
118. Akcan, R.; Yildirim, M.S.; Ilhan, H.; Guven, B.; Tamer, U.; Saglam, N. Surface enhanced Raman spectroscopy as a novel tool for rapid quantification of heroin and metabolites in saliva. *Turk. J. Med. Sci.* **2020**, *50*, 1470–1479. [CrossRef] [PubMed]
119. Azimi, S.; Docoslis, A. Recent advances in the use of surface-enhanced Raman scattering for illicit drug detection. *Sensors* **2022**, *22*, 3887. [CrossRef]
120. Haddad, A.; Green, O.; Lombardi, J.R. Detection of fentanyl in binary mixtures with cocaine by use of surface-enhanced Raman spectroscopy. *Spectrosc. Lett.* **2019**, *52*, 462–472. [CrossRef]
121. Wang, L.; Vendrell-Dones, M.O.; Deriu, C.; Dogruer, S.; Harrington, P.B.; McCord, B. Multivariate analysis aided surface-enhanced Raman spectroscopy (MVA-SERS) multiplex quantitative detection of trace fentanyl in illicit drug mixtures using a handheld Raman spectrometer. *Appl. Spectrosc.* **2021**, *75*, 1225–1236. [CrossRef] [PubMed]
122. Wilcox, P.G.; Emmons, E.D.; Pardoe, I.J.; Kline, N.D.; Guicheteau, J.A. Quantitative Raman cross-sections and band assignments for fentanyl and fentanyl analogs. *Appl. Spectrosc.* **2023**, *77*, 439–448. [CrossRef] [PubMed]
123. Shende, C.; Farquharson, A.; Brouillette, C.; Smith, W.; Farquharson, S. Quantitative measurements of codeine and fentanyl on a surface-enhanced Raman-active pad. *Molecules* **2019**, *24*, 2578. [CrossRef] [PubMed]
124. Qin, Y.; Mo, F.; Yao, S.; Wu, Y.; He, Y.; Yao, W. Facile synthesis of porous Ag crystals as SERS sensor for detection of five methamphetamine analogs. *Molecule* **2022**, *27*, 3939. [CrossRef] [PubMed]
125. Wang, Y.; Sheng, W.; Liu, X.; Guo, J.; Zhang, X.; Qi, X.; Zou, M.; Wang, C. The detection of 27 fentanyl compounds in solid and liquid drugs based on differential Raman spectroscopy. *Chemosensors* **2023**, *11*, 561. [CrossRef]
126. Grover, C.; How, J.; Close, R. Fentanyl, etizolam, and beyond: A feasibility study of a community partnership using handheld Raman spectrometry to identify substances in the local illicit drug supply. *J. Public Health Res.* **2023**, *12*, 22799036231166313. [CrossRef] [PubMed]
127. Mullin, A.; Scott, M.; Vaccaro, G.; Gittins, R.; Ferla, S.; Schifano, F.; Guirguis, A. Handheld Raman spectroscopy in the first UK home office licensed pharmacist-led community drug checking service. *Int. J. Environ. Res. Public Health* **2023**, *20*, 4793. [CrossRef] [PubMed]



128. Gerace, E.; Seganti, F.; Luciano, C.; Lombardo, T.; Di Corcia, D.; Teifel, H.; Vincenti, M.; Salomone, A. On-site identification of psychoactive drugs by portable Raman spectroscopy during drug-checking service in electronic music events. *Drug Alcohol Rev.* **2019**, *38*, 50–56. [\[CrossRef\]](#) [\[PubMed\]](#)
129. Ye, Q.; Ren, S.; Huang, H.; Duan, G.; Liu, K.; Liu, J. Fluorescent and Colorimetric Sensors Based on the Oxidation of o-Phenylenediamine. *ACS Omega* **2020**, *5*, 20698–20706. [\[CrossRef\]](#) [\[PubMed\]](#)
130. Du, X.; Hao, H.; Qin, A.; Tang, B.Z. Highly sensitive chemosensor for detection of methamphetamine by the combination of AIE luminogen and cucurbit [7] uril. *Dye Pigment.* **2020**, *180*, 108413. [\[CrossRef\]](#)
131. Zhang, K.; Chen, T.; Zhang, L.; Ma, S.; Shen, Y.; Feng, C.; Nie, P.; Yang, Z.; Zhu, C. The selective colorimetric probe based on a macrocyclic Sm(III) complex for detecting lithium ion and its performance in the psychiatric drug. *Dye Pigment.* **2020**, *174*, 108027, ISSN 0143-7208. [\[CrossRef\]](#)
132. Jornet-Martínez, N.; Campíns-Falcó, P.; Herráez-Hernández, R. A Colorimetric Membrane-Based Sensor with Improved Selectivity towards Amphetamine. *Molecules* **2021**, *26*, 6713. [\[CrossRef\]](#) [\[PubMed\]](#)
133. Sun, J.; Lu, Y.; He, L.; Pang, J.; Yang, F.; Liu, Y. Colorimetric sensor array based on gold nanoparticles: Design principles and recent advances. *TrAC Trends Anal. Chem.* **2020**, *122*, 115754, ISSN 0165-9936. [\[CrossRef\]](#)
134. Alberti, G.; Zaroni, C.; Magnaghi, L.R.; Biesuz, R. Gold and Silver Nanoparticle-Based Colorimetric Sensors: New Trends and Applications. *Chemosensors* **2021**, *9*, 305. [\[CrossRef\]](#)
135. Bastami, R.; Mansour Bayat, T.; Paolesse, R. Naked-eye detection of morphine by Au@ Ag nanoparticles-based colorimetric chemosensors. *Sensors* **2022**, *22*, 2072. [\[CrossRef\]](#) [\[PubMed\]](#)
136. Yen, Y.; Lin, Y.; Chen, T.; Chyueh, S.; Chang, H. A Carbon-Dot Sensing Probe for Screening of Date Rape Drugs: Nitro-containing Benzodiazepines. *Sens. Actuators B Chem.* **2020**, *305*, 127441, ISSN 0925-4005. [\[CrossRef\]](#)
137. Wei, S.; Li, Y.; Liang, H.; Yen, Y.; Lin, Y.; Chang, H. Photoluminescent carbon nanomaterials for sensing of illicit drugs: Focus. *Anal. Sci.* **2022**, *38*, 247–260. [\[CrossRef\]](#) [\[PubMed\]](#)
138. Liu, J.; Zhang, J.; Wang, M.; Su, X. Silicon quantum dots based dual-mode fluorometric and colorimetric sensing of D-penicillamine. *Talanta* **2021**, *224*, 121886, ISSN 0039-9140. [\[CrossRef\]](#)
139. Ye, M.; Zhu, Y.; Lu, Y.; Gan, L.; Zhang, Y.; Zhao, Y. Magnetic nanomaterials with unique nanozymes-like characteristics for colorimetric sensors: A review. *Talanta* **2021**, *230*, 122299, ISSN 0039-9140. [\[CrossRef\]](#)
140. Shaban, S.; Moon, B.; Kim, D. Selective and sensitive colorimetric detection of p-aminophenol in human urine and paracetamol drugs based on seed-mediated growth of silver nanoparticles. *Environ. Technol. Innov.* **2021**, *22*, 101517, ISSN 2352-1864. [\[CrossRef\]](#)
141. Nishan, U.; Gul, R.; Muhammad, N.; Asad, M.; Rahim, A.; Shah, M.; Iqbal, J.; Uddin, J.; Shah, A.; Shujah, S. Colorimetric based sensing of dopamine using ionic liquid functionalized drug mediated silver nanostructures. *Microchem. J.* **2020**, *159*, 105382, ISSN 0026-265X. [\[CrossRef\]](#)
142. Crowley, R.; Riley, A.; Alder, A.; Anderson III, R.; Luo, D.; Kaska, S.; Maynez, P.; Kivell, B.; Prisinzano, T. Synthetic Studies of Neoclerodane Diterpenes from *Salvia divinorum*: Design, Synthesis, and Evaluation of Analogues with Improved Potency and G-protein Activation Bias at the  $\mu$ -Opioid Receptor. *ACS Chem. Neurosci.* **2020**, *11*, 1781–1790. [\[CrossRef\]](#) [\[PubMed\]](#)
143. Soni, S.; Jain, U.; Burke, D.; Chauhan, N. Recent trends and emerging strategies for aptasensing technologies for illicit drugs detection. *J. Electroanal. Chem.* **2022**, *910*, 116128, ISSN 1572-6657. [\[CrossRef\]](#)
144. Xie, M.; Zhao, F.; Zhang, Y.; Xiong, Y.; Han, S. Recent advances in aptamer-based optical and electrochemical biosensors for detection of pesticides and veterinary drugs. *Food Control* **2022**, *131*, 108399, ISSN 0956-7135. [\[CrossRef\]](#)
145. Shkembi, X.; Botero, M.; Skouridou, V.; Jauset-Rubio, M.; Svobodova, M.; Ballester, P.; Bashammakh, A.; El-Shahawi, M.; Alyoubi, A.; O'Sullivan, C. Novel nandrolone aptamer for rapid colorimetric detection of anabolic steroids. *Anal. Biochem.* **2022**, *658*, 114937, ISSN 0003-2697. [\[CrossRef\]](#)
146. Zhao, J.; Kan, Y.; Chen, Z.; Li, H.; Zhang, W. MOFs-Modified Electrochemical Sensors and the Application in the Detection of Opioids. *Biosensors* **2023**, *13*, 284. [\[CrossRef\]](#) [\[PubMed\]](#)
147. D'Aurelio, R.; Chianella, I.; Goode, J.A.; Tothill, I.E. Molecularly Imprinted Nanoparticles Based Sensor for Cocaine Detection. *Biosensors* **2020**, *10*, 22. [\[CrossRef\]](#) [\[PubMed\]](#)
148. Akhoundian, M.; Alizadeh, T. Enzyme-free colorimetric sensor based on molecularly imprinted polymer and ninhydrin for methamphetamine detection. *Spectrochim. Acta Part A Mol. Biomol. Spectrosc.* **2023**, *285*, 121866, ISSN 1386-1425. [\[CrossRef\]](#)
149. Völlmecke, K.; Afroz, R.; Bierbach, S.; Brenker, L.J.; Frücht, S.; Glass, A.; Giebelhaus, R.; Hoppe, A.; Kanemaru, K.; Lazarek, M.; et al. Hydrogel-Based Biosensors. *Gels* **2022**, *8*, 768. [\[CrossRef\]](#) [\[PubMed\]](#)
150. Akgönüllü, S.; Denizli, A. Plasmonic nanosensors for pharmaceutical and biomedical analysis. *J. Pharm. Biomed. Anal.* **2023**, *236*, 115671, ISSN 0731-7085. [\[CrossRef\]](#)
151. Clifford, A.; Das, J.; Yousefi, H.; Mahmud, A.; Chen, J.; Kelley, S. Strategies for Biomolecular Analysis and Continuous Physiological Monitoring. *J. Am. Chem. Soc.* **2021**, *143*, 5281–5294. [\[CrossRef\]](#) [\[PubMed\]](#)
152. Ghorbanizamani, F.; Moulahoum, H.; Timur, S. Noninvasive Optical Sensor for the Detection of Cocaine and Methamphetamine in Saliva Using Rhodamine B-Labeled Polymersomes. *IEEE Sens. J.* **2022**, *22*, 1146–1153. [\[CrossRef\]](#)
153. Cho, S.; Kim, Y. Donor-acceptor Stenhouse adduct formation for the simple and rapid colorimetric detection of amphetamine-type stimulants. *Sens. Actuators B Chem.* **2022**, *355*, 131274, ISSN 0925-4005. [\[CrossRef\]](#)

154. Ramadan, H.; Salam, R.; Hadad, G.; Belal, F.; Salim, M. Eco-friendly simultaneous multi-spectrophotometric estimation of the newly approved drug combination of celecoxib and tramadol hydrochloride tablets in its dosage form. *Sci. Rep.* **2023**, *13*, 11716. [[CrossRef](#)] [[PubMed](#)]
155. Crocombe, R.; Giuntini, G.; Schiering, D.; Profeta, L.; Hargreaves, M.; Leary, P. Field-portable detection of fentanyl and its analogs: A review. *J. Forensic Sci.* **2023**, *68*, 1570–1600. [[CrossRef](#)] [[PubMed](#)]
156. Alonzo, M.; Alder, R.; Clancy, L.; Fu, S. Portable testing techniques for the analysis of drug materials. *Wiley Interdiscip. Rev. Forensic Sci.* **2022**, *4*, e1461. [[CrossRef](#)]
157. Bui, T.H.; Thangavel, B.; Sharipov, M.; Chen, K.; Shin, J.H. Smartphone-Based Portable Bio-Chemical Sensors: Exploring Recent Advancements. *Chemosensors* **2023**, *11*, 468. [[CrossRef](#)]
158. Lantam, A.; Limbut, W.; Thiagchanya, A.; Phonchai, A. A portable optical colorimetric sensor for the determination of promethazine in lean cocktail and pharmaceutical doses. *Microchem. J.* **2020**, *159*, 105519, ISSN 0026-265X. [[CrossRef](#)]
159. Kang, C.; Shrestha, K.L.; Kwon, S.; Park, S.; Kim, J.; Kwon, Y. Intein-Mediated Protein Engineering for Cell-Based Biosensors. *Biosensors* **2022**, *12*, 283. [[CrossRef](#)]
160. Anzar, N.; Suleman, S.; Parvez, S.; Narang, J. A review on Illicit drugs and biosensing advances for its rapid detection. *Process Biochem.* **2022**, *113*, 113–124, ISSN 1359-5113. [[CrossRef](#)]
161. Truta, F.; Florea, A.; Cernat, A.; Tertis, M.; Hosu, O.; De Wael, K.; Cristea, C. Tackling the Problem of Sensing Commonly Abused Drugs Through Nanomaterials and (Bio)Recognition Approaches. *Front. Chem.* **2020**, *8*, 561638. [[CrossRef](#)]
162. Kim, K.; Stoll, S.; Singh, R.; Lee, W.; Hwang, J. Recent advances in illicit drug detection sensor technology in water. *TrAC Trends Anal. Chem.* **2023**, *168*, 117295, ISSN 0165-9936. [[CrossRef](#)]
163. Ahmed, S.; Chand, R.; Kumar, S.; Mittal, N.; Srinivasan, S.; Rajabzadeh, A. Recent biosensing advances in the rapid detection of illicit drugs. *TrAC Trends Anal. Chem.* **2020**, *131*, 116006, ISSN 0165-9936. [[CrossRef](#)]
164. Bruni, A.T.; Rodrigues, C.H.P.; dos Santos, C.; de Castro, J.S.; Mariotto, L.S.; Sinhorini, L.F.C. Analytical Challenges for Identification of New Psychoactive Substances. *Braz. J. Anal. Chem.* **2020**, *9*, 52–78. [[CrossRef](#)]
165. Cao, F.; Xu, J.; Yan, S.; Yuan, X.; Yang, F.; Hou, L.; Zhao, L.; Zeng, L.; Liu, W.; Zhu, L.; et al. A surface plasmon resonance-based inhibition immunoassay for forensic determination of methamphetamine in human serum. *Forensic Chem.* **2018**, *8*, 21–27, ISSN 2468-1709. [[CrossRef](#)]
166. Dagar, M.; Yadav, S.; Sai, V.; Satija, J.; Bhatia, H. Emerging trends in point-of-care sensors for illicit drugs analysis. *Talanta* **2022**, *238*, 123048, ISSN 0039-9140. [[CrossRef](#)]
167. Goli-Malekabadi, Z.; Salarizadeh, N.; Dianatkah, M.; Amoo, M.; Shayeh, J. Chapter 11—Biosensors for drug detection. In *Advanced Sensor Technology*; Elsevier: Amsterdam, The Netherlands, 2023; pp. 383–412. ISBN 9780323902229. [[CrossRef](#)]
168. Dashtian, K.; Amourizi, F.; Shahbazi, N.; Mousavi, A.; Saboorizadeh, B.; Astaraei, S.; Zare-Dorabei, R. Chapter 5—Biosensors for drug of abuse detection. In *Advanced Sensor Technology*; Elsevier: Amsterdam, The Netherlands, 2023; pp. 125–172. ISBN 9780323902229. [[CrossRef](#)]
169. Theyagarajan, K.; Sruthi, V.; Mohanapriya, D.; Thenmozhi, K.; Senthilkumar, S. Chapter 7—Biosensor platform for testing active pharmaceutical ingredients. In *Health and Environmental Applications of Biosensing Technologies*; Elsevier: Amsterdam, the Netherlands, 2024; pp. 129–152. ISBN 9780443190391. [[CrossRef](#)]
170. Abdelazim, A.; Abourehab, M.; Abd Elhalim, L.; Almasy, A.; Ramzy, S. Green adherent spectrophotometric determination of molnupiravir based on computational calculations; application to a recently FDA-approved pharmaceutical dosage form. *Spectrochim. Acta Part A Mol. Biomol. Spectrosc.* **2023**, *285*, 121911, ISSN 1386-1425. [[CrossRef](#)]
171. Pallavi, M.; Kumar, S.; Baggi, T. Analytical methods for tramadol in pharmaceutical and forensic context—A review. *Int. J. Med. Toxicol. Leg. Med.* **2023**, *26*, 122–147. [[CrossRef](#)]
172. Chen, C.; Wang, C.; Ko, P.; Chen, Y. Nanomaterial-based adsorbents and optical sensors for illicit drug analysis. *J. Food Drug Anal.* **2020**, *28*, 654–676. [[CrossRef](#)] [[PubMed](#)]
173. Jang, S.; Uk Son, S.; Kang, B.; Kim, J.; Lim, J.; Seo, S.; Kang, T.; Jung, J.; Lee, K.; Kim, H.; et al. Electrospun Nanofibrous Membrane-Based Colorimetric Device for Rapid and Simple Screening of Amphetamine-Type Stimulants in Drinks. *Anal. Chem.* **2022**, *94*, 3535–3542. [[CrossRef](#)] [[PubMed](#)]
174. Akula, G.; Sapavatu, S.; Jadi, R.; Battineni, J.; Boggula, N. Analytical method development and validation for the estimation of tramadol in bulk and its formulations by UV-spectroscopy. *J. Adv. Sci. Res.* **2021**, *12*, 77–83. [[CrossRef](#)]
175. Razlansari, M.; Ulucan-Karnak, F.; Kahrizi, M.; Mirinejad, S.; Sargazi, S.; Mishra, S.; Rahdar, A.; Diez-Pascual, A. Nanobiosensors for detection of opioids: A review of latest advancements. *Eur. J. Pharm. Biopharm.* **2022**, *179*, 79–94, ISSN 0939-6411. [[CrossRef](#)]
176. Siddiqui, J.; Taheri, M.; Alam, A.U.; Deen, M.J. Nanomaterials in Smart Packaging Applications: A Review. *Small* **2022**, *18*, 2101171. [[CrossRef](#)] [[PubMed](#)]
177. Mohammadpour, Z.; Naghib, S. Smart nanosensors for intelligent packaging. In *Nanosensors for Smart Manufacturing*; Elsevier: Amsterdam, The Netherlands, 2021; pp. 323–346. ISBN 9780128233580. [[CrossRef](#)]
178. Tan, Z.; Zhu, C.; Han, L.; Liao, X.; Wang, C. SERS and dark-field scattering dual-mode detection of intracellular hydrogen peroxide using biocompatible Au@ COF nanosensor. *Sens. Actuators B Chem.* **2022**, *373*, 132770, ISSN 0925-4005. [[CrossRef](#)]
179. Negut, I.; Bitu, B. Polymeric Micellar Systems—A Special Emphasis on “Smart” Drug Delivery. *Pharmaceutics* **2023**, *15*, 976. [[CrossRef](#)] [[PubMed](#)]

180. Li, Z.; Wang, P. Point-of-care drug of abuse testing in the opioid epidemic. *Arch. Pathol. Lab. Med.* **2020**, *144*, 1325–1334. [[CrossRef](#)] [[PubMed](#)]
181. Singh, N.K.; Sidhu, G.K.; Gupta, K. Current and Future Perspective of Devices and Diagnostics for Opioid and OIRD. *Biomedicines* **2022**, *10*, 743. [[CrossRef](#)] [[PubMed](#)]
182. Canfield, J.R.; Agarwal, S.; Fortener, S.K.; Sprague, J.E. Fentanyl Detection Using Eosin Y Paper Assays. *J. Forensic Sci.* **2020**, *65*, 1432–1442. [[CrossRef](#)] [[PubMed](#)]
183. Lin, Y.; Sun, J.; Tang, M.; Zhang, G.; Yu, L.; Zhao, X.; He, Y. Synergistic recognition-triggered charge transfer enables rapid visual colorimetric detection of fentanyl. *Anal. Chem.* **2020**, *93*, 6544–6550. [[CrossRef](#)] [[PubMed](#)]
184. Qu, F.; Lin, L.; Nie, P.; Xia, Z. High-Precision Automatic Identification of Fentanyl-Related Drugs by Terahertz Spectroscopy with Molecular Dynamics Simulation and Spectral Similarity Mapping. *Int. J. Mol. Sci.* **2022**, *23*, 10321. [[CrossRef](#)] [[PubMed](#)]
185. Purohit, S.; Pandey, G.; Tharmavaram, M.; Rawtani, D.; Mustansar Hussain, C. Sensors for the Detection of Illicit Drugs. *Technol. Forensic Sci. Sampl. Anal. Data Regul.* **2020**, *199*, 21–238. [[CrossRef](#)]
186. Usman, M.; Baig, Y.; Nardiello, D.; Quinto, M. How new nanotechnologies are changing the opioid analysis scenery? A comparison with classical analytical methods. *Forensic Sci. Res.* **2024**, *9*, owae001. [[CrossRef](#)]
187. Wu, Y.; Feng, J.; Hu, G.; Zhang, E.; Yu, H.-H. Colorimetric Sensors for Chemical and Biological Sensing Applications. *Sensors* **2023**, *23*, 2749. [[CrossRef](#)] [[PubMed](#)]
188. Rodrigues, C.H.P.; de Mascarenhas, R.O.; Bruni, A.T. In Silico Infrared Spectroscopy as a Benchmark for Identifying Seized Samples Suspected of Being N-Ethylpentylone. *Psychoactives* **2023**, *2*, 1–22. [[CrossRef](#)]
189. Shin, Y.-H.; Wing-Gutierrez, M.T.; Choi, J.W. Review- Recent Progress in Portable Fluorescence Sensors. *J. Electrochem. Soc.* **2021**, *168*, 017502. [[CrossRef](#)]
190. Ghose, R.; Forati, A.M.; Mantsch, J.R. Impact of the COVID-19 Pandemic on Opioid Overdose Deaths: A Spatiotemporal Analysis. *J. Urban Health* **2022**, *99*, 316–327. [[CrossRef](#)] [[PubMed](#)]
191. Richards, N.; Fried, M.; Svirsky, L.; Thomas, N.; Zettler, P.J.; Howards, D. Clinicians Perspectives on Opioid Treatment Agreements: A Qualitative Analysis of Focus Groups. *AJOB Empir. Bioeth.* **2023**, *2023*, 2274606. [[CrossRef](#)] [[PubMed](#)]
192. Meng, L.F.; Wu, H.Z. Carbon Quantum Dots from Carrot as Fluorescence Probes for High-Sensitivity Detection of Lidocaine. *Appl. Ecol. Environ. Res.* **2023**, *21*, 4531–4544. [[CrossRef](#)]
193. Garcia de Arquer, P.; Talapin, D.V.; Klimov, V.I.; Arakawa, Y.; Bayer, M.; Sargent, E.H. Semiconductor quantum dots: Technological progress and future challenges. *Science* **2021**, *373*, eaaz8541. [[CrossRef](#)]
194. Bahar, E.; Yoon, H. Lidocaine: A Local Anesthetic, Its Adverse Effects and Management. *Medicina* **2021**, *57*, 782. [[CrossRef](#)] [[PubMed](#)]
195. Gan, Y.X.; Jayatissa, A.H.; Yu, Z.; Chen, X.; Li, M. Hydrothermal Synthesis of Nanomaterials. *J. Nanomater.* **2020**, *2020*, 891703. [[CrossRef](#)]
196. Sarigul, N.; Korkmaz, F.; Kurultak, I. A New Artificial Urine Protocol to Better Imitate Human Urine. *Sci. Rep.* **2019**, *9*, 20159. [[CrossRef](#)] [[PubMed](#)]
197. Shang, Y.F.; Shen, Y.Y.; Zhang, M.C.; Lv, C.M.; Wang, T.Y.; Chen, X.Q.; Lin, J. Progress in salivary glands: Endocrine glands with immune functions. *Sec. Exp. Endocrinol.* **2023**, *14*, 1061235. [[CrossRef](#)] [[PubMed](#)]
198. Aydin, B.E.; Aydin, M.; Sezgintürk, M.K. Chapter One—Biosensors for Saliva Biomarkers. *Adv. Clin. Chem.* **2023**, *113*, 1–41. [[PubMed](#)]
199. U.S. Government. Part 40 Final Rule—Dot Summary of Changes. U.S. Department of Transportation. Available online: [https://www.transportation.gov/odapc/Notice\\_Summary\\_May\\_2023](https://www.transportation.gov/odapc/Notice_Summary_May_2023) (accessed on 10 February 2024).
200. Kanter, K.; Gallagher, R.; Eweje, F.; Lee, A.; Gordon, D.; Landy, S.; Gasior, J.; Soto-Calderon, H.; Cronholm, P.F.; Cocchiario, B.; et al. Willingness to use a wearable device capable of detecting and reversing overdose among people who use opioids in Philadelphia. *Harm Reduct. J.* **2021**, *18*, 75. [[CrossRef](#)] [[PubMed](#)]
201. Huang, Y.; Cao, X.; Deng, Y.; Ji, X.; Sun, W.; Xia, S.; Wan, S.; Zhang, H.; Xing, R.; Ding, J.; et al. An overview on recent advances of reversible fluorescent probes and their biological applications. *Talanta* **2024**, *268*, 125275. [[CrossRef](#)]
202. Spencer, R.M.; Garnett, M.F.; Miniño, A.M. Urban-Rural Differences in Drug Overdoses Death Rates, 2020. *NCHS Data Brief No. 440* **2022**, 440.
203. Loch, A.S.; Burn, P.L.; Shaw, P.E. Fluorescent sensors for the detection of free-base illicit drugs—Effect of tuning the electronic properties. *Sens. Actuators B Chem.* **2023**, *387*, 133766. [[CrossRef](#)]
204. Lawson, H.D.; Walton, P.S.; Chan, C. Metal-Organic Frameworks for Drug Delivery: A Design Perspective. *ACS Appl. Mater. Interfaces* **2021**, *13*, 7004–7020. [[CrossRef](#)] [[PubMed](#)]
205. Heinz, K.; Rogge, S.M.J.; Kalytta-Mewes, A.; Volkmer, D.; Bunzen, H. MOFs for long-term gas storage: Exploiting kinetic trapping in ZIF-8 for on-demand and stimuli-controlled gas release. *Inor. Chem. Front.* **2023**, *10*, 4763–4772. [[CrossRef](#)]
206. Qian, Q.; Asinger, P.A.; Lee, M.J.; Ha, G.; Rodriguez, K.M.; Lin, S.; Benedetti, F.M.; Wu, A.X.; Chi, W.S.; Smith, Z.P. MOF-Bases Membranes for Gas Separations. *Chem. Rev.* **2020**, *120*, 8161–8266. [[CrossRef](#)] [[PubMed](#)]
207. Rosen, A.S.; Fung, V.; Huck, P.; O'Donnell, C.T.; Horton, M.K.; Truhlar, D.G.; Persson, K.A.; Notestein, J.M.; Snurr, R.Q. High-throughput predictions of metal-organic framework electronic properties: Theoretical challenges, graph neural networks, and data exploration. *Comput. Mater.* **2022**, *8*, 112. [[CrossRef](#)]

208. Wu, Z.; Zhou, H.; Han, Q.; Lin, X.; Han, D.; Li, X. A cost-effective fluorescence biosensor for cocaine based on a “mix-and-detect” strategy. *Analyst* **2020**, *145*, 4664–4670. [[CrossRef](#)] [[PubMed](#)]
209. Ju, L.; Lyuy, A.; Hao, H.; Shen, W.; Cui, H. Deep Learning-Assisted Three-Dimensional Fluorescence Difference Spectroscopy for Identification and Semiquantification of Illicit Drugs in Biofluids. *Anal. Chem.* **2019**, *91*, 9343–9347. [[CrossRef](#)]
210. Judd, D.; King, C.R.; Galke, C. The Opioid Epidemic: A Review of the Contributing Factors, Negative Consequences, and Best Practices. *Cureus* **2023**, *15*, e41621. [[CrossRef](#)] [[PubMed](#)]
211. Beatty, Z.G.; Muthusamy, A.K.; Unger, E.K.; Doubherty, D.A.; Tian, L.; Looger, L.L.; Shivange, A.V.; Bera, K.; Lester, H.A.; Nichols, A.L. Fluorescence Screens for Identifying Central Nervous System-Acting Drug-Biosensor Pairs for Subcellular and Supracellular Pharmacokinetics. *Bio-Protocol* **2022**, *12*, e4551. [[CrossRef](#)]
212. Rappleye, M.; Wait, S.J.; Lee, D.J.; Siebart, J.C.; Torp, L.; Smith, N.; Muster, J.; Matreyek, K.A.; Fowler, D.M.; Brendt, A. Optogenetics Microwell Array Screening System: A High-Throughput Engineering Platform for Genetically Encoded Fluorescent Indicators. *ACS Sens.* **2023**, *8*, 4233–4244. [[CrossRef](#)] [[PubMed](#)]
213. Itai, D.; Vanle, B.; Groningen, V.; Ishak, W.; Nuckols, T. Opioid Overdose in the Hospital Setting: A systematic review. *J. Addict. Med.* **2020**, *14*, 39–47. [[CrossRef](#)]
214. Hoots, B.E. Opioid Overdose Surveillance: Improving Data to Inform Action. *Public Health Rep.* **2021**, *136* (Suppl. 1), 5S. [[CrossRef](#)]
215. Wilke, C. Portable Spectrometers Give On-Site Drug Testing a Boost. *ACS Centr. Sci.* **2023**, *9*, 124–127. [[CrossRef](#)] [[PubMed](#)]
216. D’Orsogna, M.R.; Böttcher, L.; Chou, T. Fentanyl-driven acceleration of racial, gender and geographical disparities in drug overdose deaths in the United States. *PLoS Glob. Public Health* **2023**, *3*, e0000769. [[CrossRef](#)] [[PubMed](#)]
217. Hassan, M.H.; Khan, R.; Andreescu, S. Advances in electrochemical detection methods for measuring contaminants of emerging concerns. *Electrochem. Sci. Adv.* **2022**, *2*, e2100184. [[CrossRef](#)]
218. Shi, Y.; Wu, W. Multimodal non-invasive non-pharmacological therapies for chronic pain: Mechanisms and progress. *BMC Med.* **2023**, *21*, 372. [[CrossRef](#)] [[PubMed](#)]

**Disclaimer/Publisher’s Note:** The statements, opinions and data contained in all publications are solely those of the individual author(s) and contributor(s) and not of MDPI and/or the editor(s). MDPI and/or the editor(s) disclaim responsibility for any injury to people or property resulting from any ideas, methods, instructions or products referred to in the content.